^{13}C NUCLEAR MAGNETIC RESONANCE STUDIES

OF BIOLOGICAL SYSTEMS

A thesis presented to the University of Warwick in partial fulfilment of the requirements for the degree of

DOCTOR OF PHILOSOPHY

The work described in this thesis was carried out mainly in this department. A part of the work was carried out in the Department of Molecular Biophysics and Biochemistry, Yale University, New-Haven, Conn., U.S.A. , with the approval of Senate.

E. A. C. NWANZE

February. 1976

To Ngozi.....

ACKNOWLEDGEMENTS

I wish to express my sincere thanks to the Chairman of the Department, Professor K.R. Jennings, for making the facilities for research available to me. I also wish to express my gratitude to Professor V.M. Clark for his advice and helpful discussions throughout the period of my stay at Warwick.

I am very grateful for the guidance of my two supervisors, Dr. G.H. Dodd and Dr. O.W. Howarth. Many of our exchanges were fruitful and timely.

I am also very grateful to Professor J.E. Cronan Jr., under whose supervision the first part of this work was carried out at the Department of Molecular Biophysics and Biochemistry, Sterling Hall of Medicine, Yale University, New Haven, Connecticut 06510, U.S.A.

I am also grateful to Mr. Robert Hanks of this Department, for providing the Tetrahymena strain used, and for help in the growth of this organism.

May I also extend my thanks to all my colleagues for relevant discussions and to all others who have been helpful in one way or another during my stay.

Finally, I must express my deepest gratitude to the Government of the Midwestern State of Nigeria for a Scholarship to do Post-Graduate Studies in England.

SUMMARY

Nuclear magnetic resonance techniques have been applied to the study of two biological systems. Specifically, ^{13}C nmr spin-lattice relaxation times (T_1 s) have been applied to a model biomembrane and also to the subject of protein denaturation.

In the former case, available ^{13}C enrichment techniques have been used to concentrate the isotope in a bacterial phospholipid. Using T_1 as an index of molecular motion, it has been possible to observe the "dynamics" of the carbon skeleton of the enriched phosphatidyl ethanolamine in a mixed phosphatidyl ethanolamine – phosphatidyl serine system, over the temperature range of 30-85°C. The results obtained fit suggested motional gradients typical of the type of structure formed in media of low to high dielectricity. However, changes with temperature in the mixed lipid system may be less dramatic than have been reported for single component models. The estimated energy of relaxation processes show that a higher activation energy is associated with those nuclei in the middle of the acyl residues.

A method is described, for the first time, for the high ^{13}C specific enrichment of phosphatidyl choline acyl residues. The method is based on the predatory growth of a ciliate on an E. coli strain which is designed to incorporate acetate efficiently. Tetrahymena pyriformis which was the ciliate used, was found to metabolize the E. coli lipids resulting in a lipid distribution that is characteristic in normal growth. The enrichment levels found in the extracted lipids of Tetrahymena are interpreted in terms of the possible mechanisms of some steps in lipid metabolism. The attractions in this area are two-fold; firstly the high enrichment (20-50%) in ^{13}C of phosphatidyl choline which is usually the major lipid component of eukaryotes, and secondly the preservation of an "alternate-carbon" enrichment making subsequent study by ^{13}C nmr simpler than it would have been if direct ^{13}C-^{13}C spin coupling existed.

In the subject of protein denaturation, ^{13}C T_1 values are reported as a function of concentration of a protein denaturant in the presence and absence of a fixed protein concentration. No direct evidence is available for strong "ligand-type" protein-denaturant association. Weaker interactions cannot, however, be equally ruled out. More interestingly, Urea which is the denaturing agent in question is directly implicated in substantial associations with water via hydrogen bond formation. An increase in "lattice" disorder or "structural temperature" of the water is invoked to explain the "solubilization" of the protein. The possible role of different intermediates of denatured protein conformers is discussed.

TABLE OF CONTENTS

	Page
Acknowledgements	(i)
Summary	(ii)
Table of Contents	(iii)
List of Tables	(vi)
List of Figures	(vii)
Plates	(ix)
Chapter 1 INTRODUCTION	1
A. Biomembranes	1
B. Membrane models	2
C. Application of n.m.r. in membrane studies	4
D. Factors influencing the n.m.r. spectra of membranes	6
E. Application of spin-lattice relaxation time to membranes	9
F. Models for molecular motions in membrane bilayer	10
G. Mixed lipid models	12
Chapter 2 Materials and methods	15
A. Materials	15
B. Methods	16
(i) Growth of E. coli CY2	16
(ii) Mono-axenic growth of T. Pyriformis	17
(iii) Extraction of lipid material	18
(iv) Purification of lipids by column chromatography	18
(v) Thin-layer chromatography	19
(vi) Molecular sieve chromatography	20
(vii) Lipid determination	21
(viii) Preparation of fatty acid methyl esters	22
(ix) Determination of fatty acid	22
(x) N.m.r. sample preparation: non-polar solutions	23
(xi) N.m.r. sample preparation: aqueous dispersions	23
(xii) Spectrometer operation	24

Page

Chapter 3 ^{13}C biosynthetic enrichment of the fatty acyl residues of phosphatidyl ethanolamine 26

A. Introduction 27

B. Lesions in strain CY2 28

C. Incorporation of added acetate 29

D. Factors influencing yield of ^{13}C in fatty acids 31

E. Determination of specific enrichment in the phosphatidyl fraction of the lipid extract 32

F. Phospholipids of E. coli (evidence for differences in enrichments 34

Chapter 4 N.m.r. studies of phosphatidyl ethanolamine - phosphatidyl serine 36

A. Introduction 37

B. Vesicle size characterization 40

C. Lipid distribution in vesicles 43

D. Quality of ^{13}C spectra 45

(i) spectra in organic solvents 45

(ii) spectra of aqueous dispersions 47

E. ^{13}C n.m.r. of mixed lipid vesicles 50

F. ^{13}C spin-lattice relaxation times 53

(i) ^{13}C spin-lattice relaxation mechanism 53

(ii) ^{13}C T_1 of lipids in non-polar solutions 57

(iii) ^{13}C T_1 of aqueous dispersions of PE/PS systems (temperature function) 59

Chapter 5 ^{13}C biosynthetic enrichment of the fatty acyl residues of phosphatidyl choline 66

A. Introduction 66

B. Results 67

C. Discussion: Evidence for chain elongation 70

D. Biological implications 78

Page

Chapter 6 N.m.r. studies of protein denaturation 80

A. Introduction 80

B. Nuclear Overhauser enhancements 82

C. ^{13}C spin-lattice relaxation studies 83

D. Discussion 83

Glossary of terms and abbreviations 91

Bibliography 92

LIST OF TABLES

Table		After page
1	Criteria for distinguishing peripheral and integral membrane proteins	2
2	Efficiency of incorporation of label into fatty acids of E. coli	29
3	^{13}C chemical shifts of E. coli lipids	35
4	^{13}C enrichment of each carbon of extracted E. coli lipid	35
5	Results from molecular sieving	40
6	^{13}C chemical shifts of PE/PS dispersions	50
7	^{13}C T_1 data of lipids in non-polar solvents	57
8 (a-b)	^{13}C T_1 data of PE/PS aqueous dispersions	60
9	Activation energy of relaxation processes	63
10	Energies of relaxation processes of methylenes in synthetic polymers	64
11	Incorporation of label from E. coli into T. pyriformis	68
12	^{13}C chemical shifts of T. pyriformis lipids	72
13	^{13}C enrichment of each carbon of extracted T pyriformis lipid	73
14	Signal-to-noise ratios from double resonance experiments	82
15	^{13}C T_1 of aqueous urea solutions in the presence and absence of bovine serum albumin	83

LIST OF FIGURES

Figure		After page
1	Possible lipid-protein assocations in membrane	2
2	Effect of cholesterol on proton spectrum of sphingomyelin	3
3	Proton and ^{13}C demonstration of Chapman transition	4
4	Dependence of molal volume on vesicle radius	7
5	^{13}C n.m.r. spectrum of some naturally occurring membranes	7
6	Possible molecular reorientations in the bilayer	12
7	TCA cycle showing lesions in E. coli CY2	28
8	Amount label in lipids, amount remaining after growth and fatty acid concentration, all as a function of added acetate	29
9	Incorporated acetate μg/ml vs added acetate	30
10	Growth curve of E. coli CY2	31
11	^{13}C spectrum of fatty acid methyl esters of enriched and natural abundance lipids	32
12	Proton n.m.r. of $-OCH_3$ resonance of F.A. methyl-esters	33
13	Molecular radius vs $\text{erfc}^{-1}\sigma$	40
14	Elution profile of PE/PS on sepharose 4B	40
15	^{31}P n.m.r. spectrum of PE/PS	45
16a	^{13}C n.m.r. spectrum of E. coli PE	46
16b	^{13}C n.m.r. spectrum of egg yolk PE	46
17	^{13}C n.m.r. spectrum of PE/PS	46
18	^{13}C n.m.r. spectrum of cardiolipin	46
19	Carbon numbering system used	46
20	^{13}C n.m.r. spectrum of PE/PS dispersions	49
21	^{13}C n.m.r. spectrum of E.Y.L.	49
22	^{13}C n.m.r. spectrum of PE/PS (temperature dependence)	50

Figure		After page
23	^{13}C n.m.r. spectrum of PE/DPL (temperature dependence)	50
24a	^{13}C T_1 vs carbon number for lipids in non-polar solvents	57
24b	^{13}C PRFT of PE in chloroform	57
25(a-f)	^{13}C PRFT of PE/PS aqueous dispersions	60
26(a-b)	^{13}C T_1 of PE/PS dispersions as temperature function	61
26(c-d)	^{13}C T_1^{-1} of PE/PS dispersions as temperature function	61
27	^{13}C T_1 of PE/PS vs carbon number	62
28	Figure 27 continued	62
29	^{13}C NT_1 vs carbon number	63
30	Activation energy versus carbon number	64
31	^{13}C n.m.r. spectrum of chloroform extract from T. pyriformis	68
32a	^{13}C n.m.r. spectrum of PE from T. pyriformis	68
32b	^{13}C n.m.r. spectrum of PC from T. Pyriformis	68
33	Mass spectrum of methyl myristate and methyl palmitate from fatty acids of T. pyriformis	69
34	^{13}C n.m.r. spectra of PE from both T. pyriformis and E. coli compared	73
35	Comparison of palmitoleic acid, γ-linolenic acid residues	74
36	Proton spectrum of urea solution	81
37	^{13}C n.m.r. partially decoupled spectra of urea solutions	82
38a	^{13}C T_1 as a function of urea concentration	83
38b	^{13}C T_1^{-1} as a function of urea concentration	83
39(a-f)	Some ^{13}C PRFT of urea solutions	83
40	Schematic representation of diverse species in water structure	85

PLATES

Plate		After page
1	TLC of PC, PS, PE, DPG mixture	19
2	TLC of neutral lipid fraction of *T pyriformis* chloroform extract	68
3	TLC of polar lipid fraction of *T pyriformis* chloroform extract	68

CHAPTER I

INTRODUCTION

A. Biomembranes.

It is not an easy task to evolve a definition for the biological membrane based on structure and/or function, that will have any meaningful general application. This is so for the simple reason that considerable variability in structure and function may be found from one membrane type to another. The two major biomembrane constituents, i.e. protein and lipids, are found in the respective ratios of 20% and 80% in myelin and 49% and 44% in erythrocyte membrane: the myelin envelope of nerve fibres is functionally distinct as an electrical insulator as contrasted with the "permeability-barrier" role of red blood cells or the energy-linked oxidative phosphorylation in the membranes of the inner mitochondrion. It is not surprising therefore that descriptions such as "The surrounding envelope of cells and cell organelles " are still frequently found in the literature when a genral reference to membranes is intended.

The arrangement, or more specifically, nature of the association between the proteins and lipids may be a critical factor in determining the functionality of membranes. Unfortunately, little is known about the detailed structures of the membrane related proteins and there are still differences of opinion on the validity of crucial issues such as the distinction between integral and peripheral proteins (Singer and Nicolson, 1972). Some of the possible ways in which membrane lipids and proteins may interact include hydrophobic, electrostatic, dispersion, polarisation and covalent interactions. One may expect that for a completely integral protein in the membrane lipid matrix, hydrophobic and dispersion forces may play a more important role in determining the nature of the association

with lipids, whereas for a purely peripheral protein, polar interactions should be more important. It is in this kind of comparison that the problem of distinguishing between the integral and peripheral proteins resides. Because it is not whether a particular protein interacts with the lipid matrix almost exclusively by one kind of force but to what extent all the possible modes of interaction are participating: in other words, how deep into the lipid matrix must a peripheral protein penetrate before it can be classified as an integral protein. Figure 1 is an illustration of the "border line" problem in classifying membrane proteins as either integral or peripheral. Caution is necessary in applying the criteria (cf Table 1) for distinguishing between these classes of membrane proteins as it has been shown that depending on the severity of the treatment used for interaction, certain integral proteins may deceptively behave like peripheral proteins (Burger et al., 1968).

B. Membrane Models

Robertson (1960) postulated a universal unit membrane theory embracing the Danielli-Davson (1935) bimolecular leaflet lipid model and projected it to all cell and cell organelle membranes. Today perhaps the majority opinion of researchers in the field is that functional membranes are a kind of two-dimensional "solution" of globular integral proteins dispersed in a fluid lipid matrix (Singer, 1972). Furthermore, there is support for the so-called "separate molecular biology approach" to membrane research, whereby the structure and properties of the membrane lipids or proteins are considered separately, hoping ultimately to decide how these these two components might affect each other on being brought together in the membrane. Given the numerous reports on model membranes and the more recent ones at membrane reconstitution, it is quite likely that this approach has been followed either deliberately or accidentally.

Fig.1 Possible lipid-protein associations in membrane (b) completely peripheral (d) completely integral.

(a) cross-section of a total traversal of bilayer by protein .

In reality (c) may be most reasonable.

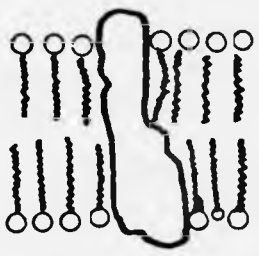

outside

a

inside

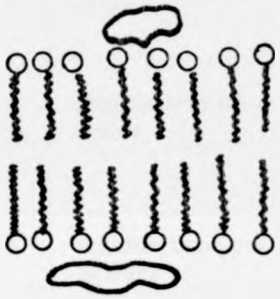

outside

b

inside

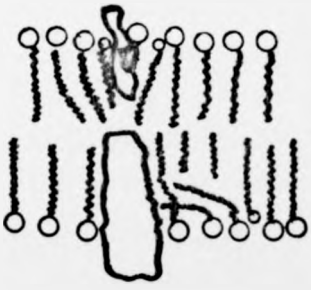

outside

c

inside

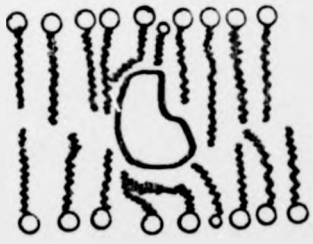

outside

d

inside

Table 1: Criteria for distinguishing peripheral and integral membrane proteins.

Property	Peripheral protein	Integral protein
1) Requirements for extraction from membrane	Mild treatment, e.g. increase in ionic strength	Strong solubilizing agents, e.g. detergents chaotropic agents.
2) Nature of lipid association when solubilized	Soluble free of lipids	Strongly associated with lipids when solubilized
3) Interaction with water	Soluble in aqueous buffers	Usually aquaphobic with regard to neutral buffers

The first experimental evidence for membrane fluidity was provided by Chapman and others (Chapman et al., 1966) using a variety of physical techniques including differential thermal analysis, X-ray diffraction and nuclear magnetic resonance spectroscopy (n.m.r.) Since then, it has been possible to demonstrate a relationship between the temperature (Tc) at which the order⇿disorder (crystal⇿liquid - crystal or Chapman) transition occurs and certain properties of the lipid matrix such as the degree of saturation of the fatty acyl residues, the length of the chains and the nature of the head group (Chapman, 1968). Furthermore, these transitions have been shown to occur in some naturally occurring membranes (Steim et al., 1969; Overath et al., 1970; Wilson and Fox, 1971; Blazyk and Steim, 1972).

The transitions observed in the natural membranes are generally broader and less defined than those in the single lipid systems. It is thought that this is merely the result of overlap of different transition temperatures from the multi-species in these membranes, although it has been suggested (Chapman, 1973) that cholesterol may act as a "fluidizing" agent of membrane lipids. This conclusion was reached from observations that in (1:1) cholesterol-lipid mixtures, the proton n.m.r. linewidths observed showed a remarkable lack of temperature dependence after an initial broadening and as compared to the case with no cholesterol present, cf Figure 2.

Among the techniques of investigation mentioned above, other physical studies in this sphere of research have included viscosity measurements (Zimmer and Schirmer, 1974), spectro-fluorimetric techniques (Trau ble and Overath, 1973; Sims et al., 1974) and electron microscopy (Nozawa et al., 1975). As judged by the quality of information obtainable, the technique of n.m.r. is undoubtedly the most powerful of the physical approaches that have been applied to membrane studies so far.

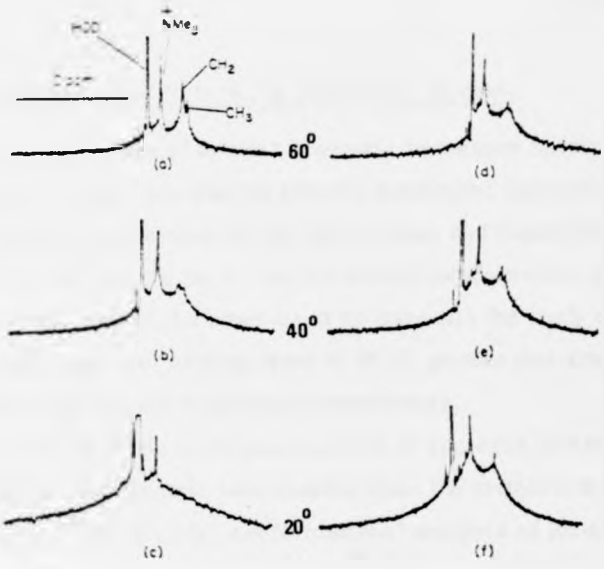

Fig. 2 Effect of cholesterol on the temperature variation of the 220 MHz ^1H n.m.r. spectrum of sphingomyelin.

(a,b,c) sphingomyelin 20% w/v dispersion in D_2O.

(d,e,f,) sphingomyelin-cholesterol (1 :1), 20% w/v dispersions in D_2O.

C. Application of N.M.R. in Membrane Studies.

The application of nuclear magnetic resonance spectroscopy to membrane studies may be broadly subdivided into two parts: on the one hand we have (i) the observation and experimentation with the "intrinsic n.m.r." or the actual component(s) of the membrane, and on the other hand we have (ii) the study of the "extrinsic signals" arising from N.M.R. probes that are not normally part of the membrane constituents.

(i) This is the more general kind of approach, and both structural and dynamic information about the membrane can be obtained. Specifically, conformational analysis of lecithins in vesicles has been deduced with ^{13}C n.m.r. (Batchelor and Prestegard, 1972); also, the demonstration of the Chapman transition in lecithins, using both ^{1}H and ^{13}C, (Figure 3). Similar transitions have also been picked up with the aid of ^{13}C n.m.r. in membranes of Acholeplasma laidlawii (Metcalfe et al., 1972). ^{31}P n.m.r. has also been successfully used to demonstrate this transition. An interesting contribution in this field is the demonstration by Bergelson and others that resonances from the "inside" and "outside" monolayers of a bilayer can be separately observed if appropriate shift reagents are employed. Such shifts have been reported for the resonances of all three nuclei (^{1}H, ^{13}C, ^{31}P) in model membranes (Bystrov et al., 1975). Considerable light has been thrown on the dynamics of membrane and membrane associated phenomena by the direct measurement of spin-lattice relaxation times (Metcalfe et al., 1971a; Lee et al., 1972; Birdsall et al., 1971).

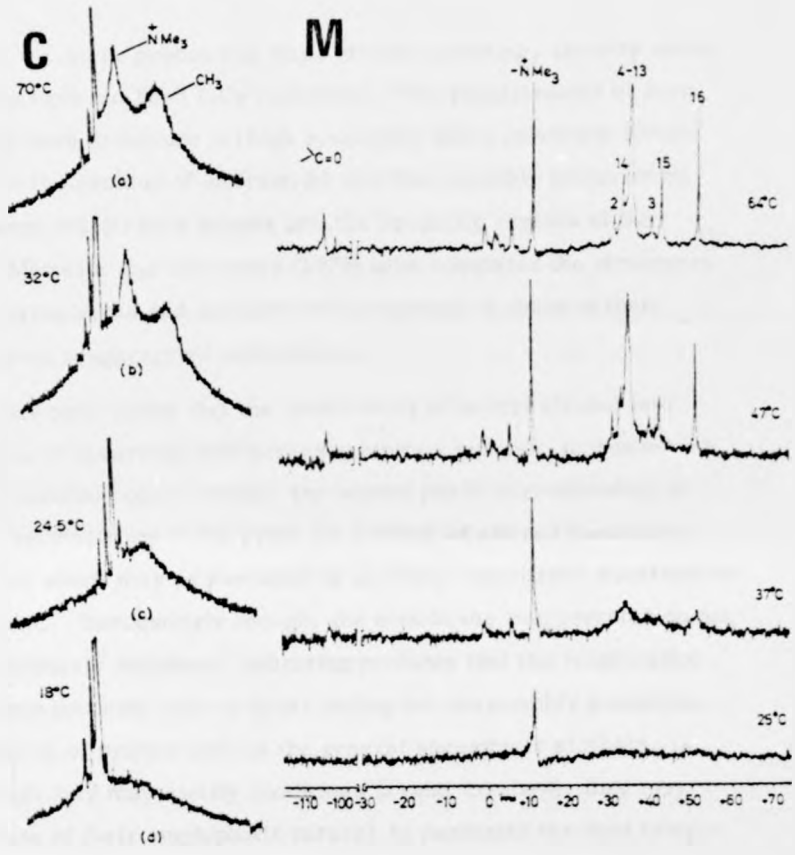

Fig.3 High resolution of ^{1}H and ^{13}C n.m.r. of phospholipids as a function of temperature.

(C) data of Chapman et al. (Chapman, 1973) showing 220 MHz ^{1}H n.m.r. of dimyristoyl dispersions in D_2O.

(M) data of Metcalfe et al. (Levine et al, 1972a) showing ^{13}C n.m.r. of sonicated dipalmitoyl lecithin in D_2O buffer.

(ii) n.m.r. probes that will, strictly speaking, classify under this heading have not been fully developed. The requirements of such probes may have to include (a) high sensitivity and a relatively simple spectrum of the nucleus of interest, (b) smallest possible perturbation of the system and (c) easy access into the lipophilic regions of the bilayer. Metcalfe and coworkers (1971b) have compared the structures of native mycoplasma and erythrocyte membranes to those of their corresponding reaggregated membranes.

It has been shown that the partitioning of benzyl alcohol into these naturally occurring membranes exhibits a biphasic response with increasing alcohol concentration; the second phase corresponding to increased permeability to the probe as a result of altered membrane architecture which may be preceded by an initial membrane stabilization against lysis. Interestingly enough, the membrane reaggregates do not show this biphasic response, indicating probably that the renaturation of membrane proteins fails to occur during the reassembly processes. The limitation of probes such as the general anaesthetic alcohols, is that although they may satisfy conditions (a) and (b) above, they may fail (because of their amphiphatic nature) to penetrate the lipid bilayer to any reasonable extent, so that only information about events in the interfacial boundary is obtained. It has been reported (Colley and Metcalfe, 1972) that there is an up-field shift associated with the choline headgroup resonance in vesicles of DPL with increasing concentration of benzyl alcohol. Furthermore, only aromatic alcohols produce this shift which decreases as the number of methylene groups between the aromatic ring and the hydroxyl function increases. This is good evidence that it is the aromatic ring current which induces the shift and can only mean that for a molecule like benzyl alcohol, most of the probe penetrate only to the extent of the lipid-water boundary. Thus, although these amphiphatic probes may have a physiological relevance,

their ability to monitor deep-seated membrane events is limited. Unsuccessful attempts in our laboratory to develop an n.m.r. "lipophilic region probe", that can be introduced into natural membranes without disrupting the membranes by sonication or detergent solubilization are briefly mentioned in the general conclusion.

The distinction between the "intrinsic" and "extrinsic" n.m.r. applications mentioned above is not to be regarded as a rigid one. On the contrary, it has been arbitrarily chosen to facilitate a brief and collective review of some of the reported applications. Indeed, many investigations embody both approaches simultaneously. Godici and Landsberger (1974) have reported ^{13}C relaxation times of egg yolk lecithin modified with stearic acid spin-labels.

D. Factors influencing the n.m.r. spectra of membranes

Unsonicated aqueous egg yolk lecithin dispersions contain particles with diameter ranging from $\sim 0.5 - 2\ \mu m$ and consisting of concentrically arranged lamellae of lipid bilayers separated by layers of water (Bangham and Horne, 1964; Chapman et al., 1968). Lack of resolution of the peaks due to possibly a combination of overlap of resonances and the general macromolecular aggregate nature of the particles makes these systems unsuitable for conventional n.m.r. studies. One of the reasons thought to account for these observed line broadenings is incomplete averaging of dipole-dipole interactions as a result of slow molecular motion (Veksli et al., 1969). Another alternative reason could be that of magnetic field inhomogeneities as suggested by the reportedly observed dependence of the transverse relaxation time (T_2) and the spectral width on the applied magnetic field (Hansen and Lawson, 1970; Penkett et al., 1968).

Exposure of these particles to ultrasonic irradiation causes a reduction in particle size and weight (Chapman et al., 1968a; Attwood and Saunders, 1965; Huang, 1969). The resulting particles have an average diameter of about 230Å and weigh between (2-4.5) x 10^6 daltons. These particles are small enough to yield high resolution ^1H n.m.r. although only three groups of resonances, corresponding to the head group methyls, the terminal methyl of the fatty acyl chain and an envelope for all the methylene protons are still resolved in the case of lecithins. The mechanism by which a high resolution spectrum is obtained after sonication is still far from being conclusively resolved. The most obvious mechanism for this narrowing of spectral lines is the rotational Brownian motion of the vesicles in the aqueous medium as argued by Finer (1974). Other workers (Sheetz and Chan, 1972) have argued that the correlation time associated with vesicle tumbling is much too long to account for the sharpness of the observed lines. This has encouraged Chan and collaborators (Seiter and Chan, 1973) to propose that there is considerably more structural disorder associated with the fluid state of the lipids in the bilayers of the smaller vesicles than in the multi-lamellae systems. It is thought that this is a direct consequence of the increased area available to each lipid molecule as the surface curvature of the vesicle increases, i.e.as radius of curvature decreases (Figure 4).

In a sense, the ^{13}C n.m.r. spectra of lipids in both sonicated and unsonicated aqueous dispersions exhibit similar phenomena in that the spectra from the smaller particles show greater line narrowing. However, the spectral resolution is a considerable order of magnitude better than in the corresponding cases of ^1H n.m.r. The spectra of some naturally occurring membranes are shown in Figure 5 and compared with the proton spectra in Figure 3, the resolution can be seen to be quite impressive. This spectral resolution is in part due

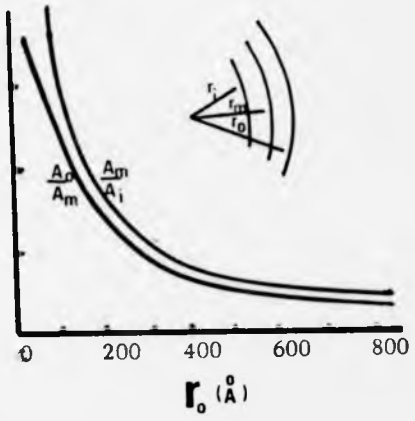

Fig. 4. Variation of ratio of charged head group to acyl chain with radius of vesicle. Data of Sheetz and Chan (1972).

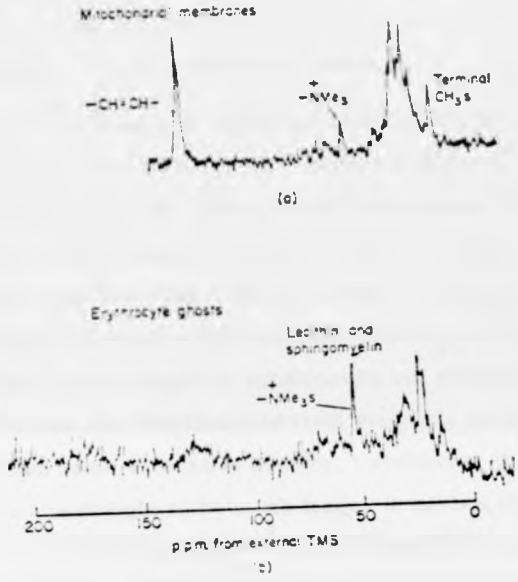

Fig. 5 ^{13}C n.m.r. spectrum on some naturally occuring membranes

Data of Keough et al.; Taken from Chapman (1973).

to the wider chemical shift range of the ^{13}C nucleus ~ 200 ppm as compared with only 10 ppm for protons and also the lower magnetogyric ratio of the ^{13}C nucleus ~ 1/4 that for the proton.

The theory of ^{13}C chemical shifts has been dealt with elsewhere (Cheney and Grant, 1967; Ramsey, 1950). Suffice it to say here, that the ^{13}C chemical shifts resemble those obtained for protons; downfield shifts being caused by electronegative substituents (~ 9 ppm for methyl and 48 ppm for hydroxyl) and by increasing s character of hybridisation (100 ppm for - HC = CH - relative to $-CH_2$). The inductive shifts due to electronegative substituents are expected to fall off rapidly with distance and contributions from magnetic anisotropy are expected to be the same size as in protons. However, linear electric field shifts are thought to be much larger in carbon than for protons. Another important factor in ^{13}C shifts may be the steric shifts and especially the steric shift which is thought to arise when two methyl groups, separated by three bonds (the centre bond being in a gauche conformation) interact. A third factor of importance influencing ^{13}C shifts may be the solvent dispersion shifts thought to arise from fluctuating molecular dipoles. It has been shown, however, (Batchelor et al., 1972), that for lipid work, only the steric shift need be considered seriously as the bulk of the carbon nuclei "buried" in the methylene envelope of the lipophilic interior of the bilayer are effectively removed from charge effects. The steric shifts, because of their additive nature, are thought to be useful in predicting the number of gauche -trans rotational isomers present in a molecule.

D. Application of Spin-Lattice Relaxation Time (T_1) to Membranes

(i) Definition :

Standard textbook definitions (Farrar and Becker, 1971; Levy and Nelson, 1972) show that T_1 characterizes the average time that a nucleus can remain in any one of two or more energy levels available to it, after the removal of the source of perturbation.

At equilibrium, nuclei are not equally distributed in all the available energy levels, but obey a Boltzmann distribution pattern as in equation (1):

$$N_u = N_l \, e^{-\Delta E/KT} \qquad \text{(1)}$$

where N_l and N_u are the nuclei populations in the lower and upper energy levels respectively, ΔE is the energy separation between the two energy levels, K is the Boltzmann constant and T is the absolute temperature. The absorption of radiofrequency energy, for example, will lead to a distortion of this ratio and subsequently the spins will tend to return to equilibrium in a time T_1 depending on the efficiency of energy exchange with their environment: - hence the term spin-lattice relaxation. T_1 values may vary over a wide range, $\sim 10^{-4}$ - 10^{4} secs. For a small diamagnetic molecule typical values are of the order of 10^{-1} - 10 secs although a value of ~ 33s has been recorded for a 2M degassed aqueous urea solution at $30^{\circ}C$ (see Chapter 6).

(ii) The application of ^1H T_1 to membranes has largely met with obstacles deriving partly from the familiarly low resolution of the p.m.r. spectra of vesicles, especially the unsonicated ones, and also possibly from a fairly strong diffusion influenced relaxation mechanism.

The differences of opinion on reported ^1H T_1's in the literature (Chan et al, 1971; Barrat, 1970; Lee et al., 1972) have highlighted the disagreement on the issue of the dominant relaxation mechanism. On the one hand, the first two reports, because they suggest a common relaxation time for all the protons in the bilayer, imply that spin-diffusion is the dominant relaxation process in these systems. In the third report, the authors have interpreted their results to mean that a heterogenous distribution of ^1H T_1's in the bilayer is characteristic of the type of structure to be expected, and that spin-diffusion is not the dominant relaxation process. This observation was made on a sonicated model. It is questionable whether their conclusion is equally applicable to the unsonicated model to which the former authors appear to have restricted their interpretation.

(iii) ^{13}C T_1 measurements in similarly sonicated vesicles clearly indicate a gradation in molecular motion along the hydrocarbon chain. The increases in molecular motion are thought to be from the glycerol backbone towards both the terminal methyls of the chains and the choline head group in the case of lecithin bilayers, (Levine et al., 1972a). The problems mentioned above with the proton T_1 values are not nearly always as present in the relaxation processes of the ^{13}C nucleus in these systems. For example, because of the low natural abundance of the ^{13}C nucleus, $\sim 1.1\%$, spin-diffusion cannot be a dominant relaxation process for this nucleus.

F. Models for Molecular Motions in Membrane Bilayer.

Isotropic motion is one which is unrestricted in space with respect to the principal axes. It can be characterised by a single correlation time (τ_c).

which can be roughly defined as the time required to execute one turn. An anisotropic motion occurs when a body is still tumbling freely but has different rates of reorientation about different principal axes: In the limit, the body is no longer tumbling perfectly freely in space and the motion may be referred to as "restricted" motion. In a phospholipid dispersion, the tumbling of the spherical vesicle is clearly isotropic The motions of the lipid molecules in the bilayer surrounding the vesicle may however, be restricted to varying degrees. The ^{1}H n.m.r. linewidths of an oriented bilayer sample have been shown to depend on the angle of the lipid chains to the applied magnetic field : the so called phospholipid "magic angle" (Finer et al., 1972; De Vries and Berendsen, 1969) suggesting that certain segments of the chains in the bilayer may be more motionally hindered. The Seiter-Chan (1973) treatment has tended to favour a model of motion in which chain protons undergo rapid motion around the chain axis while performing restricted off-axis flexing motions. These rocking motions are thought to be restricted to angles about 60-70^{o} from the long axis of the molecules. It is the lack of rotation about all possible angles that is thought to prevent narrowing of the spectral lines to the degree observed in lipids. Gauche^{+}-Gauche^{-} rotations or kink formation is invoked to explain this segmented motion. Furthermore, it is thought that this model fits the "solid-like order" packing characteristic of unsonicated bilayers in the gel phase. If the reported abrupt viscosity decrease (Zimmer and Schirmer, 1974) and a parallel volume increase (Trauble and Hayes, 1971) thought to be associated with the Chapman transition in lipid bilayers, are assumed to reflect similar changes in the immediate micro-environment of the lipid molecules, then it is obvious that a similar increase of molecular motions within this "ordered" framework will accompany the crystalline→liquid-crystalline transition. We would expect to observe an enhanced spectral resolution above the phase transition temperature.

Translational motion or lateral diffusion along the bilayer is thought to be more important for intermolecular relaxation processes and would therefore affect ^{1}H T_1 values more than ^{13}C T_1 times. Translational diffusion may yet be one of the most underestimated elements of membrane phenomena. Saffman and Delbruck (1975) have recently showed that as a consequence of the anisotropic environment in the bilayer, translational diffusion may be up to four times faster in relation to rotational diffusion than in an isotropic system. Other modes of motion in the bilayer may occur but are probably of less significance than those described above. Precession about the long axis of the chain, for example (Figure 6) may arise from a combination of the strong charged-group interactions at the bilayer surface and the tendency of the whole molecule to rotate about its long axis. Transverse diffusion or the so called "flip-flop" of phospholipids usually invoked to explain the redistribution of charged lipids between the two halves of the bilayer in an excitable membrane (McLaughlin and Harary, 1974) may proceed at very slow rates (Kornberg and McConnell, 1971), as to have no major physiological consequence. Indeed, the existence of stable asymmetrical distributions of proteins and lipids across a membrane bilayer implies that these components do not rotate from one surface of the membrane to the other at significant rates. It has been suggested also that the passage through the hydrophobic membrane interior of the polar head groups and ionic residues of lipids and proteins is thermodynamically a highly unfavourable process (Singer and Nicholson, 1972).

G. Mixed Lipid Models.

The single lipid models that have been used so extensively have contributed a significant amount to our knowledge of membrane processes.

a

b

c

d

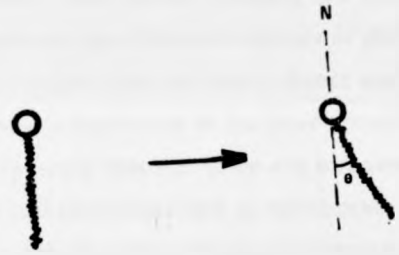

e

Fig. 6 Possible molecular re-orientations in the bilayer
(a) rotation about lipid long-axis
(b) translational diffusion
(c) transverse diffusion
(d) isomerization of rotamers
(e) precession about long axis

t = time for one event , θ = angle of precession , N = normal to bilayer surface.

The Chapman transition, as discussed previously and undoubtedly one of the major contributions to the field, was first demonstrated in one of these systems and has subsequently been shown to occur in natural membranes. However, some of the equally important membrane phenomena could not have been understood if we stuck to these simple models. The relatively low cooperativity at the transition temperature resulting in broader transitions in natural membranes was inferred from investigations on lecithin-cholesterol mixtures (Oldfield and Chapman, 1971). The interesting phenomenon of membrane asymmetry at the molecular level has no meaning in a single lipid species model. Phase segregation into different classes of phospholipids either across or along the bilayer may not have a direct equivalent in a one lipid system. The consequences of the later phenomenon in natural membranes might be very grave indeed: if we are to assume that lipids fulfil both a structural and functional role in membranes, then lipid asymmetry could lead to considerable "functional discontinuities" in the membrane.

It will probably be many years yet before we understand the precise role of each class of phospholipids found in biological membranes. Usually, it is assumed that the different phospholipids all fulfil some kind of structural role, but this need not be so. The number of enzymes showing various degrees of phospholipid dependence for activity is growing. A recent review (Coleman, 1973) listed some 26 enzymes that fulfil the two criteria for lipid dependence, viz-a-viz, loss of activity following removal of lipid and reactivation on adding lipid to the inactive enzymes. A scheme, recently published by Goldman and Albers (1973) implicates different phospholipids in possible roles in the $(Na^+ - K^+)$-ATPase activity of membranes :

$$E_1 + ATP \overset{Na^+}{\underset{Mg^{2+}}{\rightleftharpoons}} E_1P + ADP \quad \text{(phosphatidyl serine)}$$

$$E_1P \overset{Mg^{2+}}{\rightleftharpoons} E_2P \quad \text{(phosphatidyl ethanolamine phosphatidyl choline?)}$$

$$E_2P + H_2O \overset{K^+}{\rightarrow} E_2^+P_i \quad \text{(phosphatidyl serine)}$$

$$E_2 \overset{Mg^{2+}}{\rightarrow} E_1 \quad \text{(phosphatidyl ethanolamine)}$$

In conclusion, because of the need to extrapolate meaningfully the results from the model and infer membrane behaviour, it is desirable that the model simulate conditions in the membrane as closely as possible. The mixed lipid bilayer is a more relevant system than the single lipid species model.

CHAPTER 2

MATERIALS AND METHODS

A. Materials.

Egg yolk phosphatidyl choline, egg yolk ethanolamine and the monosodium salt of ox-brain phosphatidyl serine, all at the Grade I purity level, were obtained from Lipid Products, (South Nuthfield, Nr. Redhill, Surrey). Thin layer chromatography of these lipids (see methods) gave single spots and they were subsequently used without further purification. Synthetic dipalmitoyl lecithin (DPL) was purchased from Koch-Light Laboratories Ltd. Sodium [1-^{13}C-] acetate and urea ^{13}C at the 98 and 92 atom % enrichment levels respectively were purchased from Prochem, The British Oxygen Company Ltd., (Deer Park Road, London, SW19 3UF). Sodium [1-^{14}C-] acetate was obtained from the Radiochemicals Laboratories, Amersham. Bovine serum albumin (Fraction V) with an albumin content of 97% was purchased from Sigma Chemical Co., (U.S.A.).

Sepharose 4B, MN silica gel and Florisil (60-100 mesh) were obtained from (Pharmacia, Uppsala), Macherey, Nagel and Co., Düren, Germany), and (Floridin Co., Chadwell Heath, Essex) respectively. All solvents for chromatography were A.R. grade, and were freshly redistilled in an all glass distillation set-up before use. Column dimensions were (2.0 x 40 cm) and (2.5 x 40 cm) for silica gel and analytical sieve chromatography respectively. Preparative TLC plates were 20 x 20 cm.

All nuclear magnetic resonance (nmr) spectra were obtained on a Bruker WH90 with built-in Fourier transform facilities controlled by a fast analogue-to-digital converter (ADC) computer based on the Bruker data system B-NC 12. Changeable probe facilities were available and the operating frequencies for the nuclei observed were

90.02, 36.43 and 22.63 MHz for ^{1}H, ^{31}P and ^{13}C respectively. A data storage disk system (Diablo data systems) was also available. A variable temperature unit ($-150^{o}t^{o} + 200^{o}C$) was also part of the accessories. Deuteriated solvents; $CDCl_3$, CD_3OD each at 99.8 atom % isotope abundance were obtained from Aldrich Chemical Co. Inc. (Milwaukee, Wisconsin, U.S.A.) and D_2O at 99.8 atom % was obtained from Fluorochem Ltd. (Derbyshire).

Escherichia coli K12 (aceF, gltA) designated as strain CY2 was provided by Professor J.E. Cronan Jr. of the Department of Molecular Biophysics and Biochemistry, Yale University, New Haven, Connecticut 06510, U.S.A. Tetrahymena pyriformis strain W was provided by Mr. Robert Hanks of this department.

B. Methods.

(i) Growth of E. coli CY2.

Strain CY2 was usually grown in 15 litre carboys containing 10 l culture medium, with vigorous aeration at $30^{o}C$. The growth medium consisted of medium E (Vogel and Bonner, 1956,) available at 50 x strength as a stock solution. The medium was supplemented with 0.4% glucose, 0.04% sodium L-glutamate, 10 mgs/litre each of L-leucine, L-isoleucine and L-valine; 0.01% thiamine, 35 mgs/litre sodium [1-90% ^{13}C] acetate and 0.1% casein hydrolysate. For the purposes of quantitation, especially during the extraction and purification of lipids, a trace amount of sodium [1-^{14}C] acetate was usually added to these large cultures. For the 10 ml cultures, however, sufficient hot acetate to produce counts of the order of 10^{4}/min/ml was used to dilute cold acetate before growth. Growth was usually initiated by innoculation with a small amount of organisms from a pure culture. In the case of the 10 ml cultures, a wire loop-full from a solid agar streak in a petri dish was enough, but for the 10 l cultures up to 100 ml of

stationary phase liquid cultures were required to avoid unduly prolonged lag phases.

(ii) Mono-axenic growth of Tetrahymena Pyriformis.

10 litres of a late log phase E. coli strain CY2 culture were harvested by centrifugation at 7,500 g. Aseptic conditions were maintained during centrifugation by ensuring that the centrifuge bottles had been previously sterilized by autoclaving. The transfer of culture medium from the large 10 l carboys was either achieved with the aid of previously autoclaved siphon tubes attached to an evacuation pump with air-filters at the appropriate junctions or alternatively the contents of the pots were poured out in a sterile cabinet attached with a micro-mesh air screen. In this way, the E. coli cells were collected and washed in sterile distilled water three successive times before being finally suspended in another 10 l flask containing sterile distilled water. 100 ml of Tetrahymena pyriformis strain W, that had been previously cultured axenically as described by Nozawa and Thompson (1971) were similarly washed and resuspended in 100 ml of water. To avoid lysis of the tetrahymena cells, centrifugation was carried out at much reduced speeds ~ 2,000 g and, before transfer into the E. coli medium, phase contrast microscopy was used to check that the cells were still intact. The 100 ml of Tetrahymena pyriformis suspension was then used to innoculate the 10 l E. coli suspension and the carboy set up on the fermentor. Air was passed in through the sterile air filters as in the growth of the E. coli except that the stirring rate of the fermentor was kept at much reduced speeds, (11 revs/min) owing to the discovery that the tetrahymena cells quickly broke open with vigorous stirring. The thermostat was adjusted to the 28°C mark and samples were regularly taken off for phase contrast microscope observation. After no E. coli was

visible, the culture was allowed to continue for another four hours so that the ingested bacteria could be fully digested before harvesting. This was usually characterized under phase microscopy by the decline and disappearance of normally abundant food vacuoles. The cells were then subsequently harvested by centrifugation at about 2,000 x g for 2 hours, and then extracted by the Bligh and Dyer (1959) method.

(iii) Extraction of lipid material.

The method of Bligh and Dyer (1959) employing a biphasic solvent system of chloroform, methanol and water was used. The cells were first spun down at about 7,000 g and the wet cell paste extracted directly after the determination of their water content. For small quantities, it was alright to use the approximation of 80% water content in tissues, but for the larger extracts, a proper dry weight determination via freeze-drying of a small aliquot of the cell suspension was performed.

(iv) Purification of lipids by column chromatography.

The complex lipid mixture was further purified into lipid classes by column chromatography on an acid-treated florisil adsorbent (Caroll et al. 1968). An all glass column with a teflon stop-cock (2 x 40 cm) was loaded with a slurry of the adsorbent in chloroform (30 g dry wt. of florisil). Bed height after equilibration was 30 cm. About 300 g of lipid material was introduced at the top of the column bed in 5 ml of chloroform, and elution with increasing ratios of methanol in chloroform carried out as outlined below. The eluent was continuously monitored by analytical thin-layer chromatography on silica gel adsorbent mounted on (2.5 x 7.5cm) microscope slides. For the non-polar lipids, the equilibrated tank contained petroleum ether (b.p.60-80°) - ethyl ether-acetic acid (90:10:1, v/v) and for the phosphatides, a solvent

system chloroform-methanol-water (65:25:4, v/v) was used. The spots were detected by a destructive non-specific method employing 40% H_2SO_4 and heat. Flow rate was maintained at 3 mls/min.

Fraction 1.

Chloroform: neutral lipids such as sterols, glycerides.

Fraction 2.

Chloroform-methanol (90:10, v/v): cerebrosides, phosphatidic acid and cardiolipin.

Fraction 3.

Chloroform-methanol (3:1, v/v)

+

Fraction 4.

Methanol

} Traces of cardiolipin plus phosphatidyl ethanolamine phosphatidyl glycerol.

Fractions 3 and 4, pooled together, were always found to contain $\gtrsim$ 88% of the starting material (w/w). The phospholipids were further purified by concentrating their respective fractions and chromatographying these on preparative thin-layer chromatography.

(v) Thin-layer chromatography.

For preparative thin-layer chromatography, the adsorbent was pre-washed with $CHCl_3$-MeOH (1:1) and dried in an oven at 110°C for 2 hours after an initial overnight air-drying in a dust-free cabinet. The layer thickness was arranged to be 0.75 mm using an automatic spreader. The solvent system used was chloroform-methanol-water (65:25:4). An initial trial experiment with a mixture of four commercial phospholipids (PC, PS, PE, DPG) showed that sufficient resolution of these lipids under the conditions of our laboratory was possible, (Plate 1). Up to 50 mgs of lipid material in a 10% chloroform w/v) solution was usually applied with an automatic streaker, about 2.5 - 3 cm from one end of the (20 x 20 cm) plates and, after evaporating the solvent off in a nitrogen atmosphere, (usually 0.5 min), the plate was developed in an ascending solvent

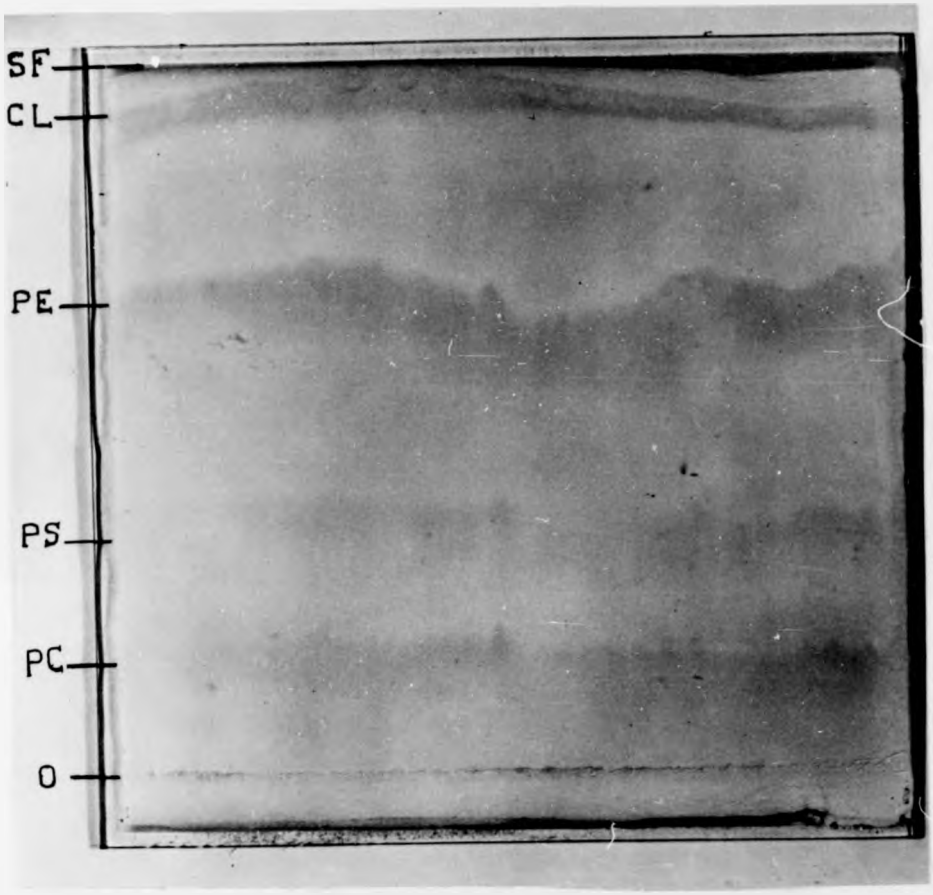

Plate 1

Preparative TLC of a phospholipid mixture on silica gel MN SF, Cl, PE, PS, PC & O stand for solvent front, cardiolipin, phosphatidyl ethanolamine, phosphatidyl serine, phosphatidyl choline and origin respectively. Spots were developed with a chloroform-methanol-water (65 : 25 : 4, v/v) mixture and viewed with 0.1% Rhodamine 6G.

flow in a pre-equilibrated tank. After elution, the area corresponding to the R_f of each lipid was scraped into a beaker and the lipids re-extracted with a chloroform methanol (2:1) mixture. The phospholipids were further shown by microslide TLC to be of the single spot-purity grade in two different solvent systems: chloroform-methanol-water (65:35:5, v/v) and chloroform-methanol-acetic acid-water (25:15:4:2, v/v).

In the separation of the lipids from Tetrahymena pyriformis, a solvent system comprising chloroform-acetic acid-methanol-water (75:25:5:2.2, v/v) was used for the development of the polar lipids and the neutral lipids were developed in a petroleum ether (b.p. 40-60°C)-diethylether-acetic acid (70:30:1, v/v) solvent system.

(vi) Molecular sieve chromatography: vesicle size determination.

A glass column (2.5 x 40 cm) fitted with a teflon tube at the drawn-out end was packed with sepharose 4B. The top of the column was connected to an eluant reservoir and the column left to run overnight to ensure close packing. A buffer (0.04M Tris-HCl pH 9.0) was used as the eluting solvent. After equilibration of the column, the top surface was protected with a plastic cup with a net in the bottom and fitting closely around the inside of the column. (Adsorbent bed height ~ 30 cm.) 8 ml of a 3% (w/v) dispersion of the mixed lipid system in the same buffer was sonicated until optical clarity and then introduced at the top of the bed with the aid of a drawn-out pasteur pipette. Elution of the column with buffer was commenced at a flow rate of 0.5 ml/min and 5 ml fractions were collected on an automatic fraction collector. The absorbance was read on a UV spectrophotmeter, (Beckman Model SP1800).

The void volume was determined as the elution volume of Dextran blue 2000 (Pharmacia, Uppsala, Sweden). The internal volume was determined from the elution volume of tritiated water (Radiochemical Centre, Amersham, Great Britain) and glycine. The two column constants a_o and b_o were determined from the elution profiles of γ-globulin and tomato bushy stunt virus (mean Stokes radius, 52 Å and 150 Å respectively.)

The absorbance was determined at 300 nm for the column effluent of lipid material. 280 nm was used for γ-globulin and 570 nm for glycine while the virus and Dextran blue were monitored at 260 nm. Tritiated water was determined by liquid scintillation (Packard Model).

(vii) Lipid determination.

All non-phosphorus containing lipids were determined directly by their dry-weight estimates. Usually, a small aliquot of the chloroform-methanol (2:1, v/v) solution was evaporated to dryness in a freeze drier, and the difference in the constant weights of the flask with and without lipid material regarded as the dry weight of the sample. Phospholipids were determined by both a similar dry-weight method and an inorganic phosphorus assay based on the modified procedure of Allen (Kates, 1972). Usually, an aliquot of the lipid sample containing up to 2.5 mg of phospholipid (estimated from the dry weight) was evaporated to dryness in a calibrated straight-walled 'pyrex' glass tube. The sample was digested with 2 ml of perchloric acid by heating over a gas burner until the colour disappeared completely. 10.5 ml of distilled water, 2 ml of Amidol solution and 1 ml of molybdate solution were each added to the cooled digest, with mixing, on a vortex mixer in that order. 25 minutes was then allowed for the molybdenum blue colour to develop, and then 9.5 ml of distilled water finally added

with mixing. The absorbance was read at 680 nm against a reagent blank and the phosphorus content estimated from a calibration curve determined under identical conditions, using 30 μg and 60 μg phosphorus standards. The phospholipid content was obtained by multiplying the amount of phosphorus present after digestion by 25, as the average phosphorus content of phospholipids is about 4%.

(viii) Preparation of fatty acid methyl esters.

50 mg of phosphlipid in chloroform-methanol (2:1 v/v) was taken into a 25 ml round-bottomed flask, and the solvent removed by vacuum over nitrogen. 5 ml of a 5% KOH solution in 50% aqueous methanol was added and the flask fitted to a reflux apparatus. The sample was heated under reflux for 1 hour. The aqueous phase was acidified with HCl and the fatty acids extracted with ether. The ether solution was then dried over anhydrous sodium sulphate before evaporation under nitrogen. The fatty acids were then taken up in 1 ml of light petroluem, 2 ml of acid methanol (1% v/v) and 3 ml of 2, 2-dimethoxypropane (Radin et al., 1960). After 1 hour at room temperature, 5 ml of distilled water was added, and the separated upper layer collected. The aqueous phase was successively washed three times with petroleum ether and the combined fractions with anhydrous Na_2SO_4.

(ix) Determination of fatty acid.

The fatty acid content was estimated by the hydroxamate assay. Usually, 0.1 μmole of the fatty acid sample was taken up in 0.5 ml of a mixture of EtOH:Et_2O (3:1 v/v). 0.2 ml of alkaline hydroxylamine (2 parts NH_2OH:1part NaOH v/v) was added and mixed on a vortex mixer. The reaction mixture was left to stand at room

temperature for 20 min and 0.1 ml of a 5M HCl solution added with mixing. This was then followed by the addition of 0.1 ml of an acid ferric chloride solution (10% $FeCl_3 \cdot 6H_2O$ in HCl, w/v) and, after mixing, the absorbance was read against a reagent blank at 520 nm. A standard, employing lauric hydroxamate (mp 91-93°) or stearic hydroxamate (mp 99-106°) in 66% EtOH was used throughout the procedure.

$$\Sigma = 1 \cdot 1 \text{ O.D units/}\mu\text{mole} \qquad (2)$$

(x) Nmr sample preparation: non-polar solutions.

All non-polar solutions for nmr runs were prepared in deuteriated chloroform as solvent with the deuterium signal providing a heteronuclear field/frequency lock. Occasionally, a small amount of deuteriated acetone ($\lesssim 5\%$ v/v) was found necessary to provide a much stronger lock than the $CDCl_3$ signal especially when long accumulation times were desired for the natural abundance material. Concentrations were in the range 10-20% w/v for the natural abundance lipids, and as little as 0.5% (w/v) was found sufficient to obtain meaningful spectra from enriched lipids. All relaxation data for lipids in non-polar solutions were obtained for total lipid concentrations of 10% (w/v) so that in a mixed lipid system of a (1:1 molar ratio) between enriched and unenriched lipids, this will amount to approximately a 5% solution of enriched lipids in terms of length of run.

When chemical shifts were desired, TMS was used as internal standard and the concentration used ranged between (1-10% v/v) depending on whether enriched or natural abundance material was being run.

(xi) Nmr sample preparation:aqueous dispersion.

A known quantity (150 mg) of lipid material in chloroform-methanol (2:1 v/v) was evaporated to dryness at 35°C over a stream

of nitrogen, and the dry lipid material then shaken with 1.5 ml of buffer (40mM Tris-HCl/100 μM edetate in 20% D_2O in triply distilled water pH 9) to give a coarse lipid dispersion. Sonication was performed in specially cut (2.0 x 5.5 cm) pyrex glass tubes with a probe type (MSE) sonicator. The sonication was carried out at 30°C and under a steady stream of pure nitrogen and the tip of the soniprobe was immersed to about half the depth of the dispersion in the tube and the power supply then tuned to maximum cavitation. For the PE/PS mixtures, the sonication time for the dispersion to attain optimum transparency was usually not more than 8 min, whereas for the PE/DPL mixtures, up to 15 min was required. The egg yolk phosphatidyl choline was sonicated for 10 min with the glass tube well immersed in a beaker of ice.

No significant increase in absorption at 234 nm was observed after sonication and TLC of the sonicated lipids showed no evidence of hydrolysis products. The sonicates were then usually filtered through a 0.1 μ Millipore filter and transferred into a 10 mm nmr tube. Nitrogen was bubbled through for about 3 min before the 'antidiffusion'current plug was fitted into the tube. For a reference standard, a 10% 1, 4-dioxane solution (for ^{13}C) or an 85% orthophosphoric acid solution (for ^{31}P) in a capillary tube was co-axially mounted. The 20% ^{2}HHO content was found to be adequate to provide a field/frequency lock. ^{1}H nmr samples were prepared in a similar buffer made up in 99.8% atom ^{2}HHO and were run in 5 mm tubes. Urea solutions were made by adding a 2% stock solution of BSA to weighed quantities of ^{13}C urea and then runin a 10 mm tube.

(xii) Spectrometer operation.

All spectra were obtained in the Fourier transform (FT) mode. An 8 K (8, 192 sampling points) data set was used, making it possible for the computer to measure chemical shifts correct to ± 0.05 p.p.m.

For the measurement of relaxation times, a pulse method (Freeman and Hill, 1971) employing a $(\pi\text{-}t\text{-}\pi/2)$ sequence was used where t, the interval between the 180° and 90° pulse, was varied in such a way as to include times on either side of the 'null' spectrum of any particular peak. A minimum recovery time for the spins of 5 x the largest T_1 in the sample was allowed between successive pulse cycles. Typically, 150-300 scans were accumulated for each spectrum of the partially relaxed FT block. A programme allowing each FID to be stored as part of the block so that the block as a whole could be processed at once was used. T_1 was calculated from the slope in equation (3) below.

$$\ln(A_{\infty} - A_t) = \ln 2A_{\infty} - {}^{t}/T_1 \qquad (3)$$

CHAPTER 3

^{13}C BIOSYNTHETIC ENRICHMENT OF THE FATTY ACYL RESIDUES OF PHOSPHATIDYL ETHANOLAMINE

CHAPTER 3

A. INTRODUCTION

With the development of the technique of Pulsed Fourier Transform n.m.r., the observation of the ^{13}C n.m.r. of a lipid material at the natural abundance level is a relatively simple matter. This applies,strictly speaking, only to the organic solutions of such material. The formation of highly populated macromolecular aggregates by lipids in organic solvents is very small compared with their aqueous dispersions. For example, in $CDCl_3$, lecithin exists as inverted micelles containing 60 - 70 molecules and only below the boiling point of a methanol solution of the same lipid do trimers begin to appear. (Price and Lewis, 1929; Elworthy and Macintosh, 1961). A well dispersed aqueous solution of the same lipid, however, will contain about 3000 molecules per vesicle, arranged in a bilayer. (This estimate is based on a vesicle average weight of about 3×10^6 Daltons, and an average molecular weight of about 750). This factor is in part responsible for the decreased resolutions and also the longer times required to attain meaningful signal/noise ratios in going from the solution to the dispersion. Although it is possible, in principle, to increase the signal/noise ratio indefinitely by accumulating more free induction decays (FIDs) it becomes uneconomical to accumulate data for more than 10 hours and worse still, this will mean up to 100 hours if spin-lattice relaxation (T_1) time measurement is required.

One obvious solution to this problem is the ^{13}C enrichment of n.m.r. samples. Both chemical and biosynthetic techniques for concentrating the ^{13}C isotope in lipids are available and have been used in conjunction with each other (Metcalfe et al, 1972). Although any carbon of choice along the fatty acyl chain can be selectively labelled by chemical methods, this usually involves arduous synthesis. On the other hand, growth of algae on $^{13}CO_2$, although economical, results in all the carbons of the chain being labelled, thus yielding a complex spectrum.

The alternative is to culture bacteria on acetate labelled on only one carbon, so as to obtain fatty acids labelled only in alternate carbons. This eliminates the complex spin-spin splittings mentioned above, but suffers the disadvantage that if wild-type bacteria are used, most of the added acetate is wasted in the medium because the internal production of acetate from pyruvate in the biochemical pathway of the organism is quite efficient.

At about the time I was embarking upon my research programme, Cronan and Batchelor (1973), had just reported a mutant of Escherichia coli designed to utilize acetate efficiently for the synthesis of its fatty acids. It is my pleasure to have spent the early stages of this work at the laboratory of Professor John E. Cronan, Jr. (Department of Molecular Biophysics and Biochemistry, Yale University, New Haven, Connecticut 06510, U.S.A.) working with this strain. The organism used was E. coli K12 strain CY2 (aceF, gltA).

B. LESIONS IN STRAIN CY 2

Added acetate in cultures of E. coli growing in glucose minimal medium is largely incorporated into fatty acid and protein (Roberts et al, 1963). A large proportion of the acetate is also converted to CO_2 and released. In order to achieve a high level of incorporation into the fatty acid alone, the incorporation of acetate into protein and the oxidation to CO_2 would have to be blocked. The relevant part of the Krebs cycle is shown in figure 7. The enzyme citrate synthetase catalyses the condensation of oxalacetate with acetate to form citrate. Mutants of E. coli defective in this enzyme can be isolated as strains requiring α-Ketoglutarate or glutamate. These mutants are called glt A mutants and have been previously shown to be unable to oxidize exogenous acetate to carbon dioxide (Gilvarg and Davis, 1956; Ashworth et al, 1965). Also, it has been shown (Harder et al, 1972) that when glt A strains are grown on medium supplemented with leucine, 95%

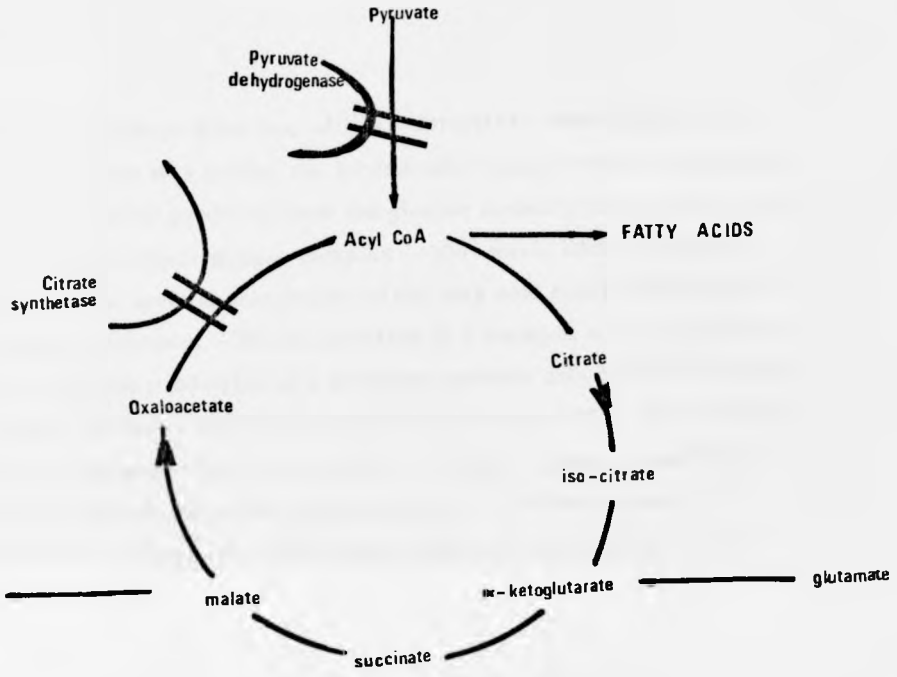

Fig. 7 TCA cycle showing positions of lesions in strain CY2.
= mutations.

of the acetate incorporated into cellular material is found in fatty acids. However, in even this strain, the incorporated acetate would be diluted by endogenous acetate produced from the glucose carbon source by the action of the pyruvate dehydrogenase complex. This would lead to a marked decrease in the specific enrichment of the fatty acid compared to that of the acetate precursor. The introduction of a mutation in the aceF gene would lead to the production of a defective pyruvate dehydrogenase complex as has been shown previously (Dietrich and Henning, 1970). The resultant organism has lesions in both the glt A and ace F genes, is unable to synthesize acetate endogenously and unable to condense acetate with oxalacetate. It requires exogenously added acetate and glutamate for growth.

C. INCORPORATION OF ADDED ACETATE

Trial runs with radioactive [1 - ^{14}C] -acetate were performed in an attempt to standardize the optimum culture conditions for CY2. A typical set of readings obtained is presented in table 2 and plotted in figure 8. The plot of the percentage of label extracted in the lipid fraction against the concentration of acetate injected into the medium before growth reveals that at high acetate concentrations, the proportion being utilized drops. It seems probable, therefore, that some endogenous synthesis of acetate still occurs. This will account for the decreased utilization of the added acetate at the higher concentrations, since the organism can presumably utilize only a given quantity of acetate at any one stage in its growth phase, irrespective of the main pool.

The alternative argument that a substantial amount of acetate may have been diverted to protein synthesis, implying the failure of the glt A gene mutation, does not seem valid, since sufficient count to account for most of the unincorporated acetate was usually found in the growth medium after cell sedimentation; cf table 2.

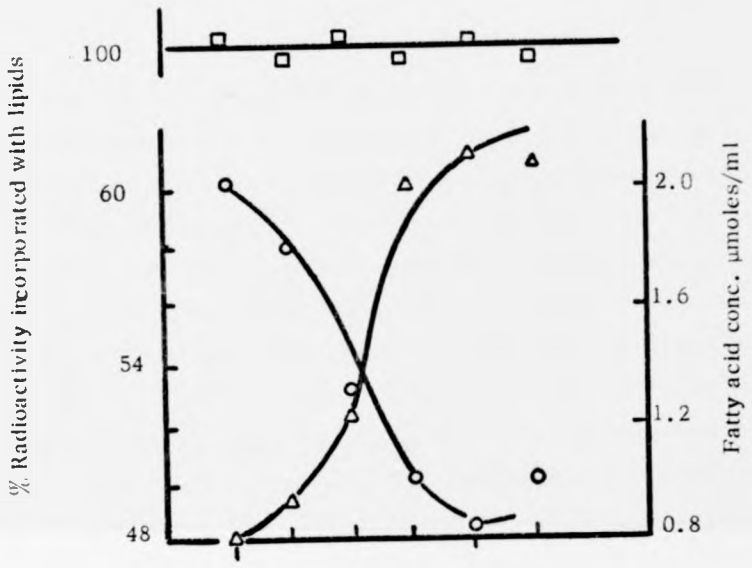

Fig. 8 % Sodium [1- ^{14}C] acetate found in (o) lipids and (□) culture after growth as a function of added acetate.
(Δ) Fatty acid present in lipids as a function of added acetate.

Table

Amt in m (ug/m
10
20
30
40
50
60

Fatty acid conc. μmoles/ml

) lipids
nction of

function

Table 2: Efficiency of incorporation of added sodium [1-^{14}C] acetate into fatty acids of E. coli.

Amt acetate in medium (ug/ml)	cpm/ml before growth	cpm/ml after growth	cpm/ml in lipid material	% total ^{14}C incorporated	Amt F.A μmole/ml
10	3.61×10^4	3.63×10^4	2.16×10^4	60	.80
20	3.70×10^4	3.68×10^4	2.15×10^4	58	.93
30	3.22×10^4	3.26×10^4	1.73×10^4	53	1.22
40	4.0×10^4	3.91×10^4	1.93×10^4	50	2.02
50	3.41×10^4	3.43×10^4	1.65×10^4	48	2.10
60	3.55×10^4	3.52×10^4	1.79×10^4	51	2.09

The value of only 50% incorporation for the concentration range (30- 40 μg/ml acetate added) is rather low compared with the previously reported data of Cronan and Batchelor,(1973). This is probably due to differences in culture conditions like harvesting of cells at different stages in the log phase. Lower values than 50% have been reported elsewhere (Batchelor, 1974). The plot of the fatty acid content of the extracted lipids shows the opposite trend to the percentage acetate incorporated. The fatty acid concentration seems to depend markedly on the amount of acetate present in the medium, although it tends to plateau off above the 40 μg/ml acetate concentration. This is good evidence that the lesion in strain CY2 is authentic, at least to the extent that the major part of the acetate in the medium is channelled into fatty acid synthesis. Presentation of the data in another form, using the calculated absolute quantities of exogenous acetate ingested by the organism, helps to illustrate this point better .(Figure 9).
This does not upset the argument of internal dilution of the acetate, because for internal dilution to occur, each organism will presumably synthesize acetate only to the extent to which the mutation in its genes has reverted to the wild type or is incomplete in the first place. In other words, the amount of endogenous acetate produced from pyruvate will be the same, irrespective of the quantity of added acetate. Thus, depending on the threshold acetate required by the organism, the amount of fatty acid produced may vary with added acetate. The endogenous production of acetate by the organism is short of the threshold requirement for growth by about 40 μg/ml, hence we have fatty acid synthesis increasing with added acetate up to this point and gradually levelling off subsequently. The plot at the top of Figure 8 shows that the amount of acetate present in the medium before and after culture growth is conserved, indicating that little or no acetate was lost as CO_2.

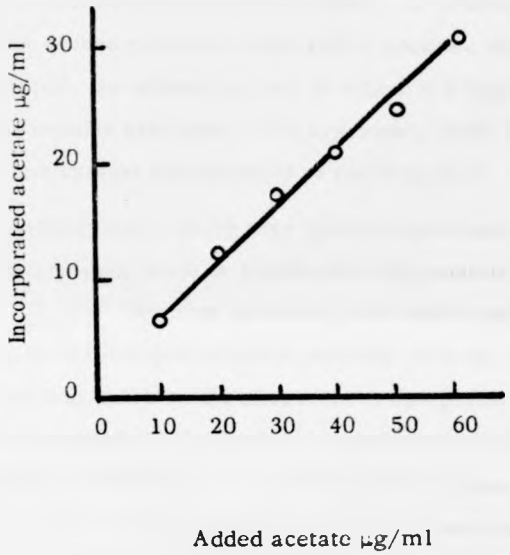

Fig. 9 Amount added acetate that is incorporated directly into lipids of E.coli CY 2

D. FACTORS INFLUENCING YIELD OF ^{13}C IN FATTY ACIDS

From the point of view of n.m.r. , it is the specific enrichment in ^{13}C of the fatty acids which is most important. This is the degree to which the enrichment in the acetate precursor [1 - 90% ^{13}C] -acetate is preserved in each labelled carbon atom. It is desirable to obtain a high proportion of incorporation of the added acetate, but as has been demonstrated, the advantage may be offset if a high quantity of endogenous acetate is equally available to the organism, since this may reduce the specific enrichment considerably in the fatty acid.

Another factor which may lead to significant amounts of acetate being endogenously made is insufficient oxygenation of the culture during growth. E.coli has been shown to grow under anaerobic conditions by switching to the phosphoroclastic pathway (Strecker, 1951). The phosphoroclastic pathway involves the anaerobic decomposition of pyruvate into acetate and formate. The acetate produced may then enter into the tricarboxylic acid cycle. It was to avoid this danger that cultures were generally grown under vigorous aeration and terminated in late log phase so as to prevent the limiting oxygen conditions of stationary phase cell densities.

In Figure 10 the exponential growth of E.coli K12 strain CY 2 is plotted on a semi-logarithmic scale. Plots are shown for different aeration conditions. The advantage of good aerobic conditions is clearly borne out given that there exists approximately a 5 hour time separation for both cultures in reaching identical cell densities, with the less aerated culture being the slower. It is with this and other arguments presented above in mind that the standard conditions for subsequent experiments were chosen.

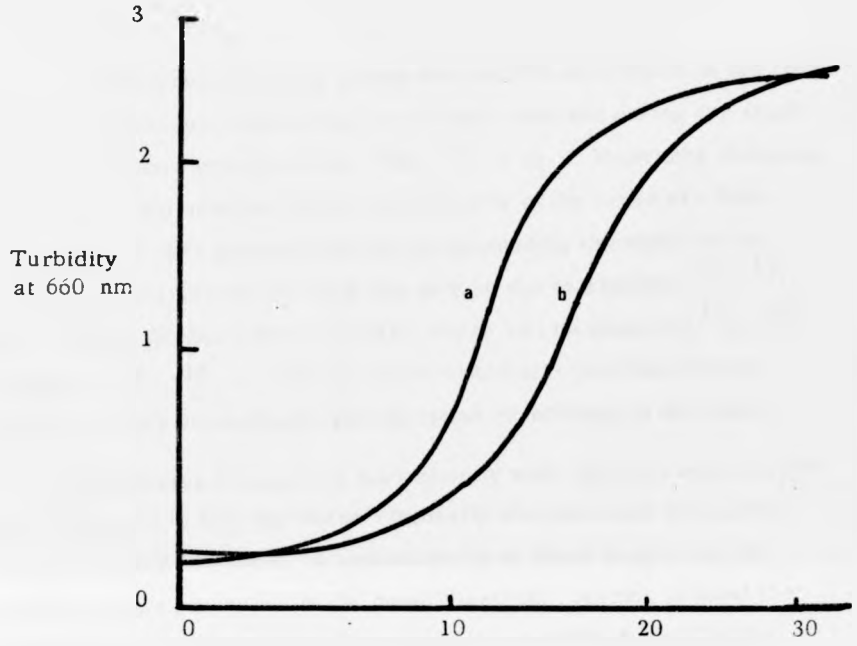

Fig. 10 Growth curve of E.coli strain CY2 (a) 5L culture in automatic fermentor. (b) 5L culture without vigorous aeration .

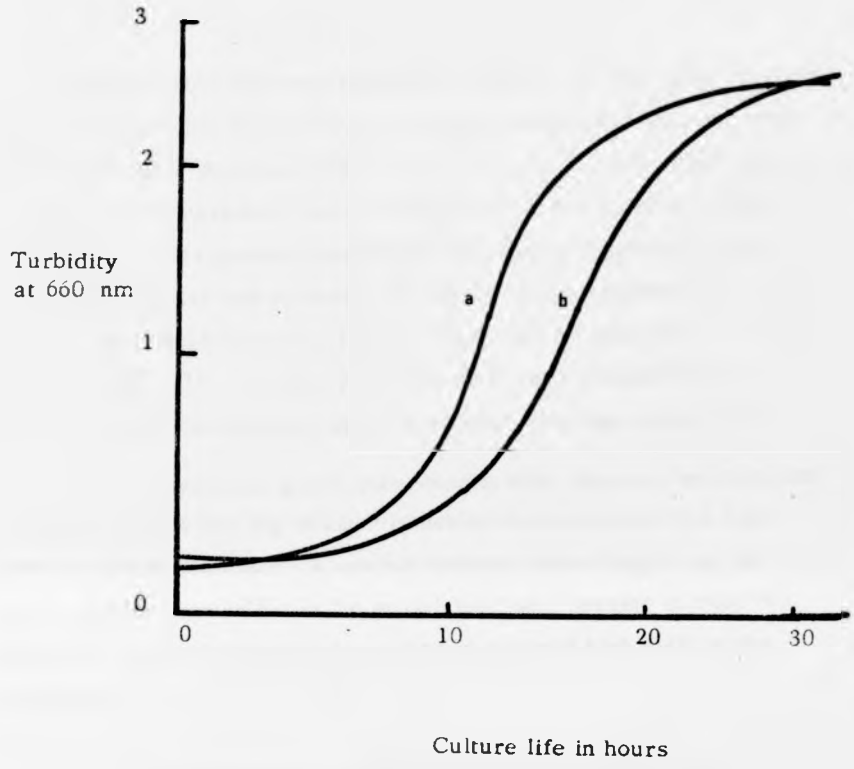

Fig. 10 Growth curve of E.coli strain CY2 (a) 5L culture in automatic fermentor. (b) 5L culture without vigorous aeration .

A third factor that may reduce the specific enrichment in the fatty acids is if significant scrambling of the label occurred during any stage in the biosynthetic incorporation. The ^{13}C n.m.r. linewidths observed in $CDCl_3$ for the enriched lipids was typically of the order of ~5Hz. This is only $\lesssim$ 3Hz greater than the corresponding linewidths in the unenriched material and at worst can only be due to alternate ^{13}C-^{13}C spin-coupling (Birdsall et al., 1974). There was no observed ^{13}C -^{13}C splittings ($J_{^{13}C-^{13}C}$ ~ 100Hz) which would have provided direct evidence for pre-biosynthetic incorporation scrambling of the label.

All cultures were grown subsequently with vigorous aeration and usually stopped in late log-phase - typically characterised by a Klett reading of about 160 units. A concentration of about 35μg/ml of the labelled acetate was added in the growth medium, bearing in mind the balance to be struck between the economic cost and high yield in the experiment.

E. DETERMINATION OF SPECIFIC ENRICHMENT IN THE PHOSPHOLIPID FRACTION OF THE LIPID EXTRACT

Phosphatidyl ethanolamine is the major lipid found in E.coli . It accounts for about 80% of the cellular phospholipids which in turn account for more than 95% of the cellular lipid material (Law, 1961). Determination of the enrichment in the PE fatty acyl chain residues should therefore give a good indication of the level of enrichment of all other lipid material. The enrichment was determined by both n.m.r. and mass spectrometry on the methyl esters of the resulting fatty acids after alkaline hydrolysis of PE. The fatty acids were separated into individual species by preparative gas chromatography . Figure 11 is a comparison of the ^{13}C n.m.r. spectrum of methyl palmitoleate for both the natural abundance and isotopically enriched cases. On prediction (based on the successive condensation of acetate units in fatty acid biosynthesis), we would expect to see a

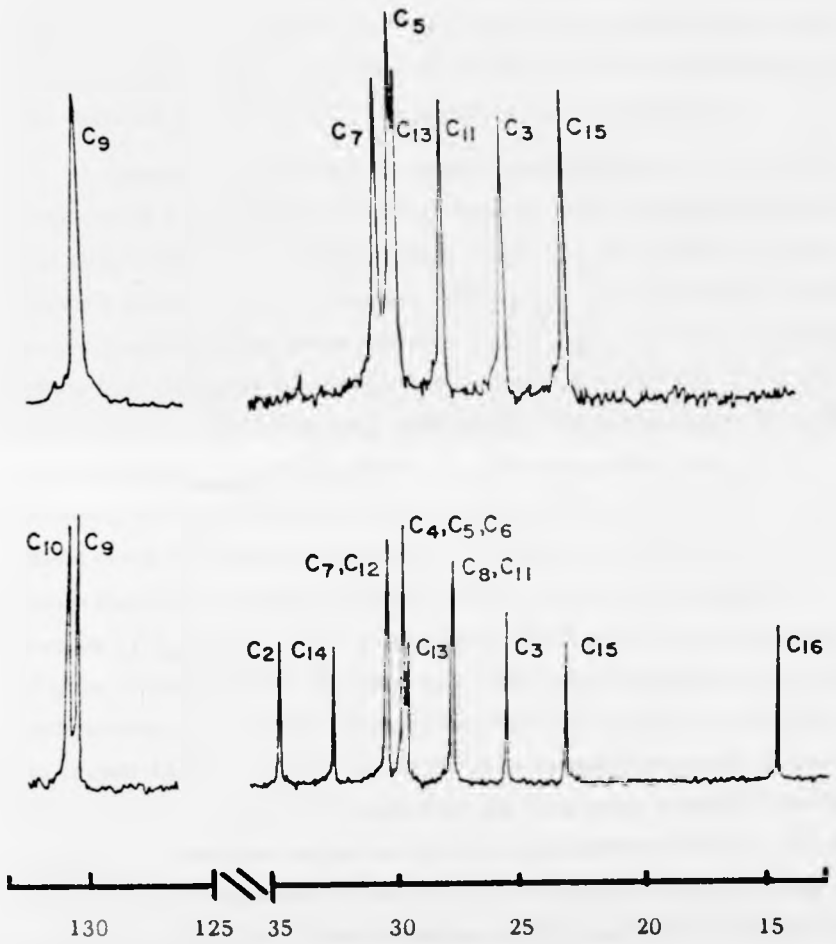

Fig. 11 ^{13}C n.m.r. of methyl palmitoleate from E.coli showing odd-carbon enrichment pattern (top compared to bottom) when organism is grown on [1-^{13}C] acetate.

significant signal/noise enhancement in only the odd carbon atoms of the enriched material, if [1 - ^{13}C] acetate has been used. This is indeed the case as shown in Figure 11. Corroborating evidence has now been obtained (Birdsall et al., 1974) to show that only the even numbered carbons are enriched when [2 - ^{13}C] acetate is the starting material.

Analysis of the carbon-13 enrichment level by n.m.r. can be achieved by a ratio method involving hydrogen atoms bonded to carbon-12 and spin coupling with neighbouring carbon-13. The carbon-13 may be directly bonded to the proton observed (J^{13}_{C-H}) or just merely coupling over a longer range of more than one bond (J^{13}_{C-X-H}). The proton spectrum of the fatty esters shows three regions identifiable with the olefin, the $-OCH_3$ and the rest of the fatty acyl chain. The latter region is much more complex due to the presence of multiple spin-spin interactions. The coupling constant of the olefin proton-carbon (J^{13}_{C-H}) is estimated on the basis of the sp^2 character of the C = C bond to be about 160 Hz (Shoolery, 1959) while that of the splitting between the OCH_3 protons and carboxylate carbon ($J^{13}_{C(O)O-C-H}$, is estimated to be about 3.5 Hz (Karabatsos, 1960). Figure 12 is the proton spectrum of the methoxy resonance of the methyl palmtoleate. The central peak is that due to the protons directly bonded to carbon-12. It is unsplit due to the zero magnetic character of carbon-12. The two surrounding peaks arise from the long range coupling with the enriched carboxylate carbon and a coupling constant of about 3.7 Hz is observed. A comparison of the areas of this doublet with that of the central peak should yield the relative abundance of carbon-13 over carbon-12. On the basis of this calculation, we obtained values of 50% for both regions typically. The experimental error in measuring the carbon - 13 abundance was ± 10%.

Mass spectrometric determination of the carbon-13 abundance on the gas chromatographically purified methyl palmitate yielded a value of 49 ± 2% .

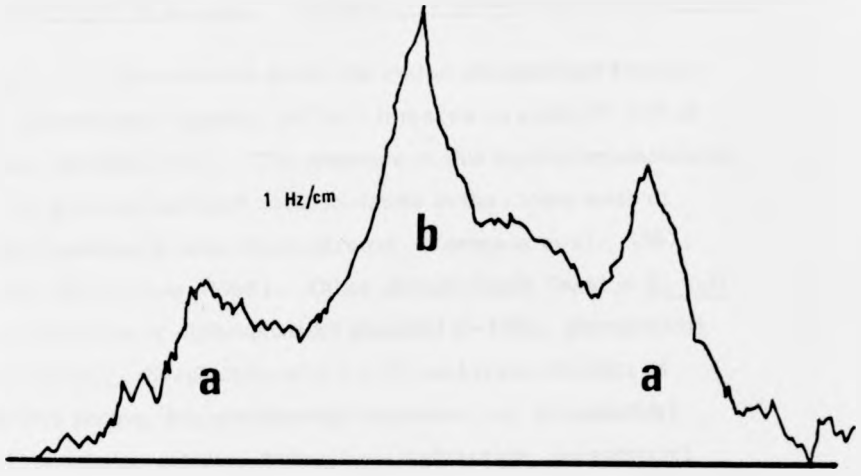

Fig.12 Proton n.m.r. of $-OCH_3$ resonance of fatty acid methyl esters from E.coli PE showing long range coupling ~ 3.6 Hz to ^{13}C at carboxylate .

$$\frac{2a}{(2a + b)} \times 100\% \sim 47\%$$

F. Phospholipids of E. coli. (Evidence for differences in enrichments).

Phosphatidyl ethanolamine is the the major phospholipid found in E. coli, (Cronan and Vagelos, 1972). It makes up about 70-80% of the cellular phospholipids. The presence in this lipid of ethanolamine, phosphate, glycerol and acyl ester moieties in the molar ratio of 1:1:1:2 has previously been demonstrated, (Kaemasa et al., 1967; De Siervo, 1969; Ames, 1968). Other phospholipids found in E. coli include cardiolipin or diphosphatidyl glycerol (5-15%), phosphatidyl glycerol (5-15%), phosphatidic acid (< 1%) and trace amounts of phosphatidyl serine, lysophosphatidyl ethanolamine, phosphatidyl glycerol phosphate, cytidine diphosphate diglyceride, phosphatidyl inositol and an as yet unidentified phosphatide designated lipid Y, (Cronan and Vagelos, 1972).

The fatty acids usually found esterified to the glycerol in the phosphatides have been shown, by co-chromatography with synthetic analogues, to comprise mainly of myristic, palmitic, palmitoleic, 9, 10-methylene hexadecanoic, cis-vaccenic and lactobacillic acids, (Kaneshiro and Marr, 1962; Hsu and Fox, 1970). Palmitic alone comprises about half the total fatty acid and is clearly the major saturated acid with myristic comprising only 2% of the total fatty acid, (Silbert and Vagelos, 1967). Under the conditions in which we have cultivated our cultures, cyclopropane fatty acid synthesis is greatly supressed, and the major fatty acid unsaturate is likely to be the palmitoleic, (Cronan, 1968).

The spectra of the cardiolipin and phosphatidyl ethanolamine lipid fractions are shown in Figures 16 and 18. The spectra are typical of ^{13}C chemical shifts of acyl residues of phospholipids. The method of comparing the integrated areas of the olefinic proton resonances of the enriched material and their ^{13}C-H satellites gives

only the enrichment at the olefine carbon. Similarly, the method of the $-OCH_3$ with its ^{13}C satellite gives the enrichment at only the carboxylate carbon. The mass spectrometry method we have used gives only the "diffuse" or average value for all the enriched carbons. In an attempt to determine the enrichment at each enriched site, I have ratioed the intensity of each peak to that of solvent (Table 4), introduced appropriate correction factors for concentration discrepancies, and compared these with corresponding values from natural abundance egg-yolk PE. The enrichment on each carbon nucleus is consistently lower for cardiolipin than in the corresponding case in PE. Furthermore, more natural abundance peaks appear to be resolved in the cardiolipin spectrum where none are observed in the PE spectrum, (cf. peaks marked n, Figure 18). There is, it appears, reason to believe that the fatty acyl chains are differently enriched in the two lipids.

If this observation is true, then it is rather surprising since cardiolipin synthesis and phosphatidyl ethanolamine synthesis are thought to have a common precursor up to the cytidine diphosphate diglyceride (CDP-diglyceride) level, (Cronan and Vagelos, 1972). Another point of note is the fairly high enrichment level of the terminal methyl (ω); $\sim 5\%$ and $\sim 10\%$ for PE and cardiolipin respectively. Since we have earlier on discounted the existence of any significant scrambling of the label, this may probably be due to the presence of trace amounts of odd-numbered fatty acid residues esterified to these lipids. Apparently, on purely statistical grounds cardiolipin can accomodate four of these (a factor of 2 more than PE) per molecule.

Table 3: ^{13}C chemical shifts of E. coli lipids in $CDCl_3$

Resolved resonances along acyl residue	8 p.p.m. from TMS at 45°C	
	PE	DPG
C1 α	173.8	173.1
C1 β	173.6	
C3	25.4	24.8
C5	29.9	29.8
C7	30.6	30.2
C9	130.1	129.3
C11	27.2	27.3
C13	29.5	29.3
C15 (ω-1)	23.2	22.6
C16 (ω)	16.0	15.9

TABLE 4

% ENRICHMENT AS ESTIMATED FOR EACH CARBON

IN E. COLI LIPIDS

Resolved Resonances along acyl chain	% ^{13}C ENRICHMENT	
	PE	CL
C1	65 60	27
C3	47	41
C (5, 7, 13)	24	19
C9	70	46
C11	28	26
C15 (ω-1)	50	41.6
C16 (ω)	5	14

CHAPTER 4

N.M.R. STUDIES OF PHOSPHATIDYL ETHANOLAMINE - PHOSPHATIDYL SERINE

CHAPTER 4

A. INTRODUCTION

In general, when the extracted lipids from any naturally occurring membrane are analyzed, there is found to be a distribution of different lipid types. These will range from long chain fatty acids to the more complex phospholipids. It is unlikely that any naturally occurring membrane known or unknown, will contain only one lipid type. Indeed, considerable differences exist at a still lower level within the lipid type. For example, two different fatty acids can be arranged on a glycero-phosphate moiety in eight different ways to give four different 3-sn-phosphatides. Four fatty acids will lead to twenty-eight different phospholipids. The nature of this structural diversity, the guide lines along which it is established and its implication on the functionality of the membrane as an entity are some of the questions being asked by membranologists today. It is unlikely that this multiplicity of structure has no consequence on the physiological behaviour of the biological membrane.

The development of appropriate model membranes (Chapman and Dodd, 1971; Yost et al, 1971; Thompson and Henn, 1970; Sessa and Weissman, 1968) has stimulated a wide variety of research into the structure and function of biological membranes. A wide range of physical techniques such as X-ray diffraction (Engleman, 1972; Wilkins et. al., 1971· Levine and Wilkins, 1971), spin-labelling (Kornberg and McConnell, 1968) and nuclear magnetic resonance (Chapman and Morrison, 1966; Metcalfe et al., 1971) has been applied with the hope of correlating between structure and function. But perhaps the most attractive of the techniques currently available to the researcher in the field of membrane studies is that of n.m.r. Some of the reasons for this have been advanced in the

introduction and in addition to them, we have the comparative richness of the information derived. For example, the Chapman or crystalline to liquid-crystalline phase transition in a lipid bilayer can be demonstrated by proton n.m.r. (Sheetz and Chan, 1972; Lee et al., 1972) in a matter of minutes. Furthermore, this transition has been observed in a naturally occurring membrane using ^{13}C n.m.r. spectroscopy among other techniques (Metcalfe et al., 1972).

Lipids in biological and model systems exhibit both thermotrophic and lyotropic mesomorphism. The phenomenon of 'melting' in the bilayer is an endothermic one and is particularly suitable to investigation by thermal techniques. Differential scanning calorimetry when applied to these systems has been quite informative (Ladbrooke and Chapman, 1969). Appropriate thermodynamic data derived from the heat involved in these melting processes (Philips et al., 1969) have led to conclusions about the relative amount of disorder associated with these transitions. The temperatures at which the phase transitions occur and perhaps the sharpness or range of these transitions may depend on a variety of variables. These include the nature of the headgroup, the hydrocarbon chain length, the degree and type of unsaturation present and also the mixing properties of the lipids present (Chapman, 1973).

The observation of discrepancies in the proton spin-lattice relaxation times in liposomes and sonicated vesicles has been discussed in the general introduction. These data, together with the dilatometry studies of Sheetz and Chan (1972) would seem to suggest that there is no basis for the comparison of results obtained with sonicated vesicles with those from unsonicated liposomes. More recently, however, differential scanning calorimetry studies have been used to dispel doubts about the suitability of vesicles as models for biological membranes. The relevant features of these results of Radda and co-workers (De Kruijff et al., 1975) are discussed in Section C and in the conclusion, together with our results on the characterization of the PE-PS (1:1) vesicles.

Most n.m.r. studies have tended to concentrate chiefly on the measurement of relaxation times. As mentioned above, questionable

conclusions can be reached when considering results from both the liposomes and sonicated systems. It must be pointed out that this discrepancy observed with proton T_1's may not apply equally to T_1 studies of other nuclei. If the inconsistency of reported ^1H T_1 in liposomes (Barrat, 1970; Chan et al., 1971) and in vesicles (Lee et al., 1972) is the direct consequence of a spin-diffusion dominated relaxation mechanism, then there is no reason to believe that a similar problem will beset ^{13}C T_1's in these systems. Unfortunately, the low spectral resolution associated with unsonicated liposomes has discouraged investigators from comparing ^{13}C T_1 values in both systems.

^{13}C T_1 values have been reported for sonicated dipalmityl lecithin bilayers (Metcalfe et al., 1971a). However, it is not known if and how this heterogenous distribution of T_1's will be preserved over a wide range of temperature. The relevance of this information to biological structure and functions is unclear.

In an attempt to answer some of these questions, we have observed the ^{13}C spin-lattice relaxation time (T_1) behaviour for a mixed lipid system over a wide temperature range. ^{13}C T_1's have been measured for all resolvable carbons in a phosphatidyl ethanolamine-phosphatidyl serine (1:1) sonicated bilayer system over the temperature range of 30-85^{o}C. The results are compared with the deuterium magnetic resonance studies of Seelig and Seelig (1974) on nonsonicated liposomes and with the ^{13}C T_1 data of Heatley (1976) on isotropically tumbling polymers. It is concluded that the mobility gradient is a consequence of a special symmetry characteristic of the type of structure formed. Furthermore, the changes with temperature are similar in both the vesicles and liposomes establishing the former as a relevant system for membrane studies.

Pure PE does not form stable bilayers (Papahadjopoulus and Miller, 1967; Litman, 1973). Luzzati (1968) has shown that PE and PC exhibit different phase behaviour.

Steim (1968) showed that PE has a higher endothermic transition temperature than PC and Philips et al. , (1972) have demonstrated that PE is more tightly packed than PC, suggesting a difference in molecular mobility. Electron microscopy has revealed that sonication of PE results in large multi-lamellar "onion-like" structures (Michaelson et al., 1974). To obtain vesicles suitable for n.m.r. studies, it is desirable to co-disperse PE with appropriately chosen lipids. Gent and Prestegard (1974) found that co-sonication of PE and PC resulted in single-shelled spherical vesicles whose radii increased as the mole fraction of PE increased. It is fairly well established now that the major lipids can be considered roughly falling into two groups in terms of their packing characteristics. Those with a 'tapered' geometry, like PC, PS and sphingomyelin and those with a "frayed" geometry like PE and cholesterol (Israelachvili and Mitchel, 1975). Furthermore, it is thought that frayed lipids might preferentially pack with tapered lipids. Thus it is rather unsettling to see so much attention given to the PE-PC system although it has been shown that PE-PS associations can occur almost to the exclusion of other lipids in biological membranes. For instance, the major phospholipids of the inner half of the erythrocyte membrane are PE and PS (Bretscher, 1972; Zwaal, et. al., 1973).

B. VESICLE SIZE CHARACTERISATION

The results obtained for the molecular sieve behaviour of the PE-PS dispersion are presented in Table 5 and Figures 13 & 14.The partition coefficient σ of the mixed lipid vesicles and those for the calibrating standards used were deduced from experimentally measured parameters according to equation (4) overleaf.

TABLE 5 DATA FROM MOLECULAR SIEVE EXPERIMENTS

Particle	Elution Volume (Vc) ml*
Dextran 2000	52 ± 2
H_2O	155 ± 9
Glycine	153 ± 5
γ - globulin	132 ± 4
[a] T.B.S.V.	93 ± 5
PE/PS (1 : 1)	112 ± 5

* means of 3 readings

a tomato bushy stunt virus.

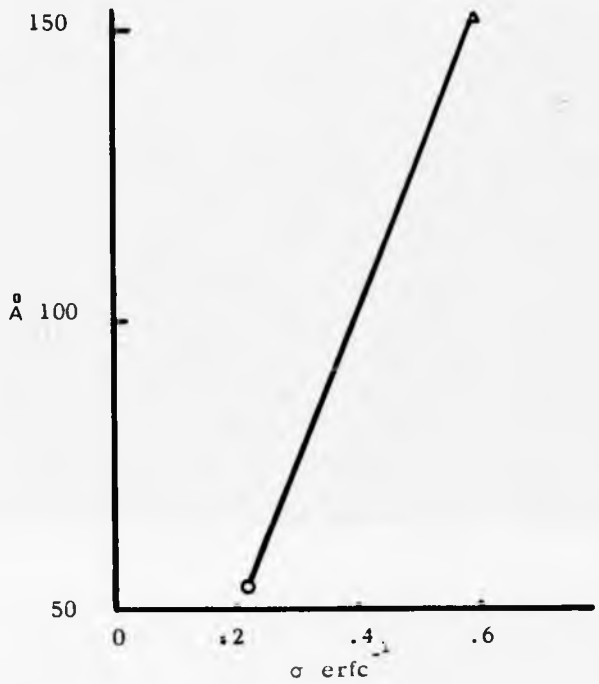

Fig.13

Molecular radius as a function of $\text{erfc}^{-1}\sigma$ on Sepharose 4B. (o)Y-globulin, ( )TBSV.

Absorbance at 300 nm

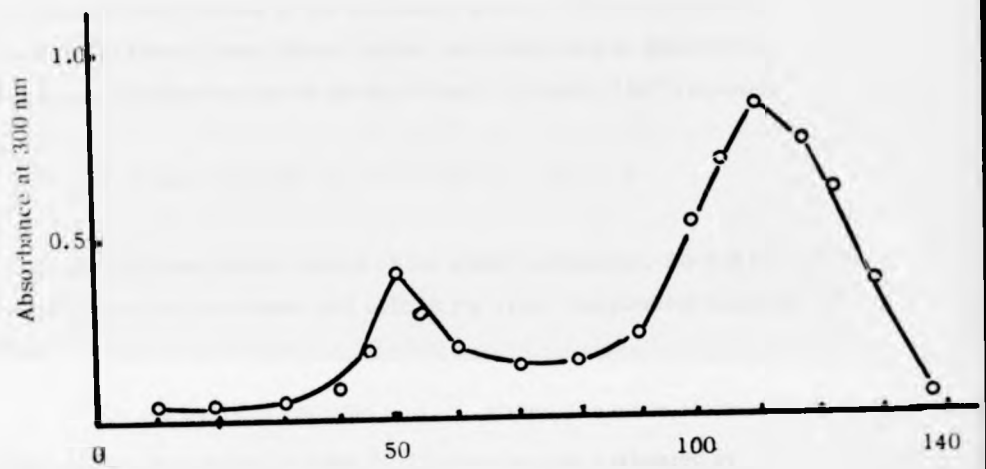

Fig. 14

Elution profile of PE/PS(1:1) with Tris-HCL pH9.

$$Ve = Vo + \sigma V_1 \qquad (4)$$

where Ve is the elution volume, Vo is the void volume of the gel and V_1 is the internal volume of the stationary phase. Three calibrating standards of known mean Stokes radius were employed in determining the column constants as given by the Acker's (Ackers, 1967) equation.

$$a = Ao + bo\,erfc^{-1}\,\sigma \qquad (5)$$

where a, is the mean Stokes radius of the eluted component, Ao and bo are constants for the column and erfc is the error complement function in σ

On the basis of equation (5) above, the mean Molecular Stokes radius determined for the PE-PS vesicles was estimated at 105 ± 5 Å . There was observed only a minor trace (Figure 14) of the fraction (1) species, claimed to elute with PC vesicles (Huang, 1969; Hauser et al.,1970; Johnson et al.,1971; Hauser ,1971). There occurred actually, a distribution of particle size ranging from 93 Å to 128 Å . The inorganic phosphate content found in the main fraction after all the 5 ml fractions had been pooled together was usually of the order of $\geq 90\%$ of that introduced into the column. Estimation of the phosphorus content of the minor lipid that eluted with the void column volume showed that this fraction constituted a variable 3 - 8 % of the total lipid injected. As a precaution, all n.m.r. samples were sieved through a 0.1 μ millipore filter before being run on the spectrometer.

The effect of ultrasonic irradiation on coarse lipid dispersions in aqueous medium has been well investigated (Sheetz et. al., 1972; Finer et. al., 1972; Hauser, 1971). It is generally agreed that provided sonication is carried out under an inert atmosphere and reasonably low temperatures, significant chemical degradation can occur via a free radical mechanism in a self-catalysed oxidation of the acyl residues of the lipids. Thin-layer chromatography of the lipid mixture before and after sonication showed only two major spots due to the PE and PS. There was a faint trace behind the major PS spot which might suggest a minor degradation of the PS fatty acyl residues to lyso-phosphatidyl serine. If any auto-oxidation has occurred at all, it will probably occur preferentially at the acyl residues of the PS , since the acyl residues of PE from E.coli are known to be predominantly mono unsaturated and also, given that auto-oxidation requires the presence of more than one olefinic function. Another effect of sonication is to break down the large macromolecular multilayers of lipids into smaller vesicles bounded by a single bilayer. It is thought (Atkinson et al., 1974) that the mean Stokes radius of the vesicles formed varies with the ionic strength of the dispersion medium for PS. Specifically, they report that the radii decrease from 125 Å in 0.1M NaCl to approximately 82 Å in salt free water. Given that I have used a buffer strength of 0.04M Tris-HCl, the results I have obtained with gel filtration are in good agreement. On the basis of theory, an increase in size of the resulting vesicles is predicted for phosphatidyl choline when co-sonicated with phosphatidyl ethanolamine (Israelachivili and Mitchel, 1975). A mean Stoke's radius of about 165 Å is predicted for a 0.5 mole fraction PE/PC dispersion. This increase is not as dramatic as that associated with a similar mole fraction of cholesterol of ~ 250 Å ,

providing evidence, therefore, that the size of the phosphatidyl choline-phosphatidyl ethanolamine vesicles is about the same as that of phosphatidyl-choline. The size reported here for the PE-PS vesicles at a 0.5 molar fraction does not seem to deviate considerably from that reported for pure phosphatidyl serine vesicles. This is probably indirect evidence that the prerogative of size determination may not rest with the geometry of the phosphatidyl ethanolamine species. Perhaps the phosphatidyl ethanolamine is merely accommodated within a predetermined framework of phosphatidyl serine vesicles.

C . LIPID DISTRIBUTION IN VESICLES

In the formation of vesicle bilayers by a mixed lipid system, there are two main ways that the lipid distribution can occur. Either there is total mixing at the molecular level, or there is incomplete mixing to some degree leading in the limit, to the phase separation into regions containing only one type of lipid. This phenomenon, known as membrane asymmetry with respect to its lipid content is known to occur in 'in vivo' membranes and has been clearly demonstrated in erythrocyte membranes (Bretscher, 1973). Although the significance is not clearly understood, it is unlikely that it has no biological consequence. It is thus necessary to look out for lipid segregation and establish to what extent it exists in laboratory models. Segregation of the lipids can occur in a variety of ways :-

(a) into patches within the layers of a bilayer;

(b) into vesicles homogenous in their lipid content ;

(c) into different bilayers of a multilayered vesicle;

(d) into different layers of bilayers.

Alternative (b) can be ruled out on the grounds of (i) the slow exchange rate of lipids, especially of PE (Wirt and Zilversmit, 1970) between vesicles in the absence of the phospholipid exchange protein factor (PEPF), (ii) the correspondingly low level of incorporation of exchanged phospholipids in the absence of this factor and (iii) the fact that intervesicular phospholipid exchange will tend to lead to bilayers homogenous in PE. Such bilayers will be unstable (Litman, 1973) and lead to ready flocculation which was not observed. On the basis of the molecular Stoke's radius determined above for the PE-PS (1:1) system, it is unlikely that there is a significant contribution from large multi-layered aggregates as suggested in alternative (c).

Lipid phase separation into types (a) or (d) are clearly possible however. It has been shown that mixing of different polar headgroup containing lipids can result in a mixed solidus liquidus system (Clowes et al., 1971; Chapman, 1973). With widely different chain lengths, monotetic mixing leading to pronounced phase separations can occur. However, with such naturally occurring lipids having a variety of chain lengths in between the two most different acyl chains, it is likely that considerable mixing may occur.

The data of Radda and co-workers (De Kruijff et al., 1975) illustrating lateral phase separations in vesicles composed of mixed phospholipid species, (figures 15 (a-d)). Figures 15(a) and (b) are the ^{31}P n.m.r. spectra of 18:1c/18:1c and 16:0/16:0 - PC vesicles respectively. The spectra have been recorded at 10^{o}C which is found to be below the order→disorder transition temperature of the latter system. The increase in linewidth associated with the resonance of this system is therefore probably due to restricted motion of the head group in the gel phase. Figure 15(c) is a similarly recorded spectrum of the mixed lipid vesicles containing a (1:1) molar ratio of the two different lipids. PC molecules of the C 16 variety in the gel phase are thought to be responsible for the broad component in this signal, while the narrower components are ascribed to liquid crystalline C 18 species in the inside and outside of the vesicles. The addition of Co^{2+} broadens the resonances from the outside bilayer resulting in the spectrum shown in Figure 15(d)

which still comprises a narrow peak superimposed on a broader component. It is thought that this is indicative of phase separation of the lipids in the inner half of the vesicle bilayer, presumably in the nature of solidus C 16 PC molecules coexisting with liquidus C 18 species.

Our results with ^{31}P n.m.r. spectrum of the PE-PS (1:1) system did not show any similar phase separations. Figure 15(e) is a 36.4 MHz ^{31}P n.m.r. spectrum of the PE-PS vesicles above their phase transition. We could not resolve resonances from the inside and outside halves of the bilayer separately. The narrow peak observed shows that to all intents and purposes the resonances due to the PE and PS phosphate moieties have identical chemical shifts suggesting similar environments for the resonating nuclei. This is probably indicative of a significant degree of 'mixing' in this system. The resonance is found not to be considerably shifted from the signal from the external reference standard (85% H_3PO_4) at 2.043 KHz and which had to be removed so that the spectrum could be recorded. Attempts to resolve the resonances from the inside of the vesicles by the addition of small amounts of non-permeating broadening agents were unsuccessful. Addition of small amounts of $MnSO_4 \sim 10^{-7}$ M resulted in rapid flocculation of the vesicles. The ease of destabilisation of these vesicles by ionic reagents is probably indicative of the importance of charge effects in the formation of the bilayer.

D. Quality of ^{13}C spectra.

(i) Spectra in organic solvents:-

The ^{13}C n.m.r. spectra of lipids in isotropic solutions show sharp resonances, $\leq$ 3 Hz wide. Linewidths observed all throughout these experiments were in good agreement with this value. Linewidths obtained in deuterated chloroform as solvent varied on the average from ~3 - 5 Hz. Bearing in mind that fairly large inverted micelles

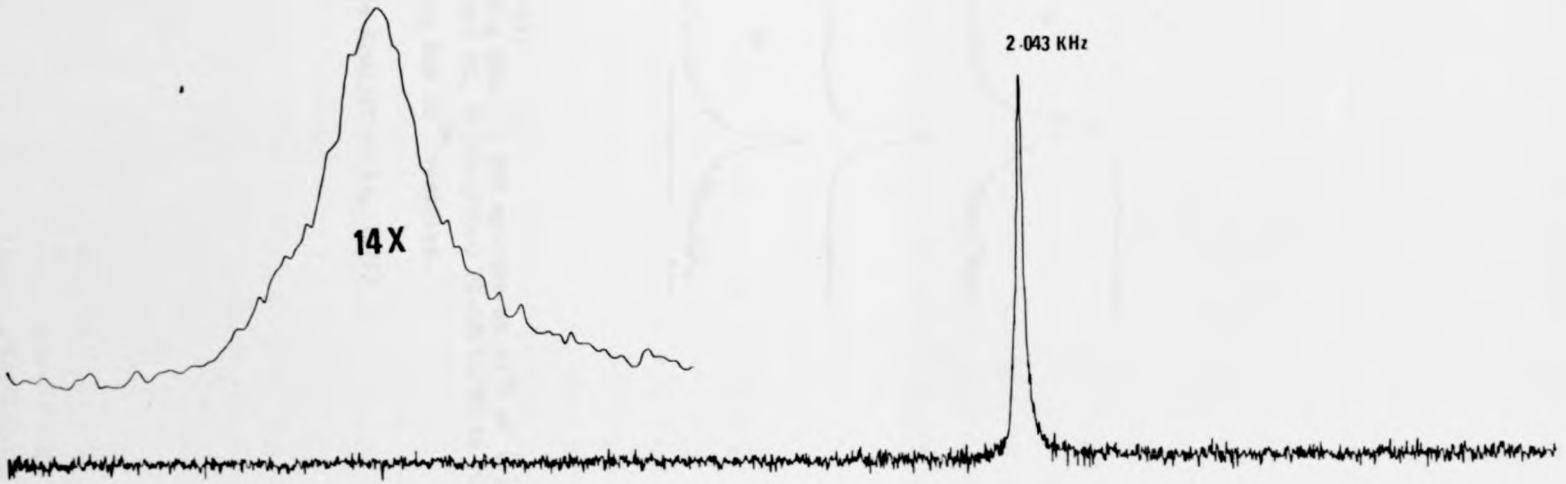

Fig. 15 **36·43MHz ^{31}Pnmr of PE°/PS (1:1) dispersions**

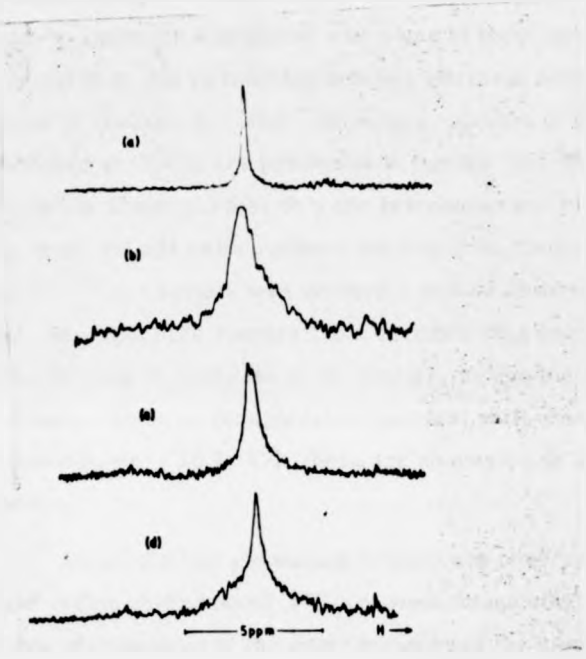

* Fig. 15(a-d); 36.4 MHz ^{31}P NMR spectra at 10°C of (a) 18:1c/18:1c PC (b) 16:0/16:0 PC, (c) 16:0/16:0 PC-18:1c/18:1c PC(1:1), (d) same as (c) plus 6mM Co^{2+} vesicles.

*(Data of De Kruijff et la, 1975)

(60 - 70 molecules) are formed in this solvent, in other words, the solution departs considerably from ideal isotropicity, we can begin to see the impressive quality of some of these spectra. On the other hand, the small increase in line width associated with some of these spectra $\sim$ 2Hz, could possibly be due to coupling between alternate carbons, as has been mentioned in Chapter 3. The ^{13}C n.m.r. spectra of some of the phospholipids in $CDCl_3$ are presented in figures (16-18). It has been established in Chapter 3 that only the resonances due to enriched carbons (in this case, all odd carbon atoms starting from the carboxylate end since [1 - ^{13}C] - acetate was utilized) will be observed. On these grounds, we expect the spectra from enriched PE alone and that from enriched PE plus PS mixtures to be similar, unless the presence of PS in the mixture leads to considerable chemical shift changes. As can be seen from figures (16 & 17) there are no noticeable differences in the two spectra.

Three distinct resonating regions are observed - (i) The low field region shifted about 173 ppm from tetramethyl silane is due to the two carboxylates of the ester moieties to the glycerol backbone. Because of their slightly different chemical environments, positions sn-1. and sn-2, respectively on the molecule, they are resonating at slightly different frequencies. The lower field peak being due to the carboxylate at position sn-1. The peak resonating at $\sim$ 130ppm is that due to the only enriched carbon of the olefinic carbons. This will be the C (9) carbon in the present nomenclature, see Figure 19 The main mass of peaks resonating up field between δ 15 -35 ppm is the contribution from the rest of the acyl chain carbons. The assignment of these resonances was based on those of model compounds and on the intensities of the resonances expected from the fatty acid composition.

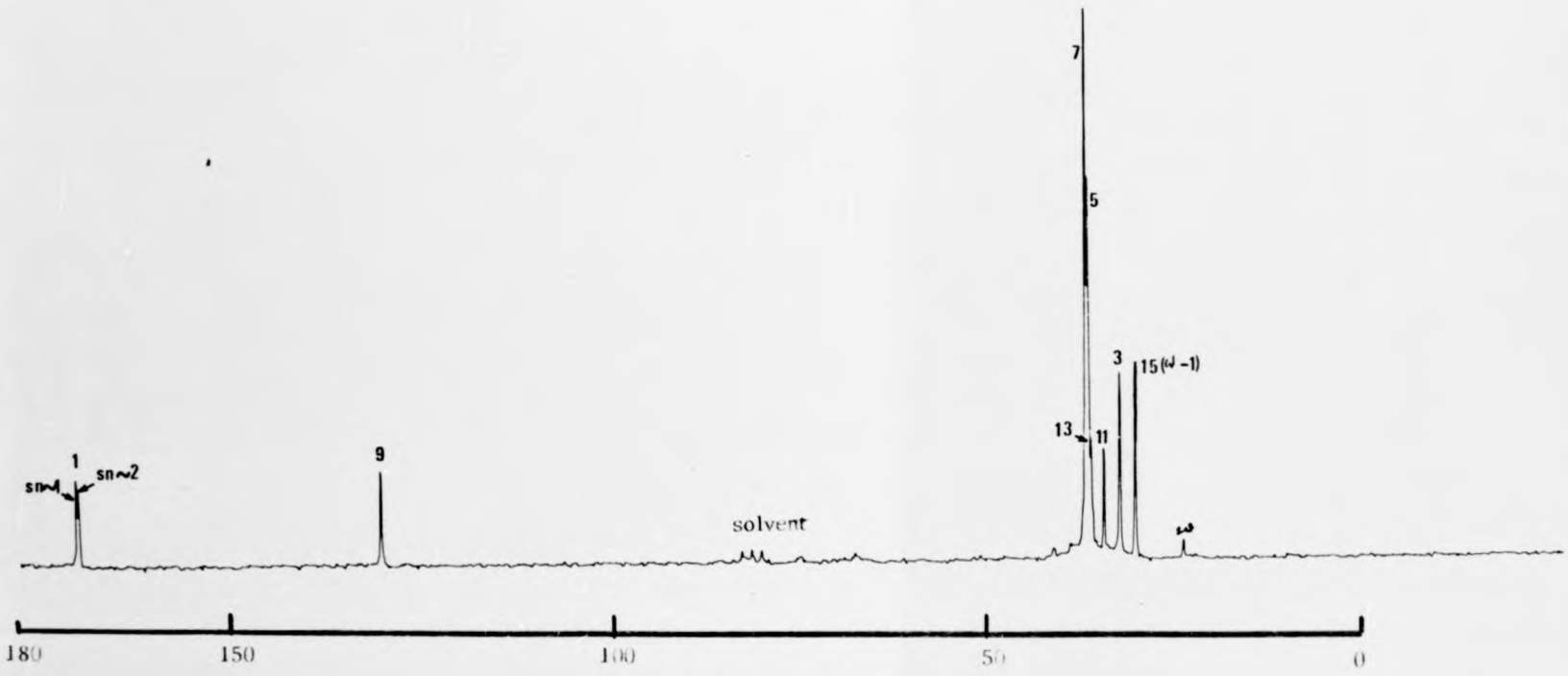

Fig. 16a 22.63 MHz ^{13}C n.m.r. of Phosphatidyl ethanolamine extracted from E.coli Y? grown on [1-^{13}C] acetate 5[illegible] FID's were Fourier transformed on 8K memory size at 40°C. Conc. 100 mgs/ml in [illegible]

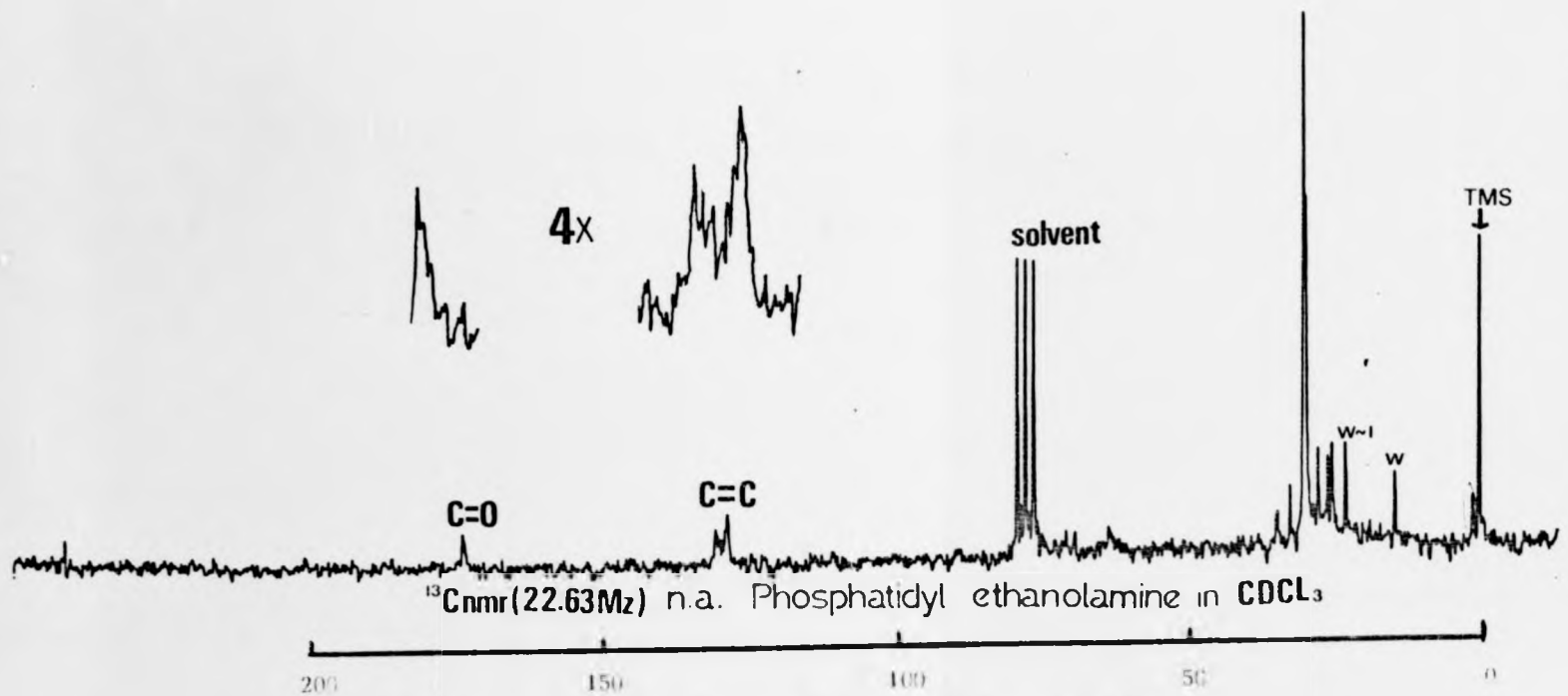

Fig.16b n.m.r. spectrum of natural abundance egg yolk PE. 100,000 FIDs were Fourier transformed on 8K. Conc. 150 mgs/ml at 40°C.

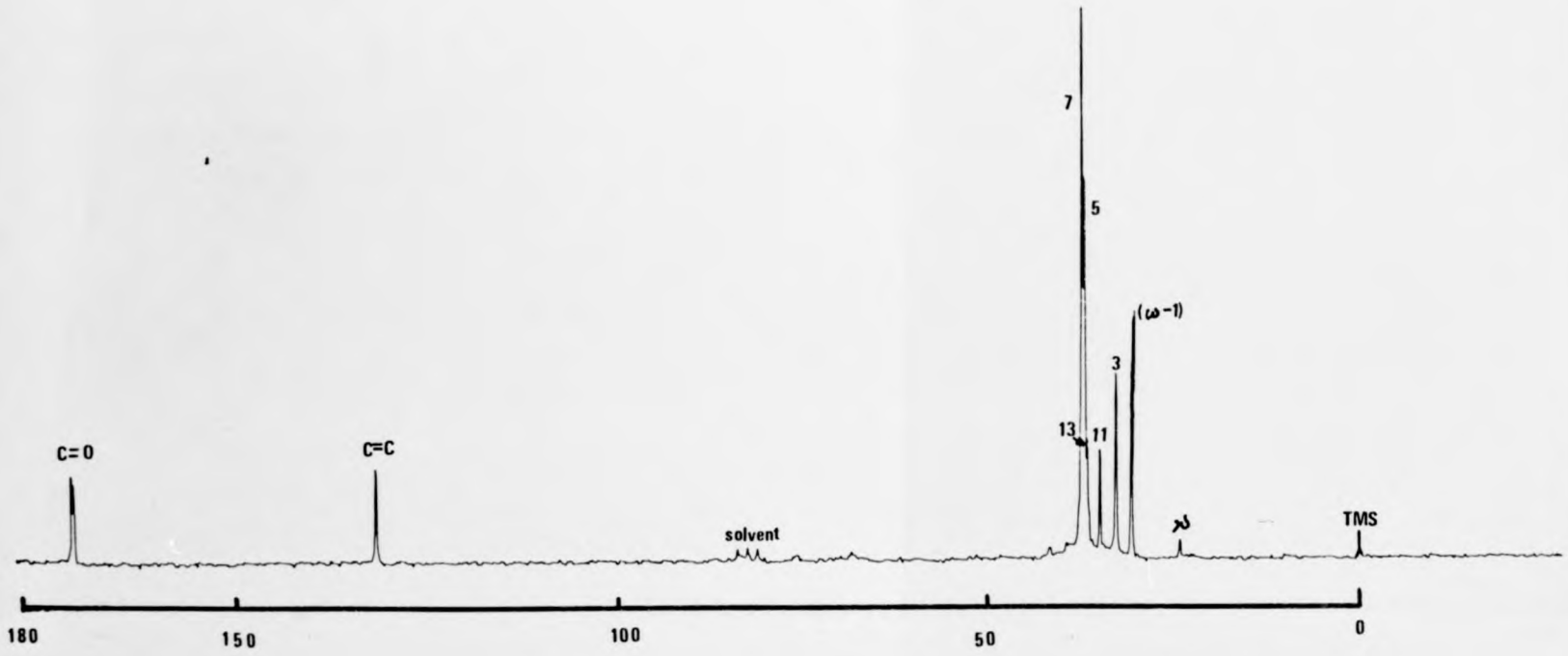

Fig.17 22.63 MHz ^{13}C n.m.r. spectrum of PE */PS (1) (w/w)

2000 scans were Fourier transformed on 8K

conc. 100 mg/ml in $CDCl_3$ at 40^{o}

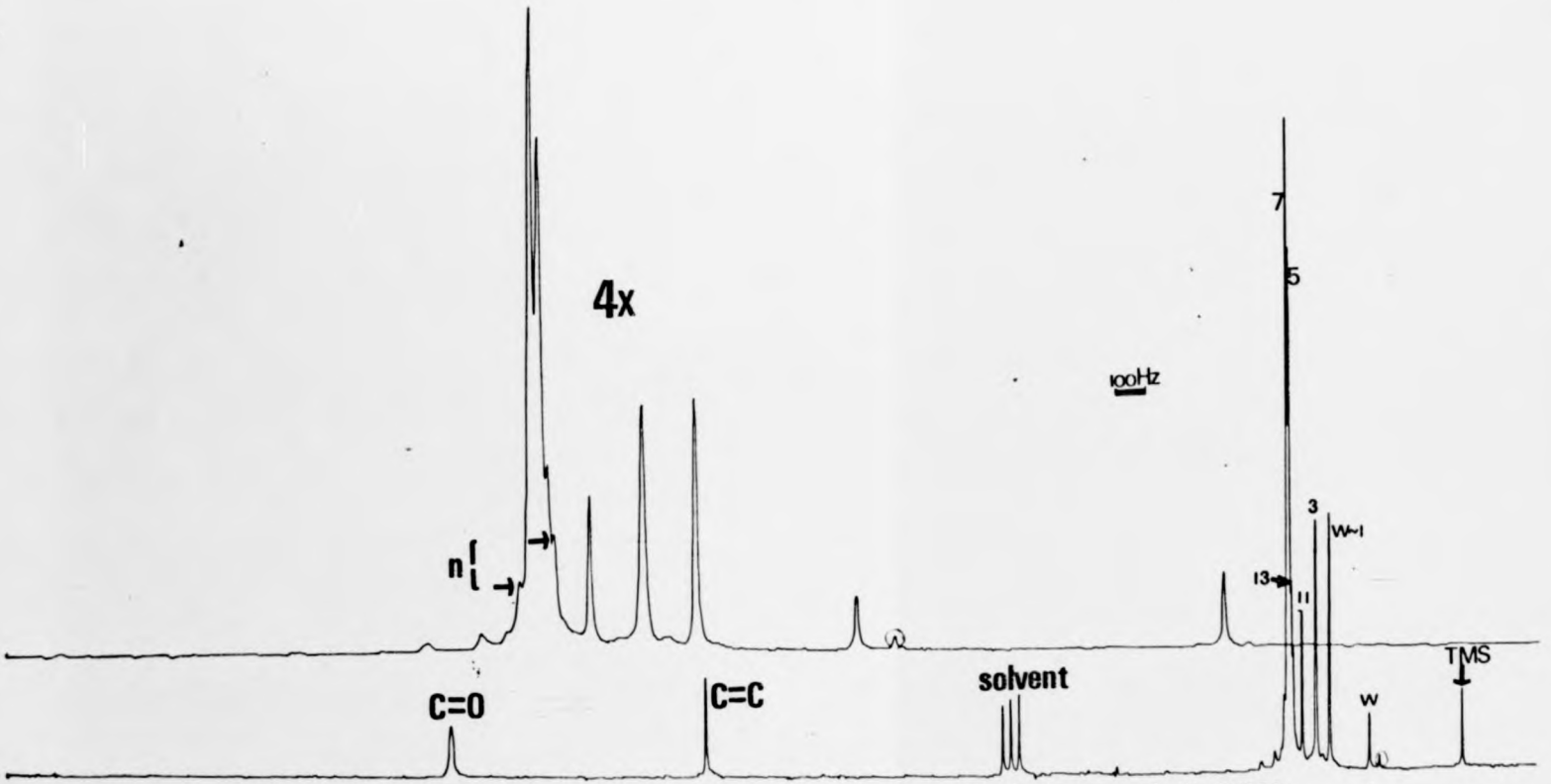

Fig. 18 22.63 MHz ^{13}C nmr of E coli DPG ($1\text{-}^{13}C$-acetate) in $CDCL_3$, 40°

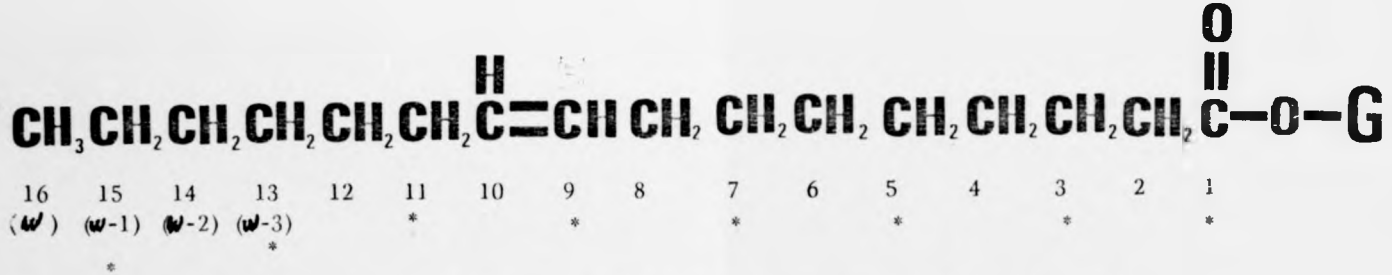

Fig. 19 Numbering system used in text as demonstrated on Palmitoleic acid. G represents either the sn -1 or sn -2 positions on a 3-sn-glycero phosphatide

* enriched sites when bacteria is grown on [1- ^{13}C] acetate

As a matter of convenience, peaks have been labelled assuming palmitoleic acid the principal fatty acid of the E.coli PE (see chapter 3). Since chemical shift is largely determined by adjacent functionality, the peaks labelled C(15) correspond to all ω-1 carbons of fatty acyl chains, C (9) corresponds to all odd-numbered carbons bearing a cis-olefinic function with saturated chains attached, C(11) corresponds to all odd-numbered methylenes α to a single olefinic function, C (3) corresponds to all carbons β to the carboxylate carbon and of course C(1) corresponds to all the carboxylate carbons. The observation that the ^{13}C shifts due to the C=O and terminal methyl of fatty acids is independent of chain length for fatty acids with more than nine carbon atoms has previously been reported (Levine et al., 1972 a).

There is no indication that the glycerol and ethanolamine carbons have been enriched in the preparation of PE [1 - ^{13}C - Ac]. The head group resonances are still at their natural abundance level or are not sufficiently enriched to give a comparable signal/noise, the inference being that acetate incorporation is probably at a "sub-phospholipid" level; the glycero-ethanolamine moiety is synthesized independent of acetate and at a later stage in phospholipid synthesis is used to esterify the fatty acids derived from acetate. It has been reported , however, that from the preparation of PE [2 - ^{13}C -Ac] of the same organism, the CH_2OCOR is enriched to about 50% of the level in other enriched carbons, suggesting that either there are two modes of incorporation of acetate or that scrambling of the label has taken place (Birdsall et al., 1974).

(ii) Spectra of aqueous dispersions

The ^{13}C spectra of sonicated lipid vesicles in aqueous dispersions (diameter ≤ 300 Å show fairly sharp resonances though somewhat broadened , $\geq 8Hz \leq 12Hz$. Large lipid bilayers (diameter $\geq 10^3$ Å) produce spectra

with much broader resonances, ≥ 25Hz (Levine et.al , 1972). Dipolar coupling with nearby nuclear spins , which unlike the applied magnetic field, lead to orientation-dependent local magnetic fields, is generally agreed to be the cause of such broadening. In the limit of very fast reorientational molecular reorganization, the fluctuating magnetic fields can only contribute inefficiently to the relaxation of excited nuclear states, leading to long lived states and the sharp lines observed for an isotropic liquid. Lipid bilayers fall between the extremes of solid and liquid behaviour in this sense. The treatment by Seiter and Chan (Seiter and Chan , 1973; Lichtenberg, et al.1973) satisfactorily accounts for lack of line narrowing due to incomplete motional averaging in the bilayer. A central issue in the Seiter-Chan treatment is the absence of isotropic motion. Fast motion is assumed about the phospholipid chain axes and slower rocking motions limited only to angles of $\sim 60 - 70^{o}$ away from the chain axis lead to incomplete rotations through all possible angles, thus preventing line narrowing to the degree observed in liquids.

The formation of bilayers with a small radius of curvature, e.g. by sonication, clearly causes an increase in the number of degrees of freedom, since the linewidth of the lipid resonances decrease. I have observed linewidths ranging between 8 - 10 Hz for the single carbon resonances of the sonicates used in these studies. Resonances outside this range were not observed except for the main methylene envelope which ranged between 12 - 18 Hz presumably due not to large macromolecular contributions but to low resolution of overlapping resonances. Bearing in mind the cautionary note that ^{13}C linewidths in general and especially of lipid dispersions, are not strictly speaking, reliable guides to elucidating molecular size, we see that linewidths of 8Hz are in good agreement with the molecular Stoke's diameter of ~ 210 Å obtained from

molecular sieve experiments.

The spectra obtained for some of the lipids studied in aqueous dispersion are presented in figures (20 and 21). It will be seen that in the main, apart from linewidth differences and the tendency to lower resolution and the consequent lower signal-to-noise ratios, the spectra are not significantly different from those obtained in organic solvents. In the ^{13}C n.m.r spectrum of egg yolk lecithin dispersion, Fig. 21. the approximation has been made again, that the fatty acid in greater abundance is contributing most of the observed signal-to-noise. Here oleic acid is assumed the principal unsaturate and we have the peaks labelled C(18), C(17) and C(16) corresponding to all ω, ω-1 and ω-2 carbons respectively. C(9) and C(10) correspond to all cis-olefinic carbons with saturated chains attached, while(δ) and C(11) correspond to all methylenes α to a single unsaturated site. The peak marked 'a' is that due to an olefinic carbon β to a second unsaturated site (Batchelor and Prestegard, 1972).

The ^{13}C chemical shifts observed in vesicles are very similar to those observed in chloroform solution, Table 6 . Batchelor and Prestegard (Batchelor and Prestegard, 1972) have shown that although solvent effects on methyl groups can be significant, similar effects on methylenes are negligible and effects on methine carbons are $\leq$ 0.2 ppm. More sizeable shifts may however occur linked with the temperature dependent rotational isomerization about carbon-carbon bonds (Grant and Cheney, 1967).

The trans isomer is usually the low energy isomer for C-C bonds in both liquid hydrocarbon solutions and in the hydrocarbon portion of a fully saturated lipid bilayer. One would therefore expect that a downfield shift would result as temperature is lowered and the trans states are populated to a greater extent. Moreover, the shifts in vesicles should be more pronounced as the Chapman transition (crystalline $\rightleftharpoons$ liquid-

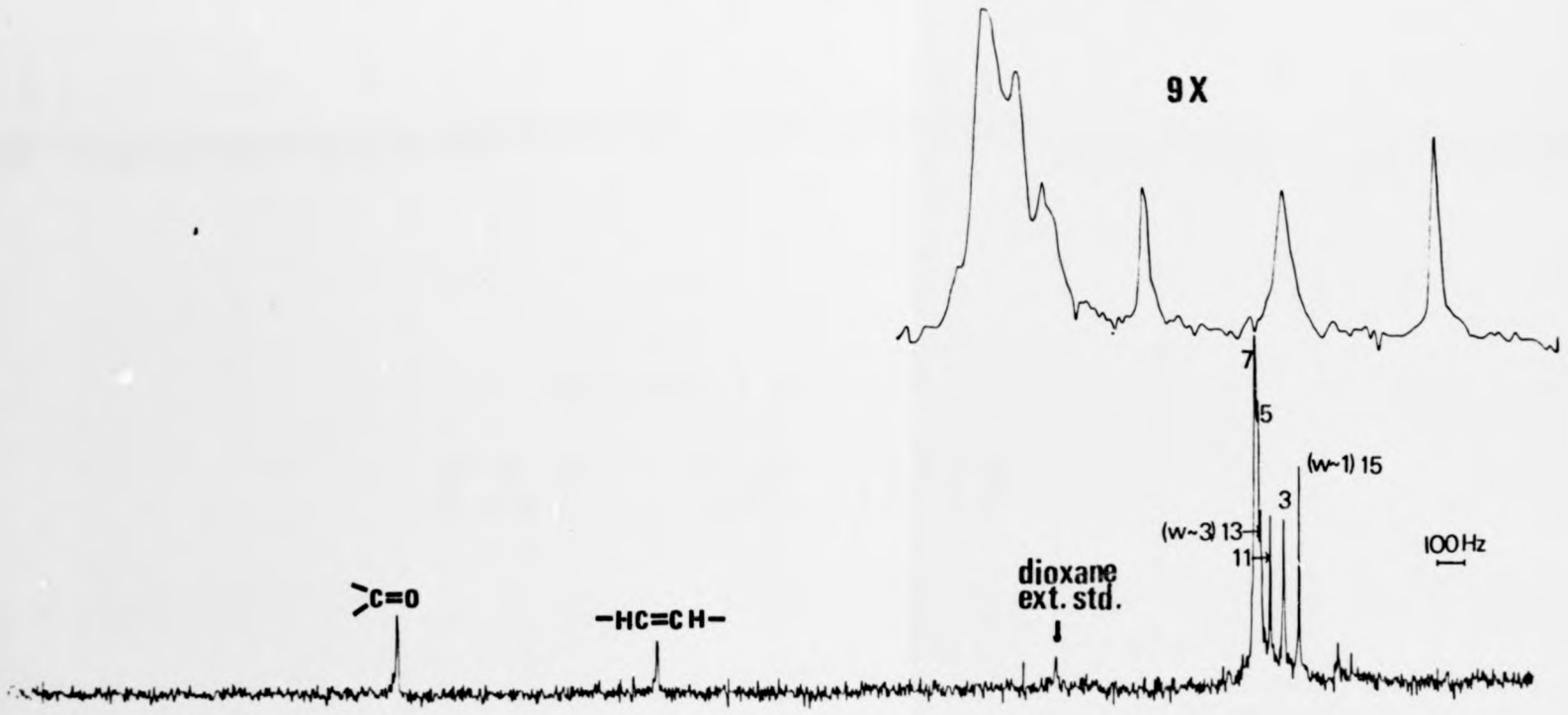

Fig. 20 22.63 Mz ^{13}C nmr PE*/PS (1:1) sonicated dispersions 45 ^{o}C

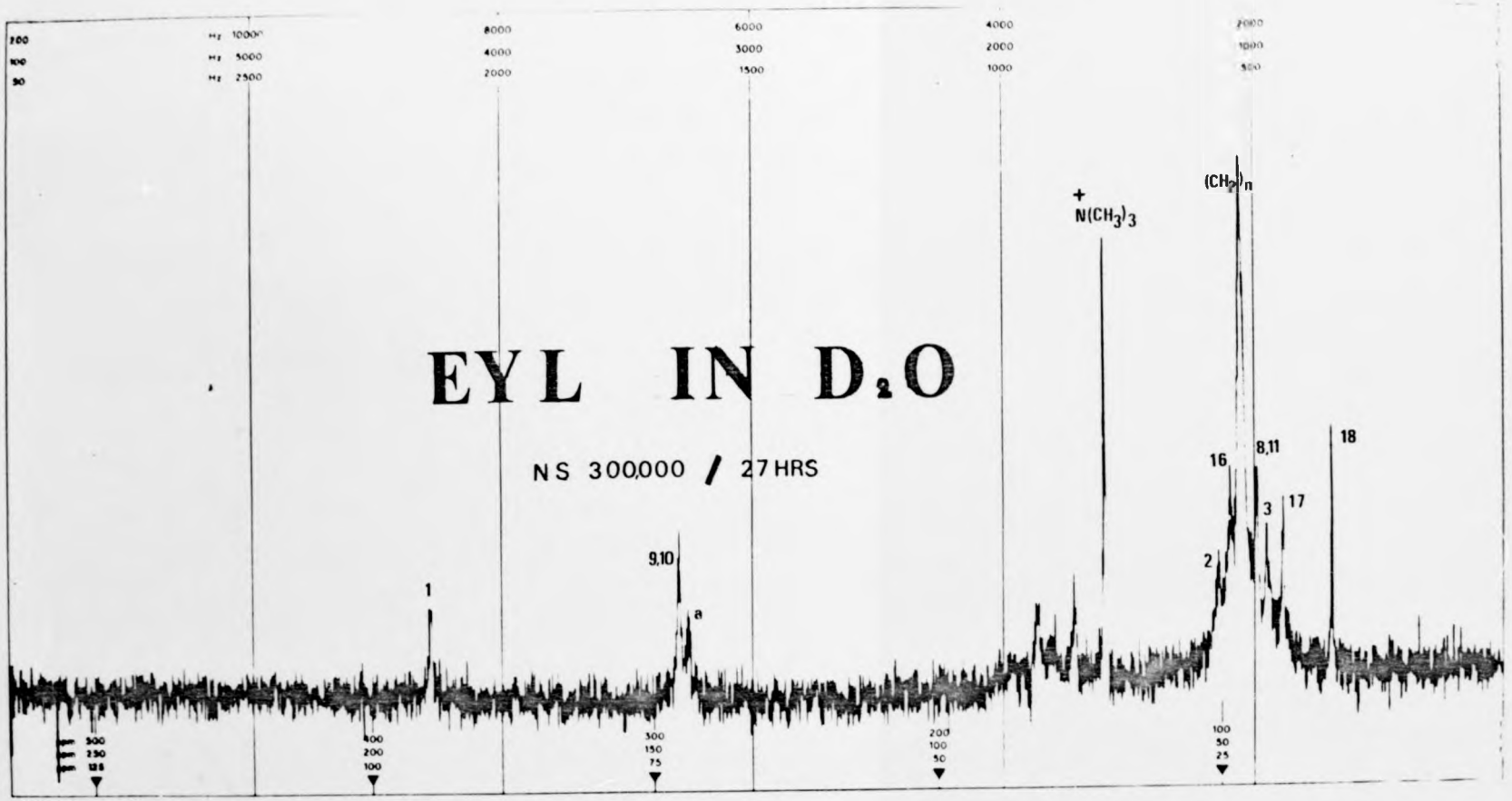
EYL IN D2O
NS 300,000 / 27 HRS
+
N(CH3)3
(CH2)n
1
9,10
a
2
16
3
8,11
17
18

Fig.21. 22.63MHz Natural Abundance ^{13}C n.m.r. at $40^{o}C$ of a 10% (w/v) Egg-yolk lecithin disperson in D_2O.

crystalline transition) is approached. This is probably because the bilayer as a distinct structural entity compared to any other structures to be found in hydrocarbon solutions, may impose peculiar conformational restrictions upon the C-C bonds. Thus, although detailed analysis of the chemical shift dependencies may yield information concerning the conformational states of the molecules in the bilayer, I have deliberately concentrated more on the measurement of spin-lattice relaxation times (T_1), given the nature (information about the fluid/dynamic states in the vesicles) of the questions I set out to answer.

E ^{13}C NMR OF MIXED LIPID VESICLES

It was desirable to establish whether any alterations occur in the observed ^{13}C n.m.r. spectra of the vesicles with temperature or at any rate, over the temperature range for which spin-lattice relaxation times were desired. Towards this end, I took the mixed lipid systems of interest [^{13}C-enriched E.coli PE/ox-brain PS (PE^*/PS) and ^{13}C-enriched E.coli PE/synthetic DPL (PE*/DPL)] through their respective Chapman transitions and above. The spectra obtained are shown in figures (22 and 23). Certain points of similarities exist in both runs and they deserve comment. The first is that both spectra show only the resonances due to the odd carbon enriched phosphatidyl ethanolamine of E.coli , although the phosphatidyl ethanolamine is only one half the total phospholipid content of each system. Thus we would expect that any temperature dependent differences that may be picked up will be chiefly due to the extent to which the other lipid component in each system has influenced the observed PE^* spectrum. The second point of similarity in both runs is that , consistent with observations on lipid phase transitions, both spectra undergo considerable line broadening near their respective "melting" points. In the case of the PE*/PS system, the position of extreme "motional arrest" as determined by extreme line broadening , seems to be around the 15^oC

Table 6: ^{13}C chemical shifts of PE^*/PS (1:1 w/w) and PE^*/DPL (1:1 w/w) in $CDCl_3$ and buffer at 45°C.

Resolved resonances along acyl residue	$CDCl_3$		Buffer	
	PE^*/DPL	PE^*/PS	PE^*/DPL	PE^-/PS
C1 α	174.1	173.8	173.8	173.3
C1 β	173.6	173.4		
C3	25.5	25.5	25.3	25.6
C5	29.5	29.6		
C7	30.2	30.2	30.0[b]	29.8[b]
C9	129.8	130.0	130.0	130.1
C11	27.6	27.7	27.8	27.7
C13	29.9	30.0		
(ω-1) C15	23.2	23.1	22.9	23.0
(ω) C16	-	-	15.8	16.0

b estimated for C5, 7, 13 envelope.

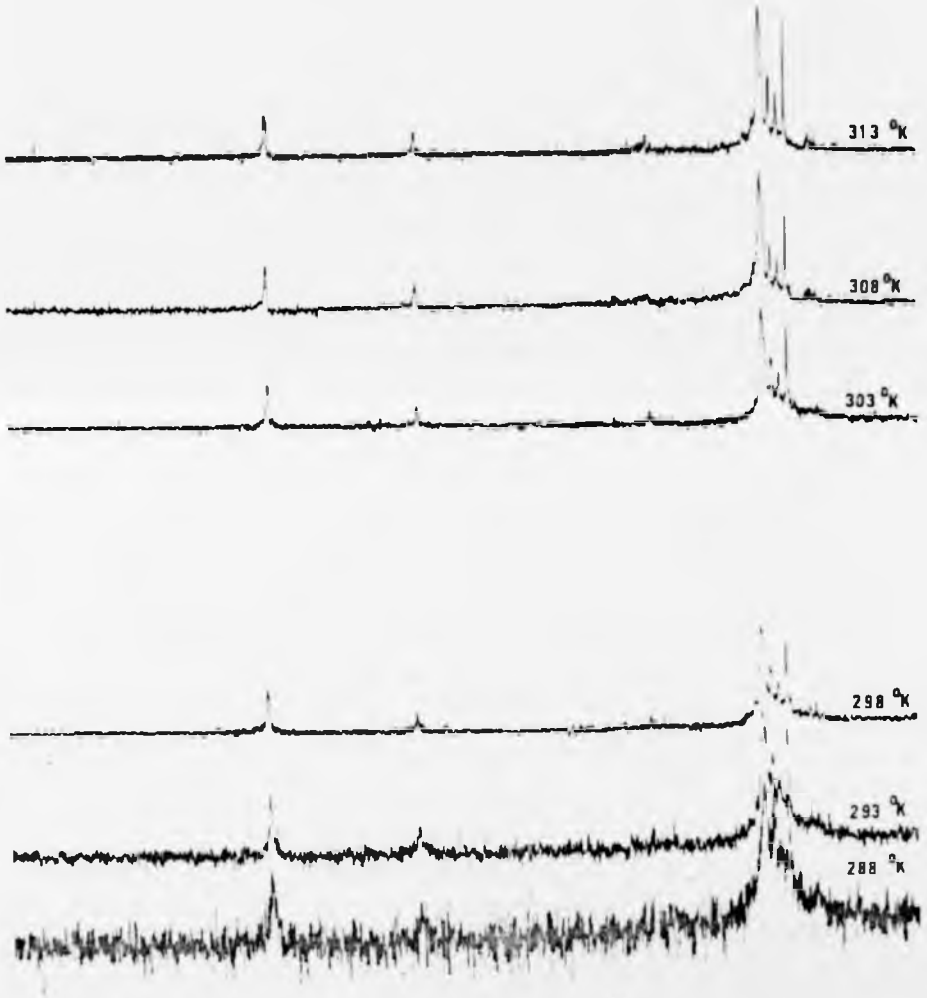

Fig. 22 22.63 MHz ^{13}C n.m.r. spectrum of PE*/PS (1:1 w/w) sonicated dispersions in 40 mM Tris-Cl, 100 μM edetate pH 9.0. Temperature was varied from 15 - 85°C in 5° steps.
Conc. 100 mg/ml. 100 FIDs were F.T.d on 8K for each spectrum

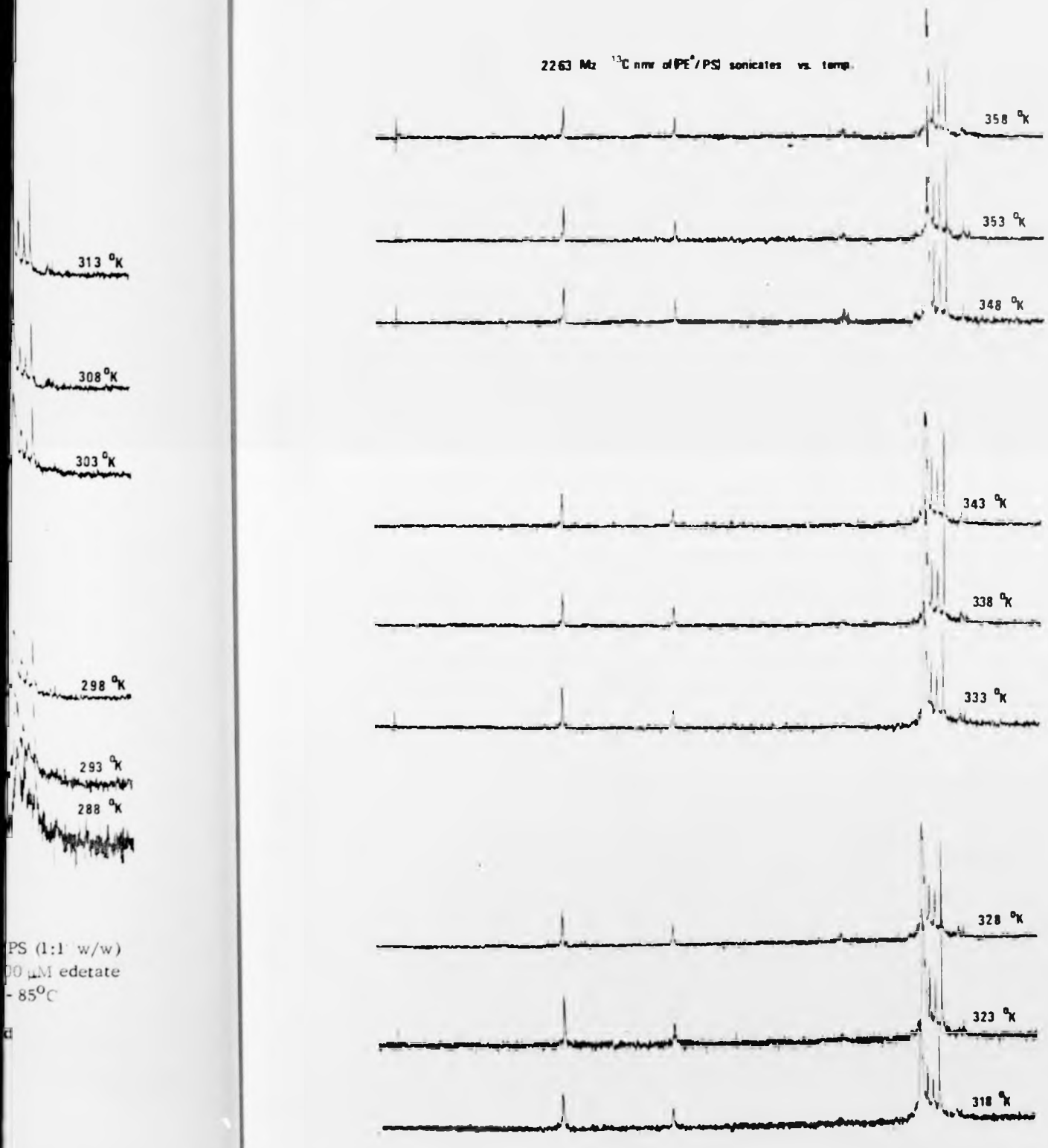

PS (1:1 w/w)
00 μM edetate
- 85°C

Fig. 23a

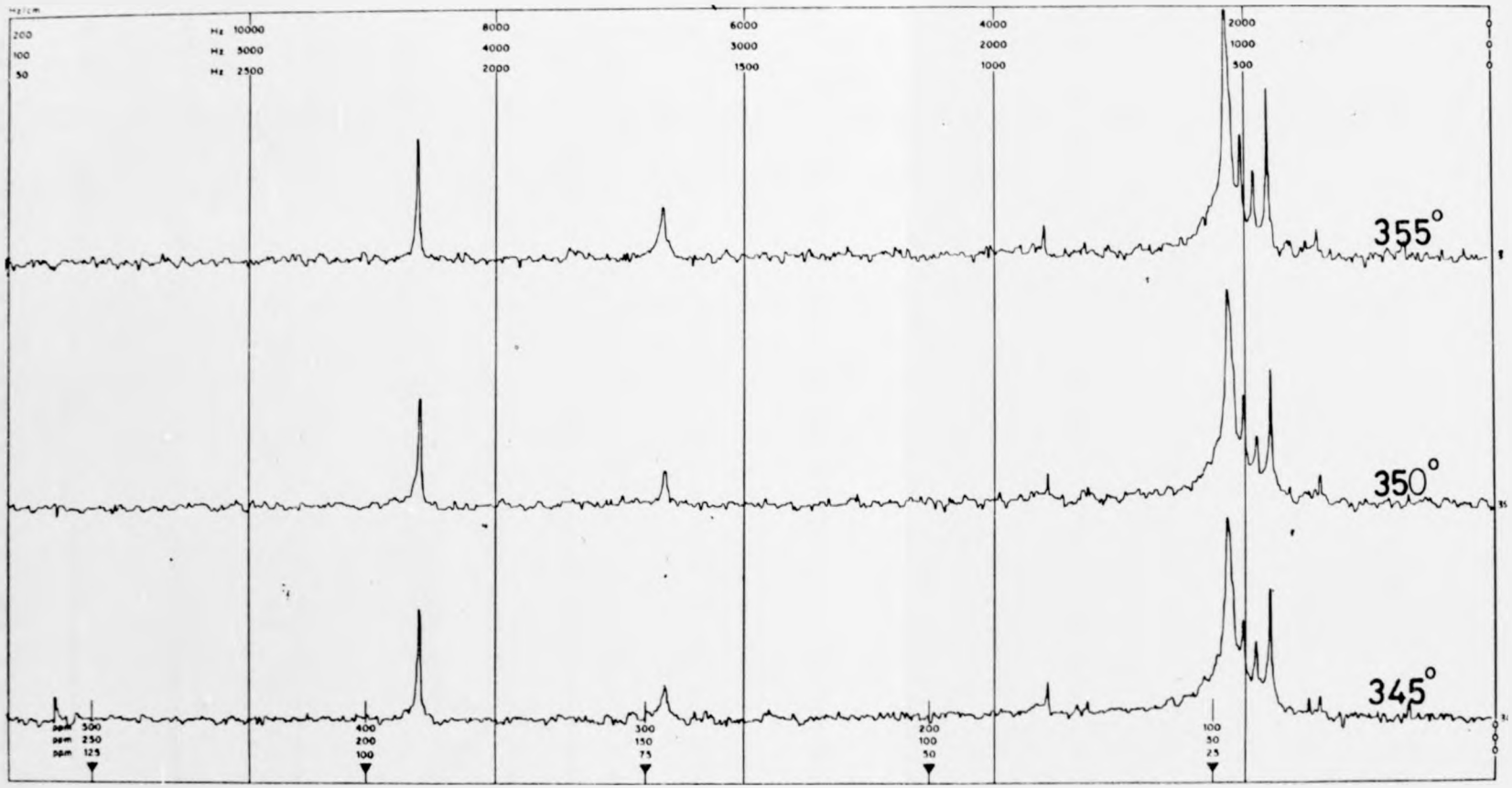

(Fig. 23b)

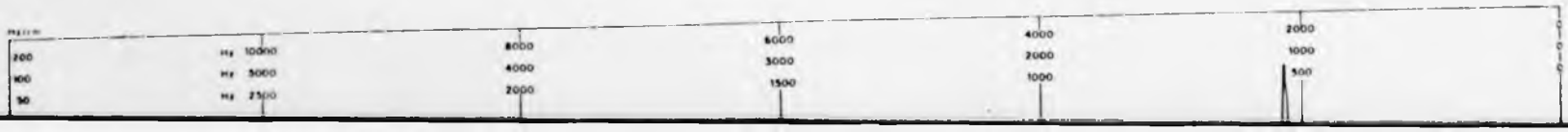

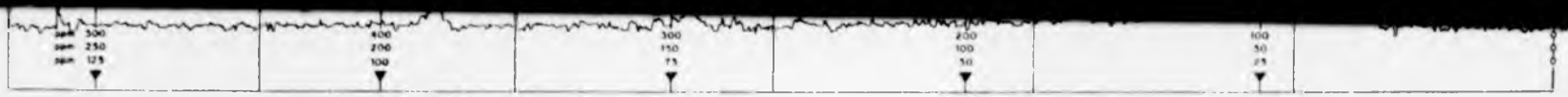

Fig. 23(a)

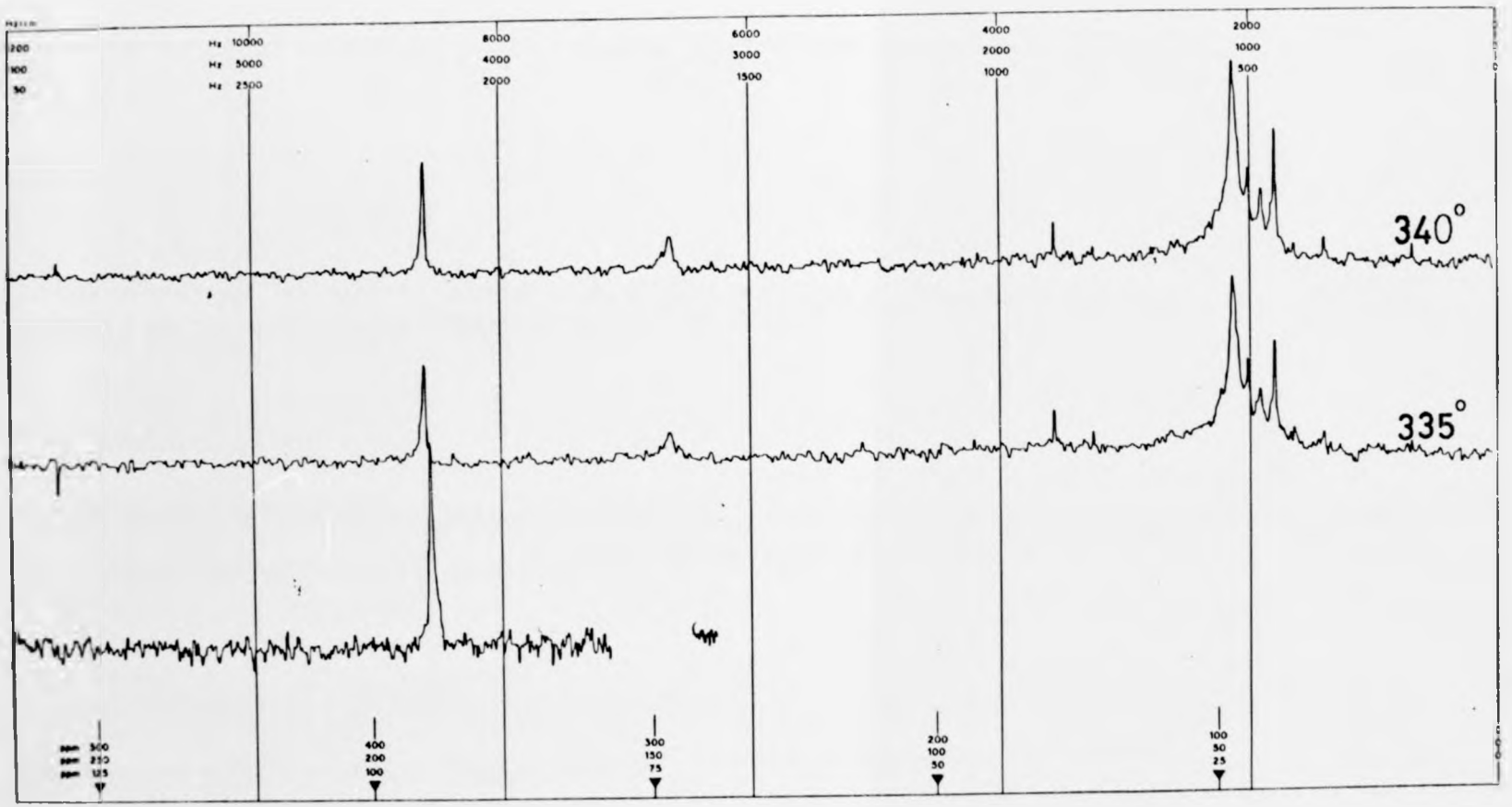

Fig. 23(b)

Fig. 23c

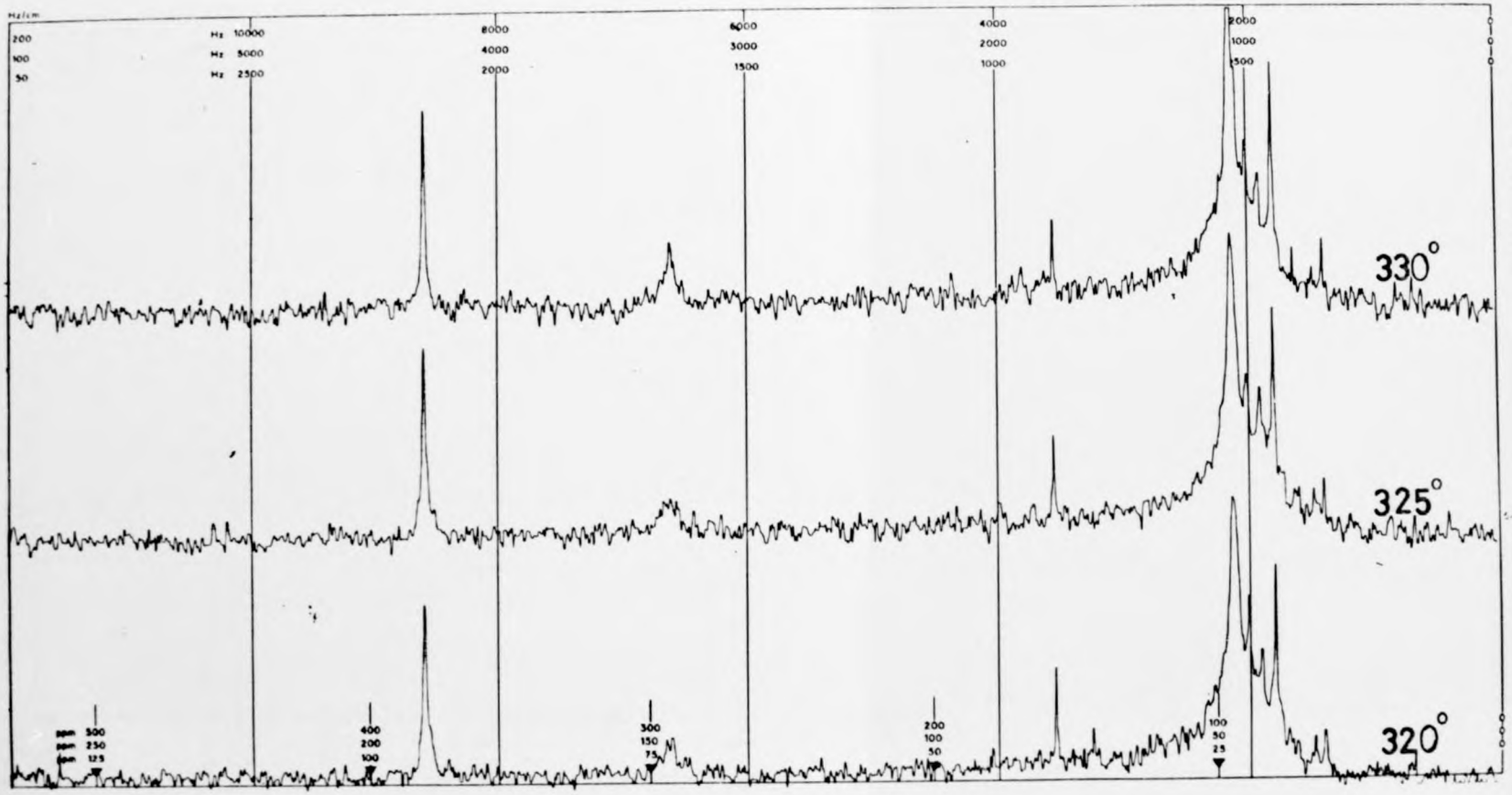

Fig. 23 (c)

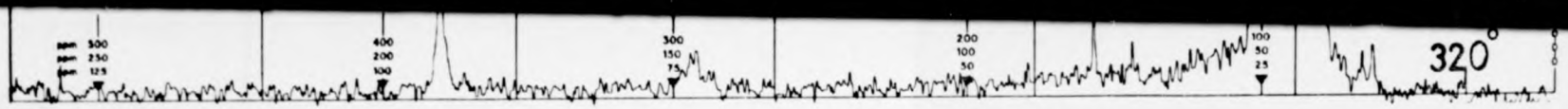

Fig. 23 (c)

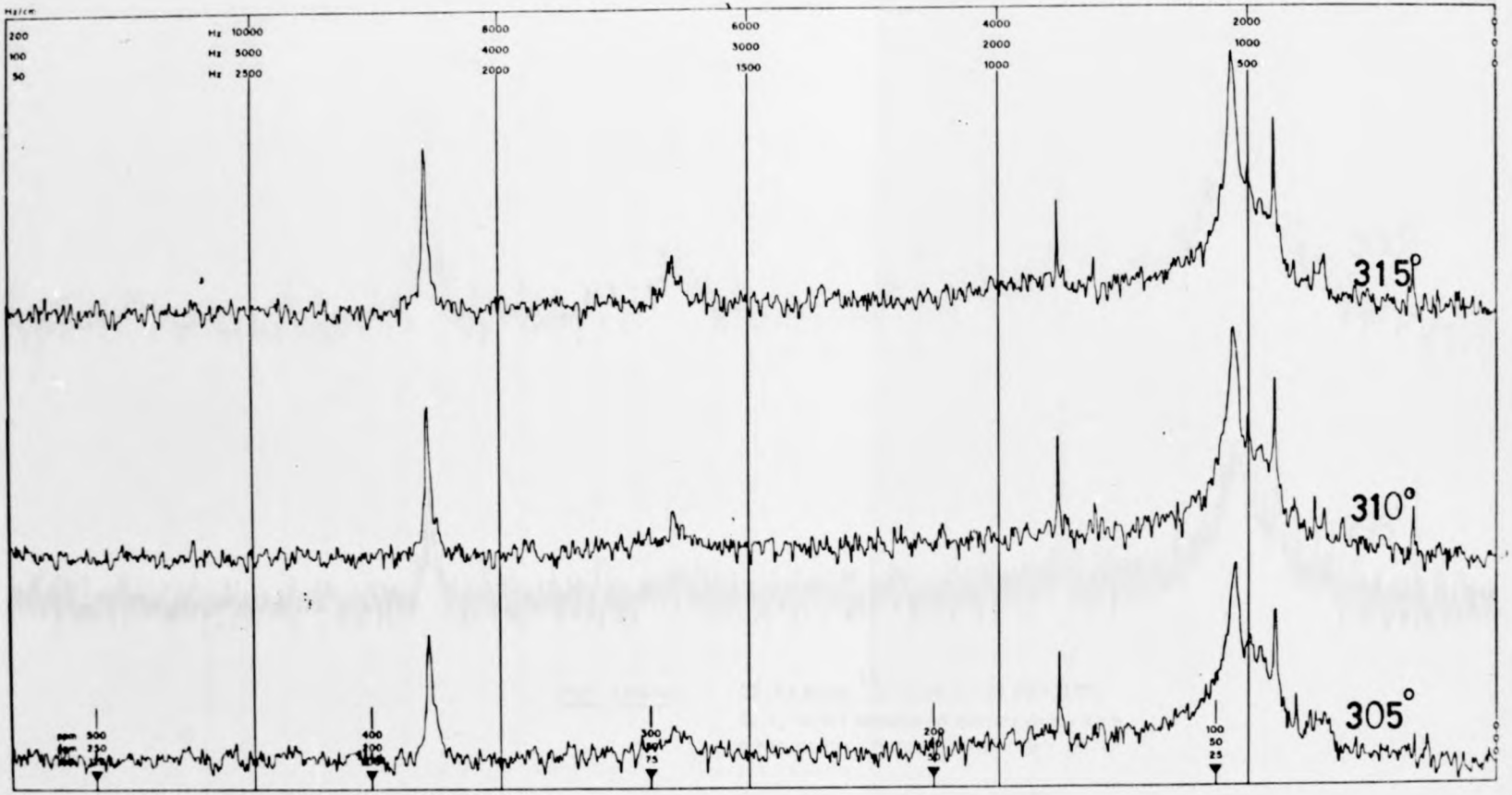

Fig. 23 (d)

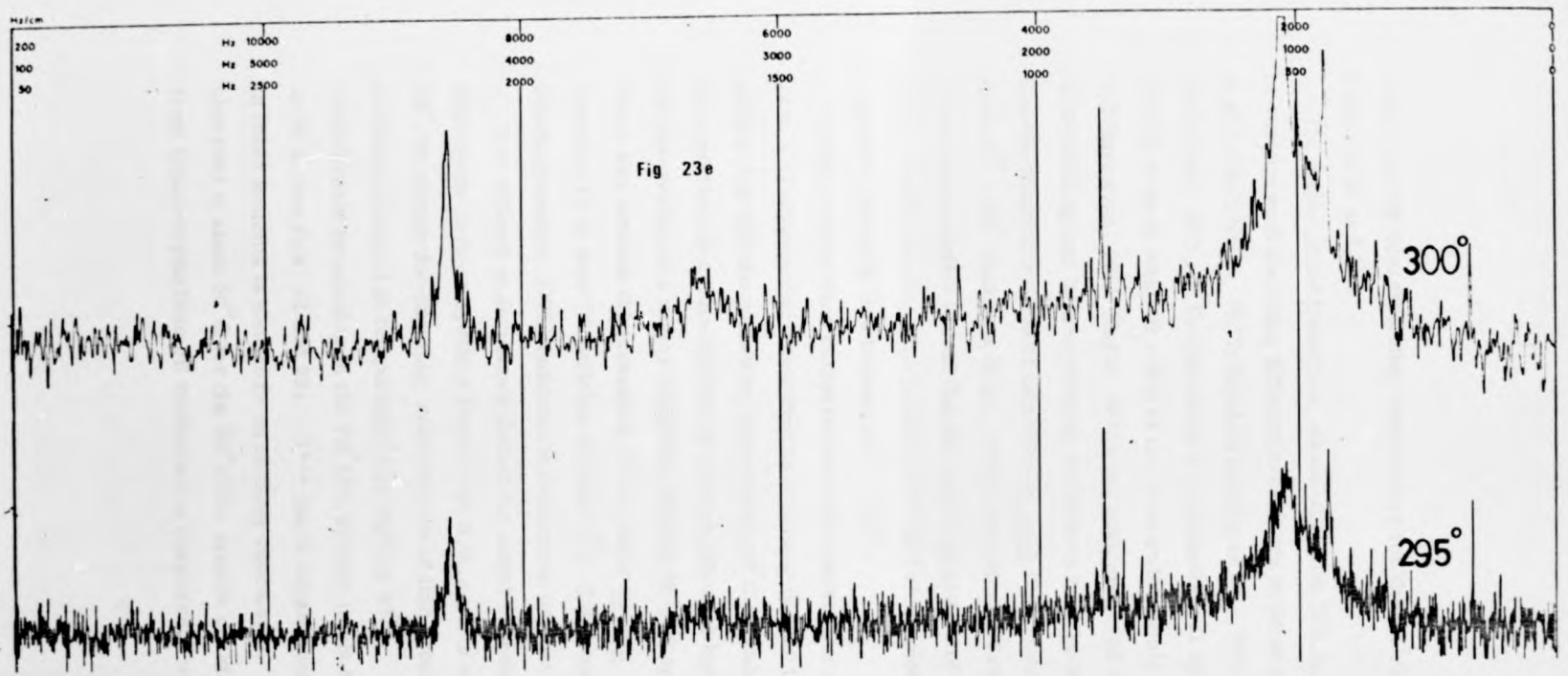

Fig. 23(a-e) 22.63 MHz ^{13}C n.m.r. of PE*/DPL (1:1, w/w) sonicated dispersions as a temperature function from 22 - 85°C

Conc. 100 mg/ml in usual buffer.

mark and the corresponding temperature for the PE*/DPL system seems to be at 32°C.

The major phase transition, associated with DPL has been estimated by various workers using different techniques to be at about 41° (Chapman et al., 1967; Nagle, 1973; Papahadjopoulus et al., 1973 and Shimshick and McConnell, 1973). Furthermore a pretransition at about 30° which is thought to be at least 10 - 20% of the main endothermic transition (Hinz and Sturtevant, 1972; Nagle, 1973) has been observed for this system. Spin-labelling and light-scattering techniques have been used to show that the phase transition of extracted E. coli membrane lipids range from 13° - 38° (Sackman et al., 1973; Overath and Träuble, 1973). In fact these studies reveal that the phase transition of the trans- 16:1 lipids, which constitute the predominant acyl chain moiety in this organism, actually lies between 24° - 28°C.

These results when compared with the spectra recorded in figures 23 (a - e) suggest that a fair degree of mixing occurs in the PE*/DPL system and that the transition observed at 32°C is probably due to a co-operative co-crystallization of the two different lipids. Similarly the observation of a major transition for the PE*/PS system at ~ 15°C which lies between the transition of the major E. coli lipids and reported Tc in pure PS vesicles at about 5°C (Jacobson and Papahadjopoulus, 1975) indicates a reasonable amount of mixing.

It is difficult to accurately define the extent of these phase transitions in these systems from these n.m.r. data alone. In the PE*/PS system for example, some degree of line broadening has probably occurred at temperatures as high as 40°C. Similarly considerable broadening in the PE*DPL system might have occurred at 50°C (see figs. 22 and 23). That phase separations are unimportant in these systems is therefore an unlikely conclusion. The signal-to-noise observed at about 30°C for the PE*/DPL system could therefore arise from liquid-crystalline PE molecules in coexistence with a "frozen"

matrix of dipalmitoyl lecithin molecules, as previously suggested by Birdsall et al.,(1974). This view derives directly from the earlier interpretation of Philips et al., (1970) that the broadening of the endotherm of mixtures of PE and PC indicates the presence of clusters of gel and liquid crystalline lipid in the bilayer.

On the other hand, our relaxation time studies on the PE*/PS vesicles and other n.m.r. data in the literature, especially the work of Seelig and Seelig (1974 and 1975) show that at any temperature different portions of the chain may possess different degrees of ordering. The order associated with the carbons near the lipid-water interface is thought to be greater than that in the middle of the bilayer. If this implies that different segments of the lipid molecule in the bilayer "freeze" at different temperatures, then n.m.r. and, in particular, ^{13}C n.m.r. is particularly suited to these studies. This may explain the observation that all the resolved resonances in figures 22 and 23 are not broadening at quite the same rates, although a general broadening of the spectrum of each of the mixed lipid systems is observable with the onset of the main transition. For example, the rates of broadening of the olefin carbon at C 9 and of the main methylene carbons at C 5, 7 and 13 appear to be considerably faster than for any of the terminal carbons, say, the ω - 1 resonance. This difference is particularly more pronounced in the PE/DPL system, (figure 23).

This observation, if true, may have interesting consequences in biological function in natural membranes. It is possible, for instance, that a "frozen" portion of the bilayer could act as an exclusion mechanism for a particular permeant molecule which then moves into regions of the bilayer containing more "fluid" phospholipid segments.

Certain differences in the ^{13}C n.m.r spectra as a function of temperature are found for the

two lipid systems. For instance, the different temperatures at which the main transition is observed in the two systems and secondly the differential rates of broadening associated with the olefine region in the two systems (in the PE*/DPL system the olefine has almost disappeared into the base line at $\sim 42^{\circ}$ while the corresponding temperature in the PE*/PS system is at $\sim 25^{\circ}$). Another obvious dissimilarity in the two spectra is the resolution observed in each case, especially at higher temperatures. The resolution associated with the spectrum of the PE*/PS system is consistently of a higher order of magnitude than that found in the spectrum of the PE*/DPL system. This is indirect evidence corroborating the size of the PE*/PS vesicles as determined by molecular sieve chromatography ~ 210 Å, to be less than that observed by other workers (Sheetz et al., 1972; Finer et al., 1972; and Litman, 1973), for the PE*/DPL system ~ 250Å . Furthermore, this is consistent with the hypothesis of a more "fluidized" packing of acid phospholipids at higher pH values than neutral or zwitterionic phosphatides (Trauble and Eibl, 1974; Jacobson and Papahadjopoulos, 1975). At temperatures above 45°, the spectrum of PE*/PS shows up to about eight carbons resolved comparable to the situation in organic solvents, whereas the maximum number of resolved resonances observed for the PE*/DPL system was six. It must be mentioned that these temperature associated changes were completely reversible over the temperature range studied. Checks for products of any major chemical degradation, using thin-layer chromatography, showed on occasions only minor trailing associated with the main spots. This could very well have been due to varying chamber humidity conditions during the chromatographic process, rather than actual chemical degradation of the lipid species.

F. ^{13}C SPIN-LATTICE RELAXATION TIMES (T_1)

(i) ^{13}C spin-lattice relaxation mechanism

Relaxation of nuclei in lipid molecules dispersed in water is complicated by the fact that internal motion of the molecules within the isotropically

tumbling vesicle occur with frequencies comparable with the resonance frequencies of the absorption phenomenon (6.28×10^8 and 1.57×10^8 radians per sec for proton and carbon-13 nuclei respectively). Detailed considerations of such motions with examples have been treated elsewhere (Woessner, 1962: Wallach, 1967; Wallach, 1969). Isotropic tumbling of the vesicles as a whole cannot be significant in $^{13}CT_1$ determinations because they will tend to predict a common relaxation time for all the carbons in the molecule which will not be consistent with experimental observations (Metcalfe et al., 1971; Levine et al., 1972). Besides, calculations based on the Stokes-Einstein equation give approximate rates of about 10^6/sec for these tumblings leading to correlation times too long for the region of interest.

Implicit in the anisotropy of the bilayer system is that several types of motions are occurring (cooperatively or non-cooperatively) simultaneously in the molecules. One obvious possibility is rotation of the whole molecules about its long axis estimated from ESR experiments to have a correlation time of about 10^{-8}-10^{-9} sec. This motional component may be important in determining the range of observed T_1s but it is not sufficient to account for the observed gradients in T_1 since rotation abouts its long axis with the molecule behaving as rigid rods will lead once again to a common T_1 value for all the nuclei. There is therefore the need to consider motions about the individual carbon-carbon bonds. The mechanism of ^{13}C relaxation times has been shown to be dominated by predominantly dipole-dipole interactions and especially in hydrocarbons, carbon-proton dipolar interactions (Farrar et al,1972).

Dipolar relaxation in the bilayer can occur either inter-molecularly or intramolecularly. The former involving relaxation by dipoles in a different molecule from the molecule bearing the nucleus under consideration

and as such is determined by, among other factors, the intermolecular separation and the lateral diffusion rate. Intramolecular dipolar relaxation is not on the other hand as dependent on the translational motions in the bilayer. The closest distance of approach of two diffusing molecules has been estimated to be of the order of 5 Å (Bloembergen et al., 1948; Burnett and Harmon, 1972) and this is at least one C - H bond length short of the separation between the carbon atom of one chain and the dipoles in another, meaning that intermolecular dipolar relaxation of the ^{13}C nucleus can only make a minimum contribution to the total relaxation experienced by the nucleus. Intramolecular relaxation and especially of directly bonded protons appears to be the chief relaxation mechanism. The intramolecular dipolar relaxation of a carbon nucleus by a directly bound proton has been given previously by Abragam (1961).

The Abragam treatment does not account for the heterogenous molecular motions in an anisotropic system directly, because the correlation time defined in the equation is only representative of the effective sum of the contributing correlation times.

We obtain, however, a direct empirical relationship between spin-lattice relaxation time and molecular motion in the expression

$$T_1 = f(1/\tau_e) \qquad \text{———} \qquad (6)$$

where τ_e is the representative of the effective sum of the participating molecular motions. Our arguments above have emphasized the relative contributions of the different correlation times to T_1; they do not preclude any motions completely and so we must express the effective correlation time τ_e as a function of all other correlation times in the system. From the introduction, we have seen that a variety of motional

possibilities are available to the molecule in the bilayer viz-a-viz, rotational motion about the long axis of the molecule, oscillatory motions within a conformation, trans-gauche isomerizations about the C - C bonds and precessional motions about the long axis of the molecules, with the always present tumbling motion of the vesicle as a whole. These will expand the τ_e term in equation 6 to read :

$$T_1 = f\left(\frac{1}{\tau_r} + \frac{1}{\tau_o} + \frac{1}{\tau_i} + \frac{1}{\tau_p} + \frac{1}{\tau_t}\right) \quad \text{——} \quad (7)$$

We can simplify equation (7) by including all the motions of the molecule within the vesicle in a common embrace as determinants of internal motion, and so equation (7) will now read

$$T_1 = f\left(\frac{1}{\tau_i'} + \frac{1}{\tau_t}\right) \quad \text{————} \quad (8)$$

where τ_i' is the correlation time characterising the average of internal motions and τ_t characterises the tumbling of the vesicles. We have deliberately left out terms due to translational or lateral diffusion and transverse or flip-flop diffusions since these are more relevant to inter-molecular relaxation. The contributions of each of these motions to the observed T_1 of each carbon of the fatty acyl chain will vary depending on the location of each carbon along the length of the chain. Besides, it is impossible with the available data to calculate the separate contributions due to each of these motions. Since we have shown earlier that τ_t is relatively unimportant in determining T_1, we see that the observed T_1's are good guides to the internal motions of each of the carbon atoms within the phospholipid molecule in the bilayer and therefore a direct index of their behaviour in the immediate micro-environment. This is the evidence for ^{13}C T_1 as an index of molecular motions in the bilayer.

(ii) ^{13}C T_1 of lipids in non-polar solutions

^{13}C T_1 for nuclei in lipids are characteristic of the type of structure that is formed. Information on the micellar behaviour of phospholipids in solvents of low dielectric constant are provided by the work of Elworthy (Elworthy, 1959; Elworthy and McIntosh, 1964). In chloroform solutions, Chapman and Morrison (1966) observed that the choline proton n.m.r. resonance of synthetic lecithins was significantly narrowed when a drop of D_2O was added to the solution. Furthermore, Walter and Hayes (1971) observed that the effect was more pronounced if H_2O was added instead of D_2O . The only possible explanation was that the choline head group was in a restricted environment (in this case inverted micelles) and that part of the driving force for the formation of these structures was disrupted by hydration forces when the hydrophilic regions came into contact with added water. Since then, direct evidence for the inverted micelle structure in terms of reduced T_1 values for the choline headgroup have been obtained (Lee et al., 1971; Levine et al., 1972). The ^{13}C T_1 values I have observed in deuterio-chloroform solutions show a gradient of increasing molecular motion from the glycerol backbone towards the terminal methyl of the acyl chain, Figure 24a and Table 7 . Furthermore, correlations with the nature of the micelle formed in this solvent by different phospholipid species and mixtures are observed. T_1 values have been obtained for three lipid systems in chloroform at $45^{\circ}C$ and at a total lipid concentration of 10% w/v. In the first determination, T_1 values were measured for PE * alone. The other two measurements were for mixed lipid systems of PE*/PS (1:1) and PE*/DPL (1:1) under identical conditions. In all these measurements enriched PE [1-^{13}C-Ac] from E.coli, was used so that only resonances from the labelled carbons of the PE have been observed. Table 7 shows the distribution of T_1 for the three different systems. There is a systematic increase of T_1 from the C(3) towards the C(15) carbons in

TABLE 7

^{13}C T_1[a] VALUES FOR PHOSPHOLIPIDS IN NON-POLAR[b] SOLVENTS AT 45°C

PHOSPHOLIPID TYPE	CARBON NUMBER OF ACYL CHAIN					
	C1	C3	C5,7,13	C9	C11	C15
PE	1.13 ± .04	0.27 ± .02	0.68 ± .03	1.04 ± .04	1.18 ± .03	2.88 ± .04
PE*/PS	2.10 ± .05	0.42 ± .01	0.88 ± .01	1.15 ± .03	1.26 ± .02	3.68 ± .05
PE*/DPL	2.12 ± .03	0.41 ± .03	0.82 ± .04	1.16 ± .03	1.28 ± .02	3.64 ± .05

[a] Errors are std. deviations of slopes of T_1 through at least seven points . T_1 reproducibility is within 10% .

[b] Deuteriated chloroform.

T_1 (secs)

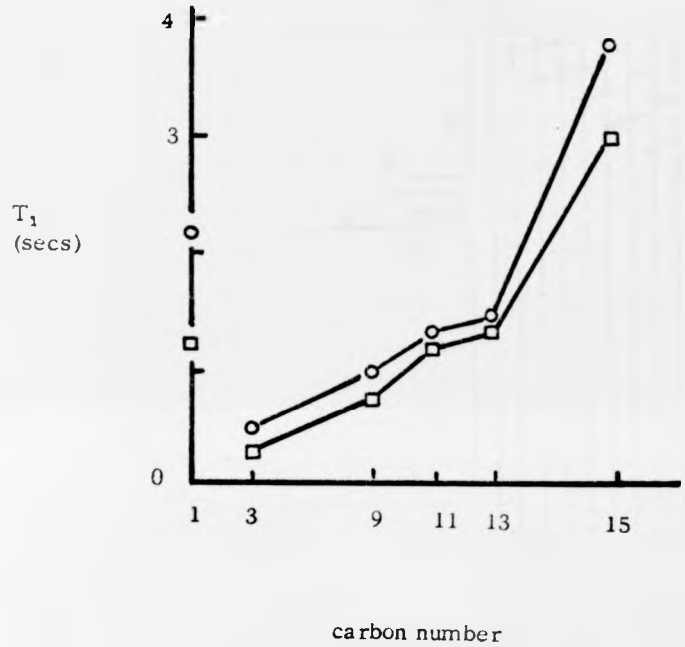

Fig. 24a T_1 variation with location within phospholipid micelles in chloroform.
(o) PE*/DPL (1:1, w/w), ( ) PE * Data for the carboxylate have been unlinked to the rest deliberately.

a Errors are std. deviations of slopes of T_1 through at least seven points and is within 10%.

b Deuteriated chloroform.

Fig. 24b ^{13}C PRFT of E.coli CY2 PE obtained using a (π - t - π / 2) pulse sequence. t is given on the right hand side in seconds.

conc. 100 mg/ml in $CDCl_3$ at 45^{o}

each case, in agreement with the inverted micellar model for these lipids in the low dielectric medium. The T_1 value for the C(1) nucleus is inconsistent with the trend in the rest, probably because of the lack of an efficient relaxation mechanism for this nucleus, in view of the absence of any directly bonded protons.

A more interesting observation, however, is that the values of T_1 for the case where PE* is the only lipid species in the system are consistently lower than corresponding values in any of the other two systems. The values for both PE*/PS and PE*/DPL are indistinguishable within limits of experimental error. Tighter packing of the phosphatidyl ethanolamine molecules in the micelle as a result of strong head-group interaction is unlikely to be the reason for this motional restriction associated with the all PE micellar unit, since from both n.m.r. and infra-red evidence, both PE and PC have been shown to exist more probably in the dipolar ionic form in chloroform (Chapman and Morrison, 1966). In other words, similar electrostatic forces are to be expected in the core of inverted micellar units formed by each of these phospholipids. There are two other plausible explanations. Firstly, for some reason that is hard to imagine (given the close similarities between the acyl chains in both the PE and DPL molecules), the PE molecules pack more tightly along their long axis leading to more restricted motions along the length of the chain or secondly, pure PE forms larger sized and consequently larger membered micelles (> 70 molecules per micelle). The arguments of Sheetz and Chan (1972), that as the radius of curvature of the vesicle increases there is a consequent drop in molal volume in the aggregate, would then apply , leading to a drop in the degree of freedom of the molecules in the macromolecular aggregate. The effect of PC (which on its own forms only small membered micelles of about 60 - 70 molecules) in a mixed PE/PC system would be to disperse the PE into smaller membered aggregates.

A similar explanation could apply to PS in the PE/PS micelles. The correlation time of the tumbling aggregate given by :

$$\tau_t = \frac{4\pi \eta a^3}{3} \qquad (9)$$

where η is bulk viscosity of medium and a is the radius of the tumbling aggregate, the rest of the symbols having their usual meanings, cannot be the chief determinants of the observed effect for reasons that have been advanced in the previous sub-section. Finally, the plot of T_1 against carbon number along the acyl chains for each of the three different systems studied, Figure 24a shows the inherent anisotropic motions associated with the lipid molecules in the macromolecular units. Inconsistent with a strictly linear gradient, a sharp increase in T_1 is observed for all the carbon atoms further than carbon number 11 towards the terminal methyl. Perhaps more resolved resonances in the middle of the chain are required to accurately pin-point the beginning of this sudden increase, although it is doubtful that it will be found to be strongly associated with the unsaturation at carbon 10. This is an improvement in the earlier definition of this point at carbon (14) by Levine and collaborators (Levine et al., 1972b). Clearly, if any model is to have meaningful application to this system, this sharp deviation from linearity will have to be taken into account and the coincidence of its origin with the termination of a π-electron orbital should not be neglected.

(iii) ^{13}C T_1 of aqueous dispersions of PE/PS systems (temperature function)

The carbon-13 spin lattice relaxation times for a mixed E.coli phosphatidyl ethanolamine-ox-brain phosphatidyl serine system at molar ratios of 1 : 1 in tris-buffer pH 9 have been measured. The measurements were taken at 5° temperature intervals over the temperature range 30°-85°,

resulting in a total of sixty T_1 values. The Chapman transition temperature for this system has been previously established to be below this temperature range using ^{13}C n.m.r. spectral linewidths (see Section E). Although measurements below $30^{o}C$ were also attempted, they have not been reported because the calculation of T_1 from these low temperature partially relaxed Fourier transforms (PRFT) were generally unreliable due to uncertainties about their inversion points as a result of considerable broadening, as the main transition is approached. The phosphatidyl-ethanolamine species was enriched to about 50% in the odd carbon atoms of its acyl chains.

Relaxation times have been calculated (see Materials and Methods) for each of the six clearly resolved resonances in the system corresponding to carbon numbers (C(1), C(3), C(5,7,13 complex), C(11) and C(15) assuming the carboxylate of the glycero-fatty acid ester linkage to be carbon C(1). The general trend in the T_1 values is consistent with increasing molecular motion from the glycerol backbone down towards the terminal methyl carbon. This motional gradient appears to be preserved over the whole temperature range for which spin-lattice relaxation times have been measured. Because all the carbons of the glycerol and ethanolamine moieties are probably still at their natural abundance level of ^{13}C enrichment ($\sim 1.1\%$) it has not been possible to obtain data for them as well as for the even number carbon atoms of the fatty acyl chain. It has previously been shown, however, that molecular motion increases from the glycerol carbons towards the terminal carbon(s) of the polar head group in vesicles prepared from both synthetic and naturally occurring lecithins (Metcalfe et al., 1971a).

Typical partially relaxed Fourier Transforms (PRFT) obtained for the mixed lipid system are shown in Figure 25. The resonances are numbered to correspond with the nomenclature in Figure 19

Table 8b: lnT_1, T_1^{-1} and NT_1 change with temperature for PE*/PS (1:1 w/w) aqueous dispersions.

Reciprocal temp. $^oK^{-1}$ x 10^3	C 1			C 3			C5, 7 & 13			C 9			C 11			C 15		
	lnT_1	T_1^{-1}	NT_1	lnT_1	T_1^{-1}	NT_1	lnT_1	T_1^{-1}	NT_1	lnT_1	T_1^{-1}	NT_1	lnT_1	T_1^{-1}	NT_1	lnT_1	T_1^{-1}	NT_1
2.793	1.482	.227	0	-0.198	1.220	1.64	0.438	0.645	3.10	0.742	0.476	2.10	1.099	0.333	6.04	1.567	0.208	9.60
2.833	1.324	.266	0	-0.301	1.351	1.48	0.166	0.847	2.36	0.553	0.575	1.74	0.916	0.400	5.00	1.335	0.263	7.62
2.874	1.199	.301	0	-0.386	1.471	1.36	-0.051	1.053	1.90	0.405	0.667	1.50	0.693	0.500	4.02	1.182	0.307	6.52
2.915	0.867	.420	0	0.511	1.667	1.20	-0.105	1.111	1.80	0.231	0.794	1.26	0.378	0.685	2.92	1.050	0.350	5.72
2.959	0.788	.454	0	0.693	2.000	1.00	-0.248	1.282	1.56	0.182	0.833	1.20	0.336	0.714	2.80	0.936	0.392	5.10
3.003	0.673	.510	0	0.916	2.500	0.80	-0.357	1.429	1.40	0.000	1.00	1.01	0.247	0.781	2.56	0.833	0.435	4.60
3.048	0.631	.532	0	1.204	3.333	0.60	-0.510	1.667	1.20	-0.105	1.111	0.90	0.166	0.847	2.36	0.756	0.469	4.26
3.096	0.609	.543	0	1.427	4.167	0.48	-0.580	1.785	1.12	-0.128	1.136	0.88	0.039	0.962	2.08	0.693	0.500	4.02
3.145	0.565	.568	0	1.514	4.545	0.44	-1.734	2.083	0.96	-0.328	1.388	0.72	-0.083	1.087	1.84	0.588	0.555	3.60
3.195	0.488	.613	0	1.609	5.000	0.40	-0.867	2.380	0.84	-0.478	1.613	0.62	-0.223	1.250	1.60	0.470	0.625	3.26
3.247	0.405	.667	0	1.833	6.250	0.32	-1.204	3.333	0.60	-0.693	2.000	0.50	-0.511	1.667	1.20	0.336	0.714	2.80
3.300	0.351	.704	0	1.966	7.143	0.28	-1.609	5.000	0.40	-0.916	2.500	0.40	-0.916	2.500	0.80	0.182	0.833	2.42

Table 8a: $^{13}C\ T_1$[b] values measured for the fatty acyl residues of a sonicated aqueous[c] dispersion of

3.300	0.351	.704	0	1.966	7.143	0.28	-1.609	5.000	0.40	-0.916	2.500	0.40						

Table 8a: $^{13}C\ T_1$[b] values measured for the fatty acyl residues of a sonicated aqueous[c] dispersion of a PE*/PS (1:1 w/w) lipid system from 30 - 85°

Temperature in °C	T_1 in seconds for each enriched site.					
	C1	C3	C5, 7, 13	C9	C11	C15
30	1.42 ± .02	0.14 ± .01	0.20* ± .01	0.40 ± .02	0.40 ± .03	1.21 ± .02
35	1.50 ± .03	0.16 ± .02	0.30 ± .01	0.50 ± .01	0.60 ± .01	1.40 ± .01
40	1.63 ± .02	0.20 ± .02	0.42 ± .01	0.62 ± .02	0.80 ± .01	1.63 ± .03
45	1.76 ± .05	0.22 ± .01	0.48 ± .03	0.72 ± .01	0.92 ± .02	1.82 ± .01
50	1.84 ± .03	0.24 ± .01	0.56 ± .01	0.88 ± .02	1.04 ± .01	2.01 ± .02
55	1.88 ± .01	0.30 ± .01	0.60 ± .01	0.90 ± .01	1.18 ± .02	2.13 ± .01
60	1.96 ± .06	0.40 ± .02	0.70 ± .02	1.01 ± .01	1.28 ± .01	2.30 ± .02
65	2.20 ± .02	0.50 ± .01	0.78 ± .04	1.20 ± .02	1.40 ± .01	2.55 ± .01
70	2.38 ± .08	0.60 ± .02	0.90 ± .01	1.26 ± .01	1.46 ± .02	2.86 ± .03
75	3.32 ± .04	0.68 ± .01	0.95 ± .03	1.50 ± .01	2.01 ± .03	3.26 ± .02
80	3.76 ± .02	0.74 ± .05	1.18 ± .02	1.74 ± .02	2.50 ± .03	3.81 ± .04
85	4.40 ± .01	0.82 ± .02	1.55 ± .03	2.10 ± .01	3.02 ± .02	4.80 ± .03

b errors are quoted as std deviations from slopes of equation (3) through at least six experimental pivots. T_1 reproducible within ± 10% experimentally.

c 40 mM Tris-HCl/100 μM sodium edetate pH 9.0

* PE from *E. coli* grown on sodium [1 - ^{13}C] acetate.

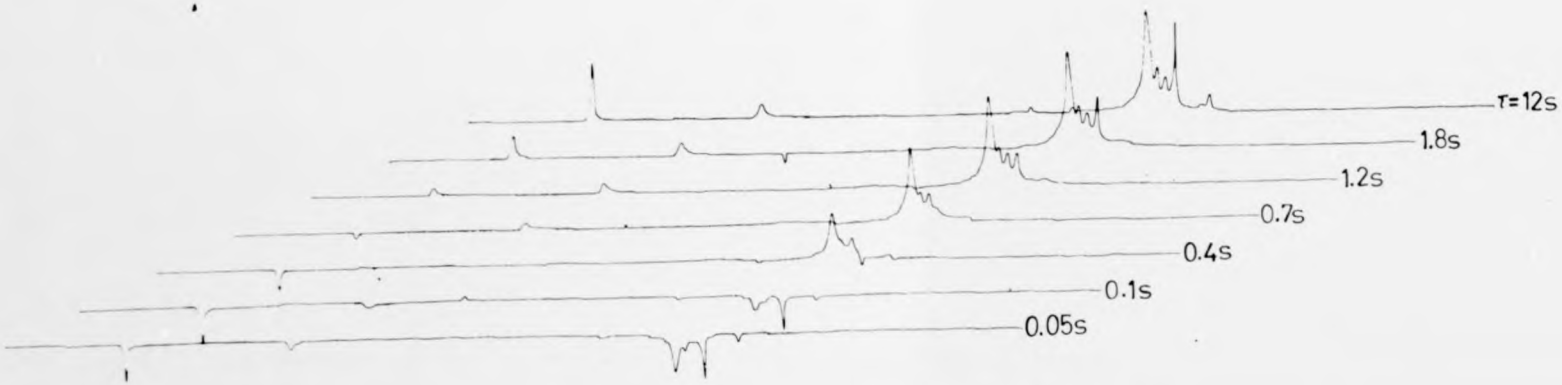

Fig. 25a PRFT of aqueous sonicated dispersions of a mixed lipid [PE/PS, (1: 1 , w/w)] system at 40°C

See "Methods for details .

Fig. 25a [PE/PS, (1: 1 , w/w)] system at 40° C

See "Methods for details .

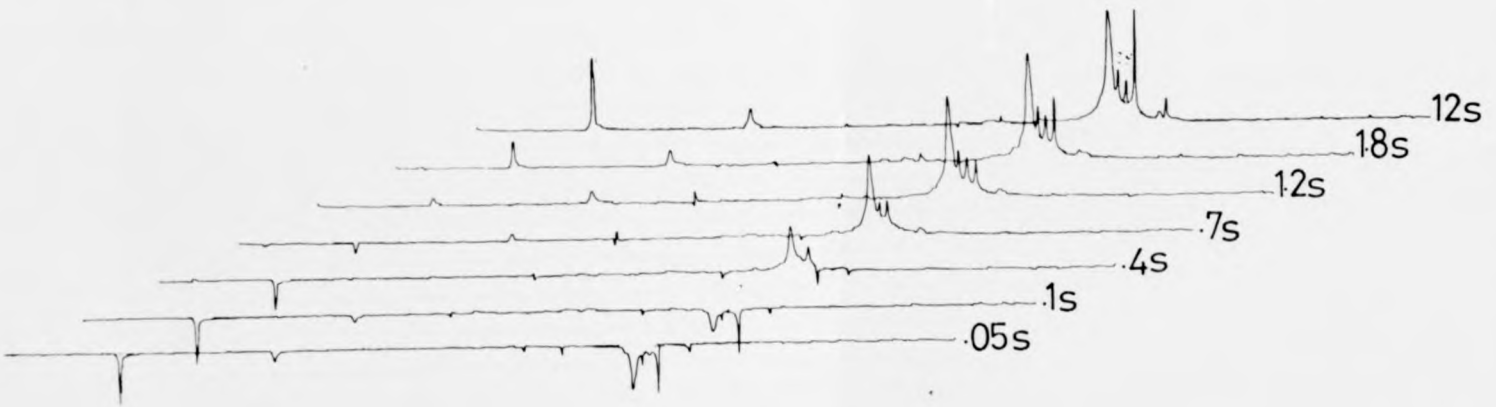

Fig. 25b PRFT of aqueous sonicated dispersions of a mixed lipid [PE°/PS (1:1, w/w) system at 45° C

See "Methods" for details.

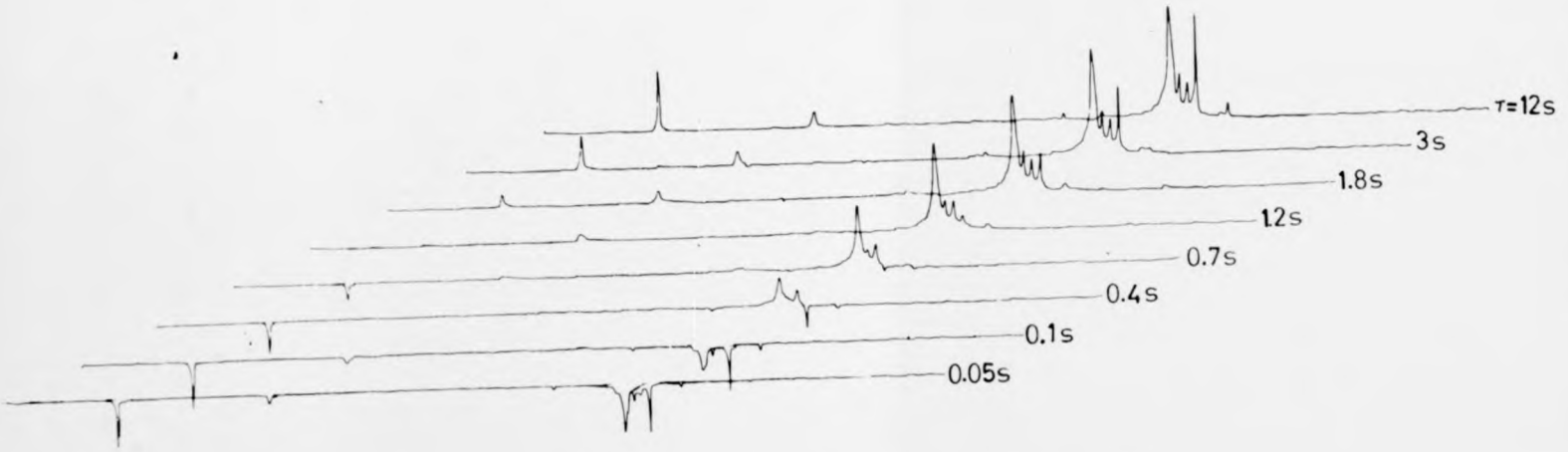

Fig. 25c PRFT of aqueous sonicated dispersions of a mixed lipid [PE*/PS (1:1, w/w)] system at 55°C

See "Methods" for details.

Fig. 25c PRFT of aqueous sonicated dispersions of a mixed lipid [PE*/PS (1:1, w/w)] system at 55°C

See "Methods" for details.

Fig. 25d PRFT of aqueous sonicated dispersions of a mixed lipis [PE*/PS 1.1 w/w)] system at 65°C.

See Methods for details

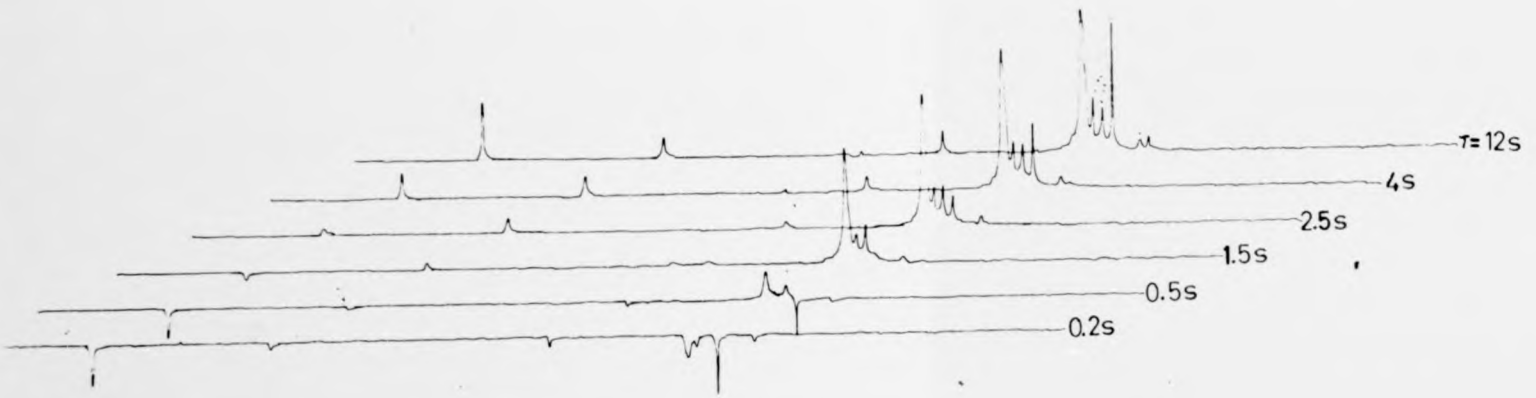

Fig. 25 e PRFT of aqueous sonicated dispersions of a mixed lipid [PE*/PS (1:1, w/w)] system at 80°C

See Methods for details

[PE*/PS (1:1, w/w)] system at 80°C

See Methods for details

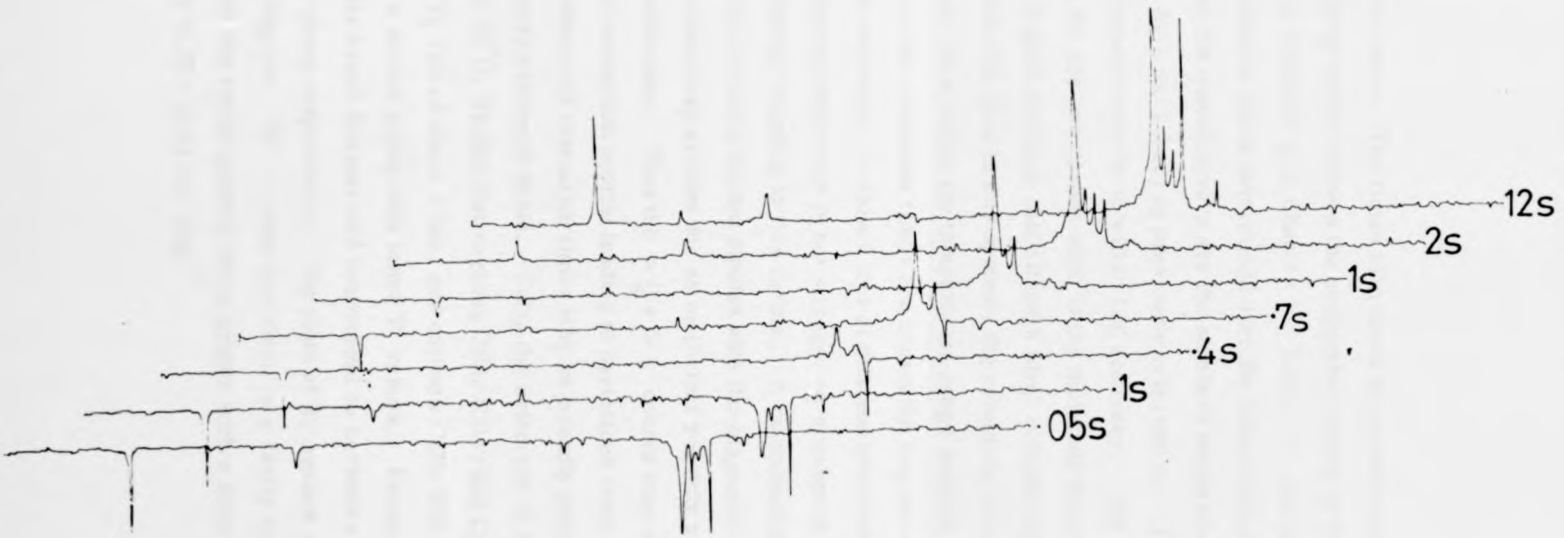

Fig. 25f

PRFT of aqueous sonicated dispersions of a mixed lipid [PE*/PS (1:1, w/w)] system at 85°C

See Methods for details

and referred to above. The times expressed in seconds on the right hand side are the delay times between the respective pulses in the π -t- $\pi/2$ pulse sequence referred to in Chapter 2. Table 8 contains the sixty-odd relaxation times determined over the temperature range 30 - 85°C and the quoted errors are the standard deviations on the slopes of log $(A_\infty - A_t)$ vs t (sec) as previously referred to. T_1 was reproducible experimentally to within 10% accuracy. The fact that the measured T_1 for any one carbon atom in the molecule increases with temperature is good evidence that although ideal solution behaviour may be far from the case in this system, the condition $\omega\tau_c \lesssim 1$ still applies, at least within the temperature range studied. The carboxylate carbon relaxation times are unusually long for their mid-region position in the molecule. A closer look at this nucleus, however, reveals that this anamolous behaviour is not strange, on account of the lack of an efficient dipolar-coupling to this carbon. A combination of neighbouring and adjacent non-directly bonded dipoles with the magnetic anisotropy of the oxygen nucleus may account for an inefficient yet only available relaxation mechanism. Thus the $>\underset{\sim}{C}=O$ centre may experience a characteristic relaxation profile leading to deviations from the predicted trend. The observed relaxation times may be broadly grouped into two parts on a purely arbitrary basis. Using the criterion of a T_1 value of 1 second at 50°C, we see that carbons C(1), C(11) and C(15) fall into one group of T_1 values above 1 sec. and carbons C(3), C(5,7,13) and C(9) fall into a second group with lower T_1 values. Except for C(1) in group one, this broad division will correspond to carbons at the end and middle of the chain respectively. The plots of T_1 against temperature presented in Figure 26 show that there is a fairly linear increase associated with the initial portion of the graphs with a slope of approximately 0.02 - 0.03 sec deg^{-1}.

Fig. 26 (a-b) Relaxation time as a function of temperature for a PE*/PS mixed lipid system.

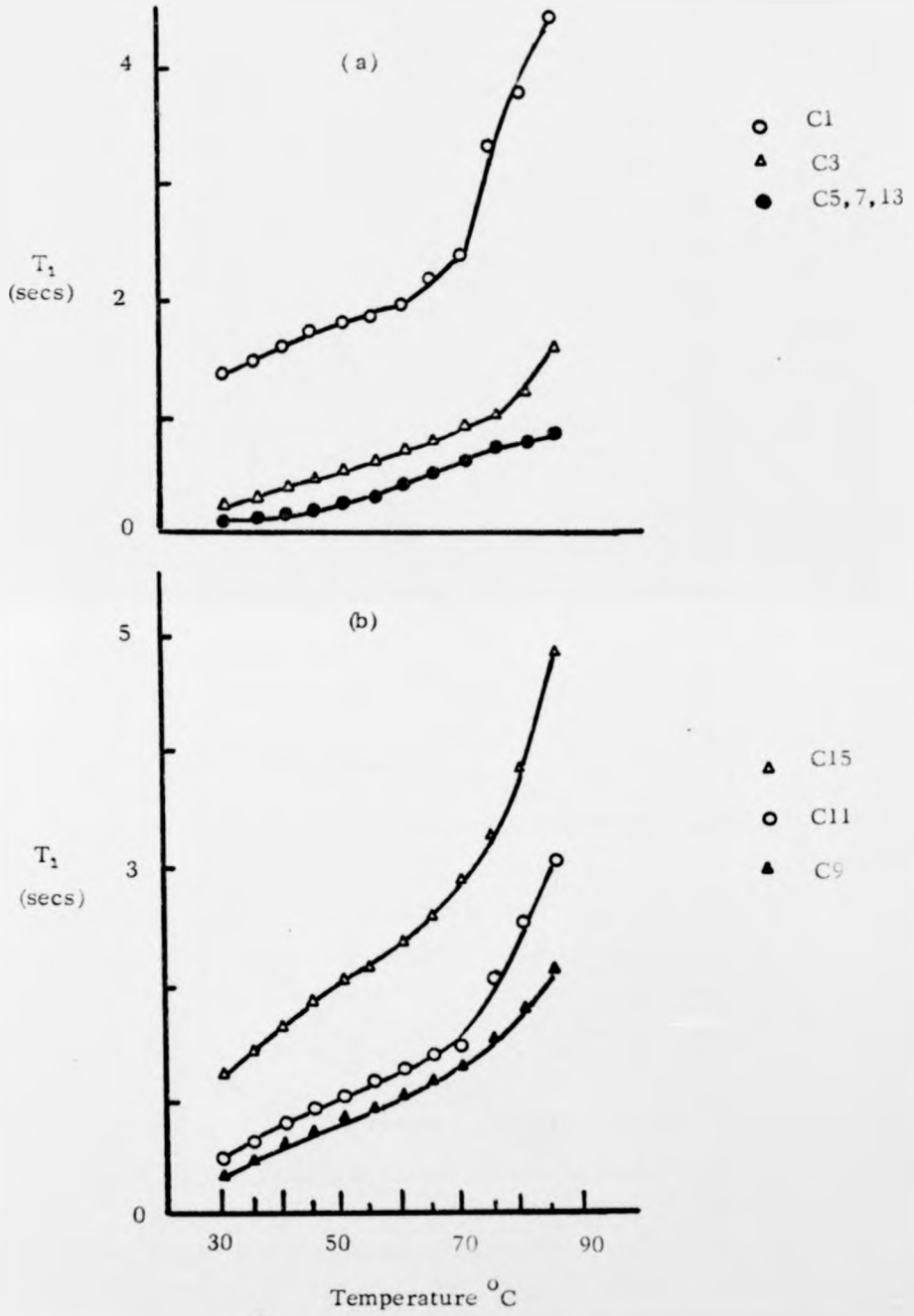
(a)
4
2
0
T_1 (secs)
C1
C3
C5,7,13
(b)
5
3
0
T_1 (secs)
C15
C11
C9
30
50
70
90
Temperature °C

T_1^{-1}
(sec^{-1}

Fig. 26 (c & d) Relaxation rate as a function of temperature for a PE*/PS mixed lipid system

T_1^{-1}
(secs^{-1}

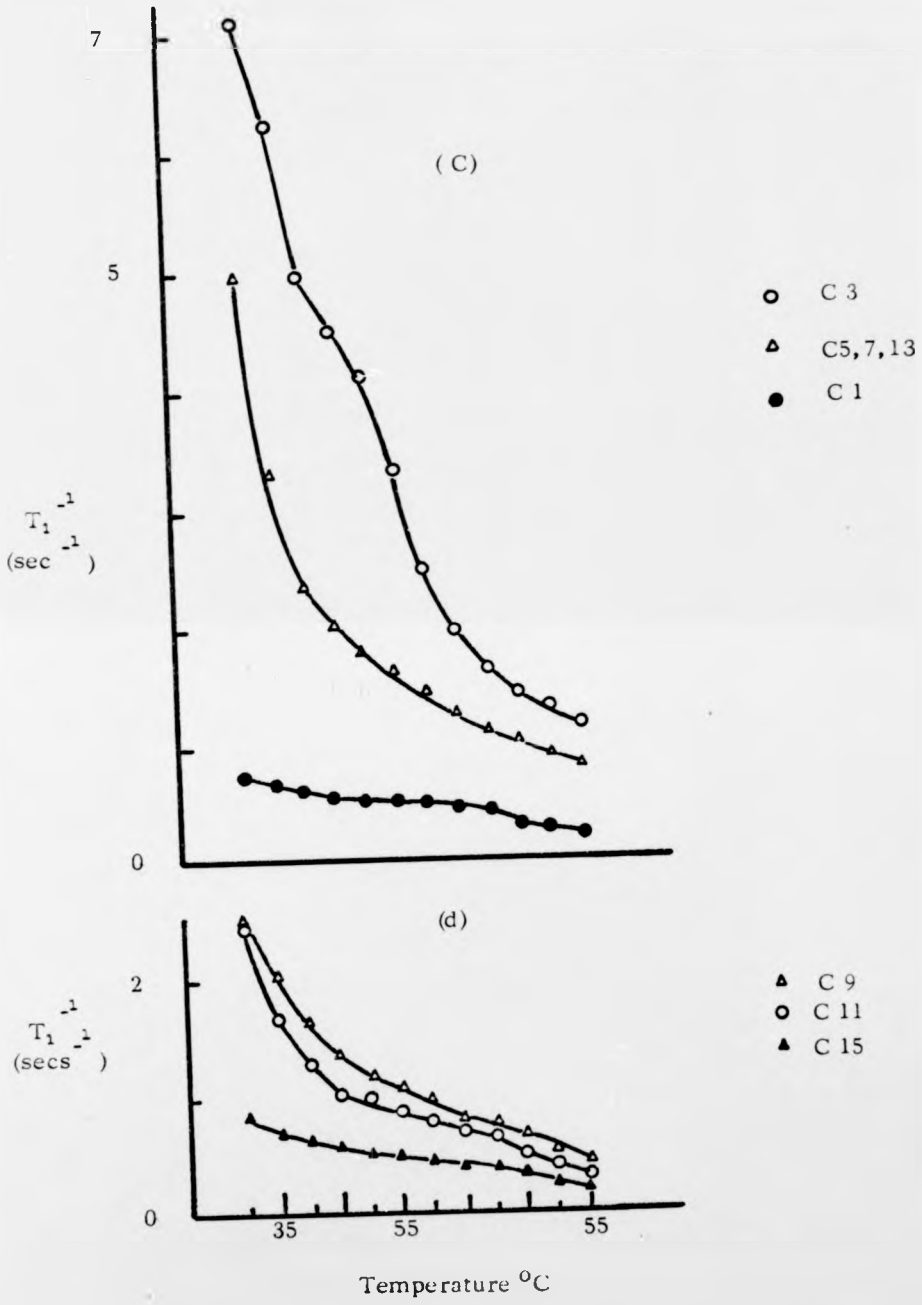
7
5
0
(C)
C 3
C5, 7, 13
C 1
T_1^{-1}
(sec^{-1})
(d)
2
0
35
55
55
C 9
C 11
C 15
T_1^{-1}
(secs^{-1})
Temperature ^{o}C

Deviation from linearity occurs for the group one nuclei at about $70^{o}C$, resulting in a new gradient of ~ 0.1 sec deg $^{-1}$ and a similar story applies to the group two carbons, except that this deviation is observed only after the $75^{o}C$ temperature mark. This deviation from the initial linearity represents an increase in T_1 of the order of ~ 3 fold. This observation may probably fit into a pattern whereby as the temperature increases, those components of molecular motion in the system that are favoured to differing degrees tend to average out, leading to a more 'isotropic' matrix and that at a critical temperature (i.e.temperature at which deviation from initial ideality is observed) a sudden acceleration into more uniform motions occurs. We would expect this temperature to be lower for the end-terminal carbons, i.e. group 1, than for the 'buried' carbons, since the former possess the larger kinetic energy initially by virtue of their longer T_1 values. The relaxation rate for the carbon centres C3, C9, C11 and the C5,2,13 envelope is significantly greater than for the carbon at the methyl end (Figures 26 (c-d). One way the nuclei could achieve this enhancement is through tighter packing in the mid-regions of the residues.

In the plots of T_1 against carbon number of the fatty acyl chain, Figures 27 and 28, carbon atoms (C(1) and C(5,7,13) have been deliberately left out; the former because, even though it may respond to the source of perturbation in a similar manner to the other carbons, it does not fit into the trend of T_1 values in the first place as stated above, and the latter because being an envelope of more than one resonance peak, may contain contributions from different resonating nuclei in ratios which we have no direct way of establishing. These plots outline the general trend of T_1 increasing towards the terminal groups. There appears to be another deviation from linearity at carbons C(11) especially at the lower range of temperature studied , cf $(30\text{-}40^{o})$. One can only infer that a sharp change of molecular motion occurs somewhere between the C(12) and C(15) carbons. Levine et al, 1972b) were unable to conclude whether this sharp increase falls right back to the middle of the chain further than the carbon C(15) nucleus. Although

T_1 (secs)

Figs. 27 & 28. Acyl residue ^{13}C T_1 heterogeneity as a function of temperature for PE*/PS mixed lipid system.

T_1 (secs)

(Fig. 27)

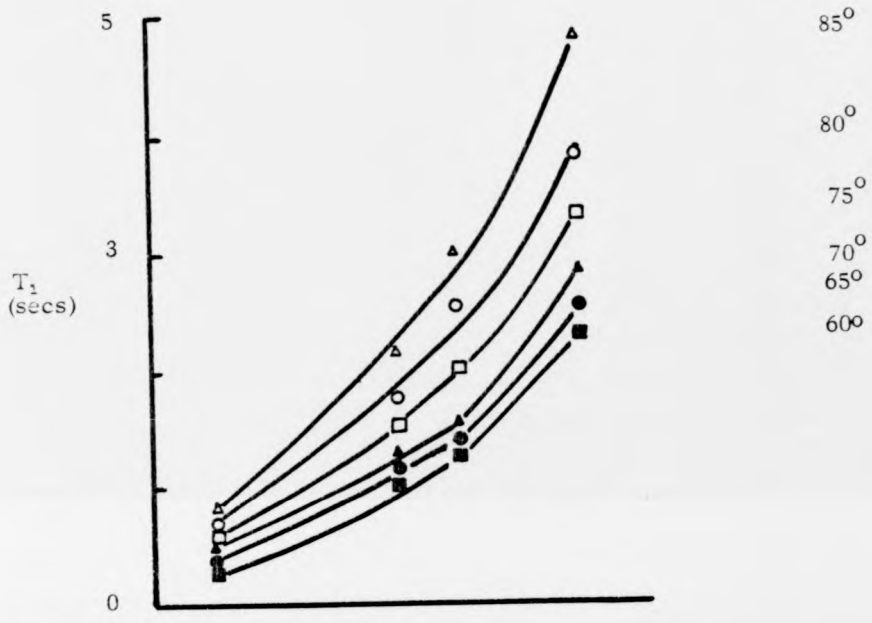
5
3
0
T_1
(secs)
85°
80°
75°
70°
65°
60°

(Fig. 28)

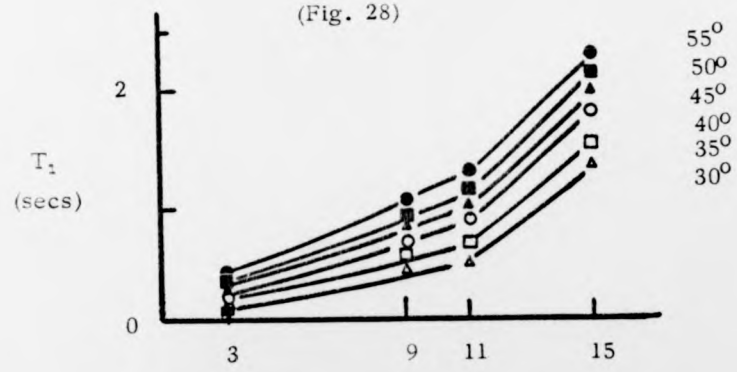
2
0
T_1
(secs)
3
9
11
15
carbon number
55°
50°
45°
40°
35°
30°

there is no evidence in these results to conclusively establish the origins of this motional increase to the carbons anywhere between C(11) and C(15), it is probably unlikely that this sharp increase falls back further than the C(11) centre since there appears to be only a fairly linear increase before this centre. It is unlikely for instance that the C(10) nucleus will show any remarkable deviation from the portion of the plot between C(9) and C(11).

The plot in Figure 29 shows the relationship between NT_1 and carbon number along the chain, where N is the number of directly bonded dipoles. The two curves shown are for the two limits of the temperature range studied and the space between them can be considered representative for all the temperatures in between. Once again, the lower curve shows the much more moderate continuity associated with the gradient of relaxation processes along the chain at low temperatures as contrasted with the sharp discontinuity at higher temperatures. With this treatment the sharp increase in relaxation times associated with the end carbons appears to have its origins from C(11). Attempts at calculating the activation energies (ΔE) of the effective relaxation processes have been made. The relationship

$$\tau_e = \tau^o \exp \Delta E/RT \qquad (10)$$

where τ_e is the effective correlation time and is reciprocally related to the relaxation time T_1 , τ^o being a constant for the system and the other symbols having their usual meanings was used. The values obtained for each of the carbon atoms in a particular range of temperature are presented in Table 9. Plots of $\ln T_1$ vs the inverse of absolute temperature were used to calculate ΔE. If the plots are all assumed to determine a linear plot and a straight line consequently fitted by the method of least squares, the activation energies calculated are those given at the top of Table 9. The largest energies of activation for the processes

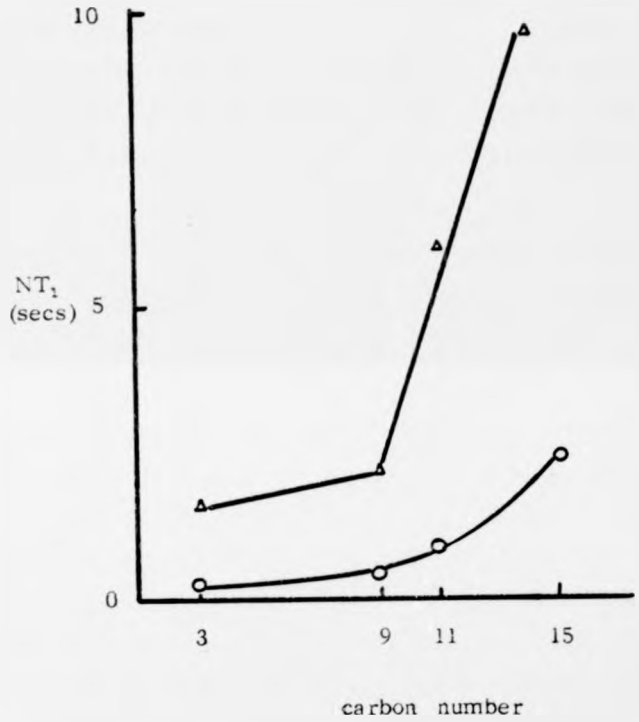

Fig. 29 Plot of NT_1 as a function of carbon number where N is no. of directly bound protons; (0) at 30^{o}, (Δ) at 85^{o}.

TABLE 9

TABLE 9

ΔE KJ MOLE^{-1} FOR T_1 RELAXATION PROCESSES IN PE*/PS (1:1 w/w) DISPERSIONS

Temperature Range ^{o}C	ΔE at resolved resonances					
	C1	C3	C5,7 & 13	C9	C11	C15
85 - 30^{o}	11.5	28.8	29.6	23.8	23.9	19.9
85 - 75^{o}	28.9	19.1	50.0	34.6	41.6	39.5
70 - 40^{o}	13.7	21.6	27.5	25.6	21.7	20.9
40 - 30^{o}	10.3	26.9	55.9	32.9	52.3	22.5

relaxation seem to be associated with the carbons in the middle of the chain. Activation energies of the relaxation processes have also been evaluated for each of three regions within the main temperature range studied. These regions are the three most linear portions of the plots of Ln T_1 against the reciprocal of temperature. Although the actual values of ΔE obtained for each region differ considerably, the trend found for the weighted average as above appears to be remarkably preserved, cf. Table 9 and Figure 30 which shows the variation of ΔE with chain number.

G. Conclusion.

A brief summary of the results reported in this chapter is as follows:-

(i) From molecular sieve experiments, the average diameter of vesicles of the fraction (II) type is determined to be $\sim 210 \pm 10$Å for PE-PS (1:1) mixed lipid dispersions.

(ii) The dependence of the ^{13}C n.m.r. spectra on temperature indicates a broad transition temperature in both PE*-PS and PE*-DPL vesicles. This transition occurs between $\sim$ 15 - 30°C for the former and 30 - 40° for the latter lipid mixtures.

(iii) The observed linewidths suggest that most of the PE molecules in the two mixtures exist in sufficiently "fluid" states to give meaningful spectra. Using ^{31}P n.m.r., it was not possible to establish any phase separations in the PE-PS system, neither was it possible to resolve resonances from both the inside and outside of the vesicle, suggesting that the packing on both sides of the vesicle is probably similar. From the results with broadening reagents, charge effects in the stabilization of this lipid system are considered to be important.

(iv) ^{13}C T_1's of non-polar solutions of these lipids are interpreted to mean that the inverted micelles formed in chloroform is larger and probably more populated when PE is the only lipid than when PE-PS or PE-DPL mixtures are used.

(v) ^{13}C T_1's of aqueous sonicated dispersions of PE-PS (1:1) have been obtained above the order → disorder transition temperature, cf. 30 - 85°C.

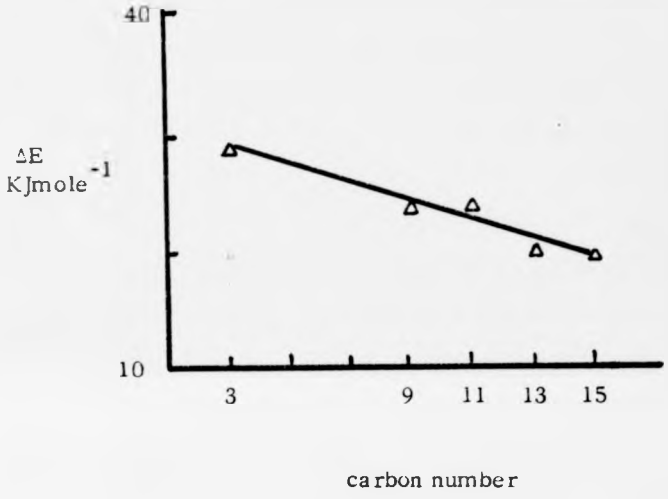

Figure 30 Variation of the energy of activation for T_1 processes with location in the bilayer.

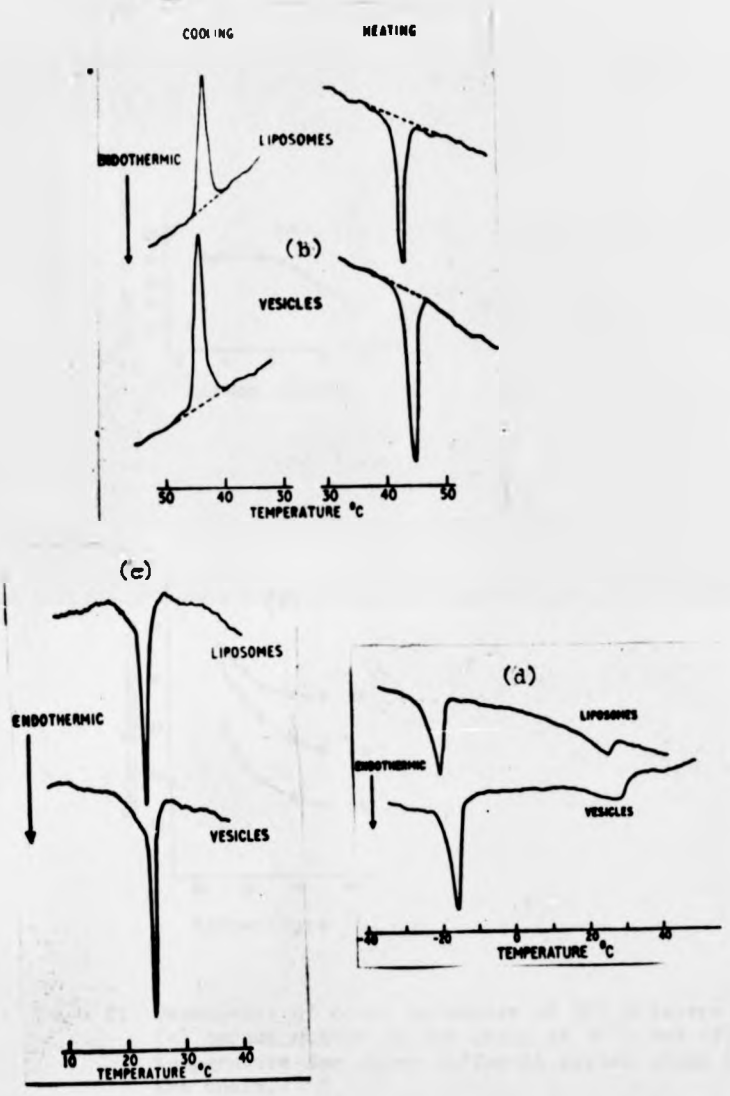

Fig. 30b-d; (b)DSC of 16:0/16:0PC, (c)14:0/14:0 PC and (d)16:0/16:0 PC-18:1c/18:1c PC(1:1) liposomes and vesicles. Only heating scans are shown in(c&d).

(Data of De Kruijff et la., 1975)

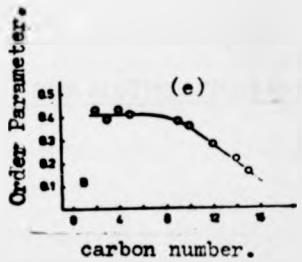

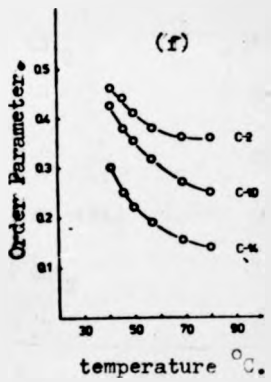

Fig. 30e & f: Dependence of order parameter of DPL bilayers on (e) carbon number in the chain at 50°C and (f) temperature for three different carbon atoms in the chain.

*Data of(Seelig and Seelig, 1974)

TABLE 10

E KJ MOLE $^{-1}$ FOR METHYLENES IN SYNTHETIC POLYMERS*

POLYMER	GROUP	$^{13}CT_1$ IN SECS.	TEMP. ^{o}C	E KJ MOLE $^{-1}$
PE O[a]	CH_2	1.1	30	16
PP O[a]	"	0.60	"	21
PIB[a]	"	0.15	"	18
PMMA[a]	α -CH_3	0.10	"	23
PE[a]	CH_2	1.35	100	10.1
PP[b]	"	0.57	"	14.3

PEO, PPO, PIB, PMMA, PE and PP stand for polyethylene oxide, polypropylene oxide, polyisobutylene oxide, polymethacrylate, polyethylene and polypropylene respectively.

* Communicated by F. Heatley (see text).

a values of F. Heatley

b values of Inoue et al.

These results clearly show a higher degree of disorder associated with the carbons nearer the chain terminal methyl than those near the glycerol backbone. In the bilayer, these would represent regions buried deep in the middle of the bilayer and those at the lipid-water interface respectively. (vi) The calculated activation energies for these relaxation processes reveal the higher activation energies associated with these carbons nearest the lipid-water boundary. It is suggested that one way in which these carbons, in segments closest to the aqueous phase, can offset these unfavourable activation energies is to pack more tightly than, say, carbons in the middle of the bilayer.

Finally, it is desirable to establish whether these results have any bearing whatsoever on natural membranes which the model is purported to represent. In the past, the validity of sonicated vesicles as models for biological membranes has been challenged on the grounds that the results obtained with them have not always been found to correspond with those from liposomes or natural membranes. A recent investigation employing differential scanning calorimetry has demonstrated the gel → liquid-crystalline transition of bilayers in liposomes to be unaffected by sonication (De Kruiff et al., 1975). Some of the results in this paper have already been presented in section C, and the other relevant parts are included here. These calorimetry studies by Radda and others show that the main endothermic transition remains largely unaffected in liposomes and vesicles of PC, (figures 30 (b) and (c)), whether heating or cooling curves are employed. Furthermore, in mixtures of PC with widely differing chain lengths, when phase separation is to be expected, identical lipid asymmetry are thought to occur in both liposomes and vesicles formed from similar lipid mixtures, (figure 30(d).)

A more direct comparison with our results is provided by the work of Seelig and Seelig, (1974 and 1975) using deuterium magnetic resonance spectroscopy. The estimation of the segmental order parameter from the observed residual quadrupole splitting in deuteriated bilayers is thought to confer an added advantage to the application of dmr in membrane systems. This is so because the high spectral resolution necessary for the

measurement of T_1's (in, say, ^{13}C n.m.r.) is no longer a limiting factor since fairly well resolved quadrupole splittings can be observed in liposomes without sonication. An obvious weakness of this approach, however, is that fluidity, which very nearly often is the relevant phenomenon in membrane function, has no known simple relationship with the order parameter. It would appear that the rate of molecular reorientations which is closely related to relaxation times (especially if dipolar interactions dominate the relaxation processes, e.g. ^{13}C T_1) is more relevant to the concept of fluidity (Seelig and Seelig, 1974). However, these authors' results on liposomes do make an interesting comparison with our own results reported here. Their results are presented in figures 30 (e) and (f). It is seen that the chain segments are less ordered near the terminal methyls of the acyl chain, i.e. in the mid-regions of the bilayer, and that there is a progressive increase in order parameter towards the glycerol backbone, (figure 30 (e)). A marked discontinuity appears to be associated with the region around the C 10 carbon of DPL liposomes as compared with our results, (figures 27 - 29). That the order parameter appears to remain constant for the first nine segments is at variance with our results, and is probably due to the fully saturated chains of equal chain length used by these authors. The dependence of the order parameter on temperature, (figure 30(f)) shows an initial rapid increase in disorder associated with each labelled portion of the chain. As temperature is increased further, a less pronounced increase in disorder appears to set in. This observation is compared to our results in figures 26(c) and (d). These observations we have ascribed to an averaging out of molecular motions as a result of increased isotropic behaviour.

Finally, our results and those of Seelig and collaborators, when contrasted with the results of Heatley (1976) on polymer solutions, show that the gradation in order associated with lipid molecules in both liposomes and vesicles is the consequence of a special symmetry characteristic of the bilayer common to both membrane models. The activation energies of ^{13}C T_1 processes associated with the methylene

carbons in these polymers is of the order of ~ 20 KJ mol^{-1}, cf. Table 10. Only the activation energies of the terminal carbons in the PE-PS system are in reasonable agreement with this value. Activation energies for carbons between the first and eleventh segment of the chain are considerably higher, cf. Table 9.

From these considerations, it would appear that sonicated lipid vesicles are still sensible models for studying biological membranes, especially when experimental limitations prevent the direct employment of natural membranes or non-sonicated liposomes. Even without this demonstration, vesicles still have their direct biological equivalence in certain specialised membranes such as the highly curved membranes of mitochondrial cristae and the retinal rod. The controversial results that are sometimes obtained with sonicated and nonsonicated systems can now almost safely be viewed as deriving from certain peculiar limitations of the technique applied rather than from differences in the properties of the two systems.

CHAPTER 5

^{13}C BIOSYNTHETIC ENRICHMENT OF THE FATTY ACYL RESIDUES OF PHOSPHATIDYL CHOLINE

A. INTRODUCTION

The reasons for the requirement of, and the problems preventing, the ready availability of phospholipids suitably enriched in the ^{13}C abundance of acyl residues have been enumerated in Chapter 3. The isolation of bacterial mutants possessing appropriate genetic lesions, permitting a high efficiency of incorporation of exogenous substrates into fatty acids is one way of combating some of these problems. One of the major attractions of bacteria in this field is the relative ease with which these mutants can be isolated and cultured as single strain types without fear of cellular diversity as in higher organisms: and another advantage closely linked to the first is the rapid cell cycle in bacterial growth with generation times typically in the region of 2 ± 1 hr resulting in the quick establishment of large populations in fairly short times with concomitant conversion of substrate into end product readily.

However, phosphatidyl choline which is very often the major phospholipid of most eucaryote membranes, is hardly ever present, at any rate in any significant amounts, in bacterial membranes. If we are going to be able to apply the powerful technique of n.m.r. to the study of this important phospholipid as was done in Chapter 4, for the phosphatidyl ethanolamine, then it is desirable that a suitable method for preparation of similarly enriched lipids be available.

There are many eucaryotic micro-organisms which approximate, in terms of their growth cycle behaviour, some of the attractive qualities enumerated above for the choice of bacteria in biosynthetic enrichment techniques. One obvious example is the well studied ciliate Tetrahymena Pyriformis . Besides having a rapid bacteria-like growth (generation time ~ 4 hours) the ciliate is fairly easy to culture axenically. Furthermore, apart from de novo fatty acid biosynthesis, demonstratable during growth in chemically defined fatty acid-free media, Tetrahymena can incorporate exogenous long-chain fatty acids of great variety into its lipids directly (Lees and Korn, 1966). However, when grown on the standard (proteose-peptone) medium the incorporation of any added acetate or fatty acid substrates will decrease due to dilution from similar substrates present naturally in these media. Besides, a considerable amount of material incorporated and en route to lipid synthesis may end up one way or another lost in respired CO_2.

Tetrahymena and several other micro-organisms will prey on bacteria growing in their immediate niche . A review of this phenomenon and some suggestions on its possible relevance in "ecological combat" has been treated by Curds and Cockburn (1968).

This chapter is a report of the results of our reasoning that if Tetrahymena can be cultivated mono-axenically on E.coli K12 strain CY2, then it may be possible to have the highly ^{13}C enriched phospholipids of CY2 incorporated into the eucaryote with possible modification (but with no major alterations in pattern of enrichment) into phosphatidyl choline.

B. RESULTS

Initially a series of experiments on a small scale (10 ml) were run in order to define the growth conditions necessary for the experiments.

These experiments demonstrated that either the E.coli growth medium or the bacterial metabolic products were toxic to the Tetrahymena and that it was necessary to wash the bacteria thoroughly before introducing the Tetrahymena into a suspension of the bacteria in sterile distilled water. The incorporation of the ingested E.coli was monitored by liquid scintillation counting of the "hot" ^{14}C label. Three separate experiments on the small scale (see Table 11) gave an incorporation of radioactivity with the Tetrahymena lipid extract of $44 \pm 3\%$ of total E.coli label. The results of a large scale preparation (10 L) were comparable (Table 11).

The large scale experiments were repeated using E.coli [1-^{13}C] acetate-labelled and the extracted lipids were fractionated to give phospholipids. The neutral lipid fraction when chromatographed by TLC gave the characteristic sterol spot of Tetrahymenol (see Plate 2). The polar lipid fraction from axenically cultivated Tetrahymena and from organisms cultivated under our mono-oxenic conditions showed identical analyses by TLC. Furthermore, the relative intensities of the spots were comparable when the same amount of lipid was streaked in both cases (see Plate 3).

The ^{13}C n.m.r. spectra obtained from the Tetrahymena phospholipids (Figures 31 & 32) confirm the biosynthetic incorporation of label into the organism via the E.coli lipid. Furthermore, the spectrum of phosphatidyl choline from the organism reveals the signal-to-noise enhancement from those enriched carbons in the acyl residues. The spectra are in general typical of ^{13}C n.m.r. spectra of phospholipids in non-polar solution and show the three main regions [viz-a-viz, carboxylate (~173 ppm), olefin (~130 ppm), and alkyl (~35 -15 ppm)] observed in the enriched E.coli lipid (see Figures 31 and 32). Certain differences are obvious, however.

Plate 2

Preparative TLC of neutral lipid fraction from Tetrahymena pyriformis grown on E.coli CY2. F.A., G, T. and O are for fatty acid, glycerides tetrahymenol and origin respectively.

Petroleum ether, bp 40-60° - diethyl ether-acetic acid (70: 30: 1 v/v) was used to develop the spots and they were visualized by charring with 40% H_2SO_4 and heat.

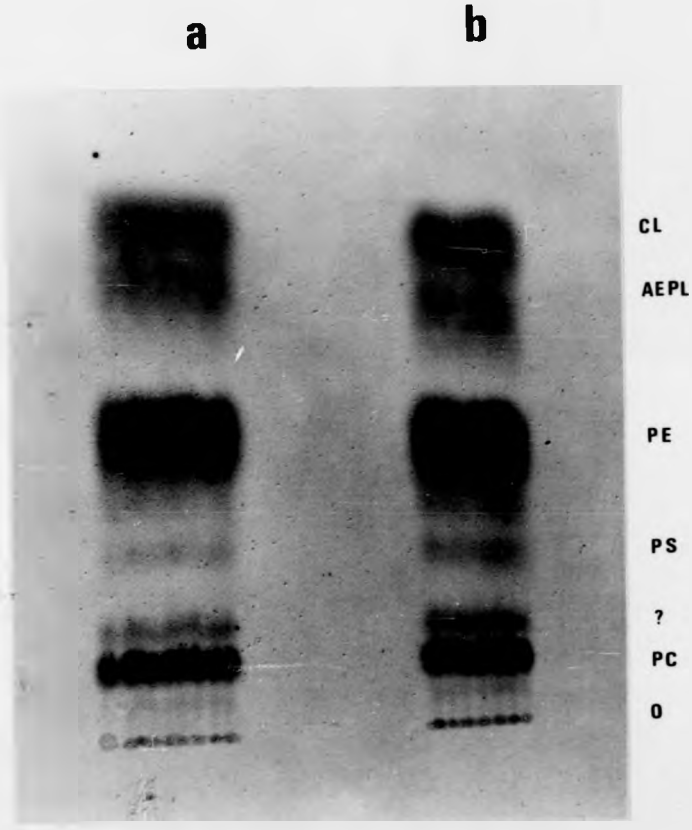

Plate 3

Preparative TLC of polar lipid fraction from Tetrahymena pyriformis.
(a) Organisms grown mono-axenically on E. coli CY2
(b) Organisms grown axenically on proteos-peptone medium.

PC, PS, PE, AEPL and CL stand for phosphatidyl choline, phosphatidyl serine, phosphatidyl ethanolamie, amino ethyl phosphono-lipid and cardiolipin respectively.

TABLE II

EFFICIENCY OF INCORPORATION OF CY2 RADIOACTIVITY IN T. PYRIFORMIS LIPIDS

^{14}C LABELLING

Culture Size		cpm/ml added to CY2 growth medium	cpm/ml in CY2 cells after growth	cpm/ml in CY2 lipids after growth	cpm/ml in T.pyriformis lipid extract	% CY2 lipid converted to T.pyr. lipid
10 ml	I	2.91×10^4	2.21×10^4	2.18×10^4	0.95×10^4	45
	II	3.22×10^4	2.62×10^4	2.59×10^4	1.32×10^4	50
	III	4.10×10^4	3.45×10^4	3.42×10^4	1.21×10^4	39
10L		7.30×10^2	5.60×10^2	5.54×10^2	3.05×10^2	55.6

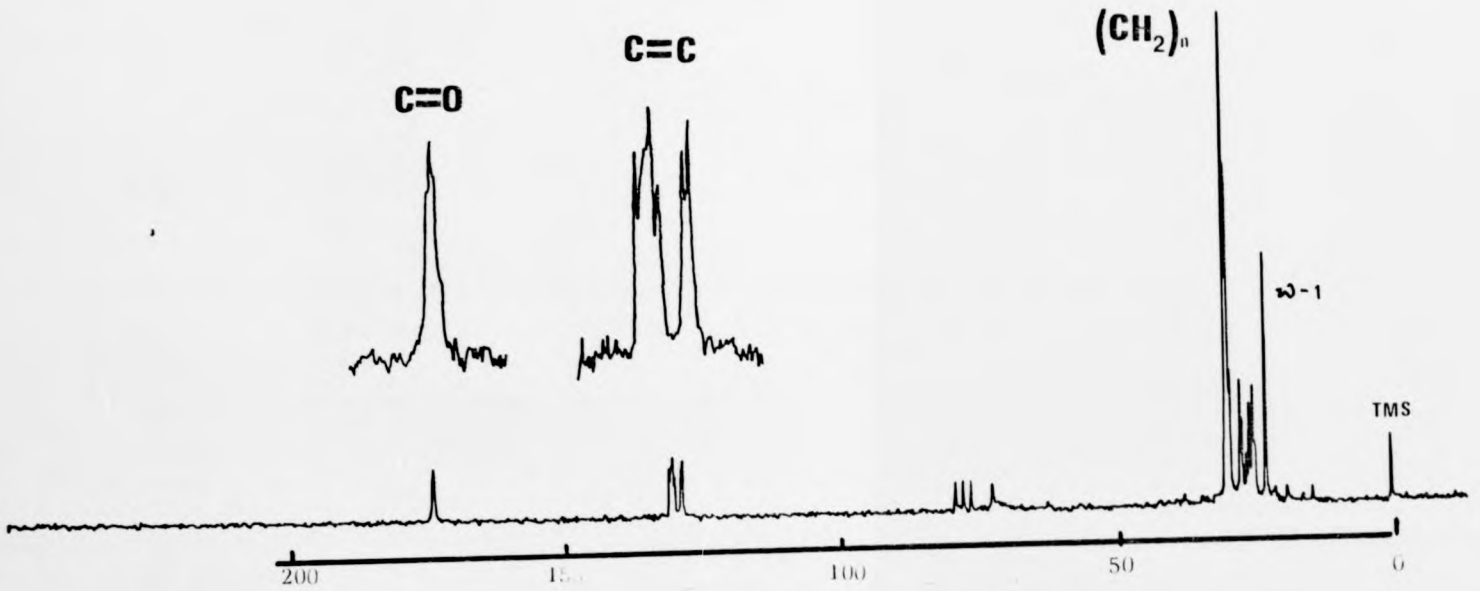
C=O
C=C
(CH2)n
ω-1
TMS
200
150
100
50
0

Fig. 31. Chloroform Extract of lipids from T.pyriformis grown on ^{13}C labelled E.coli ;CY2 .
1000 FiD's were accumulated and Fourier transformed on an 8K data set. 90^{o} Pulse length 21 μsec.
Conc. 50 mg/ml in $CDCl_3$.

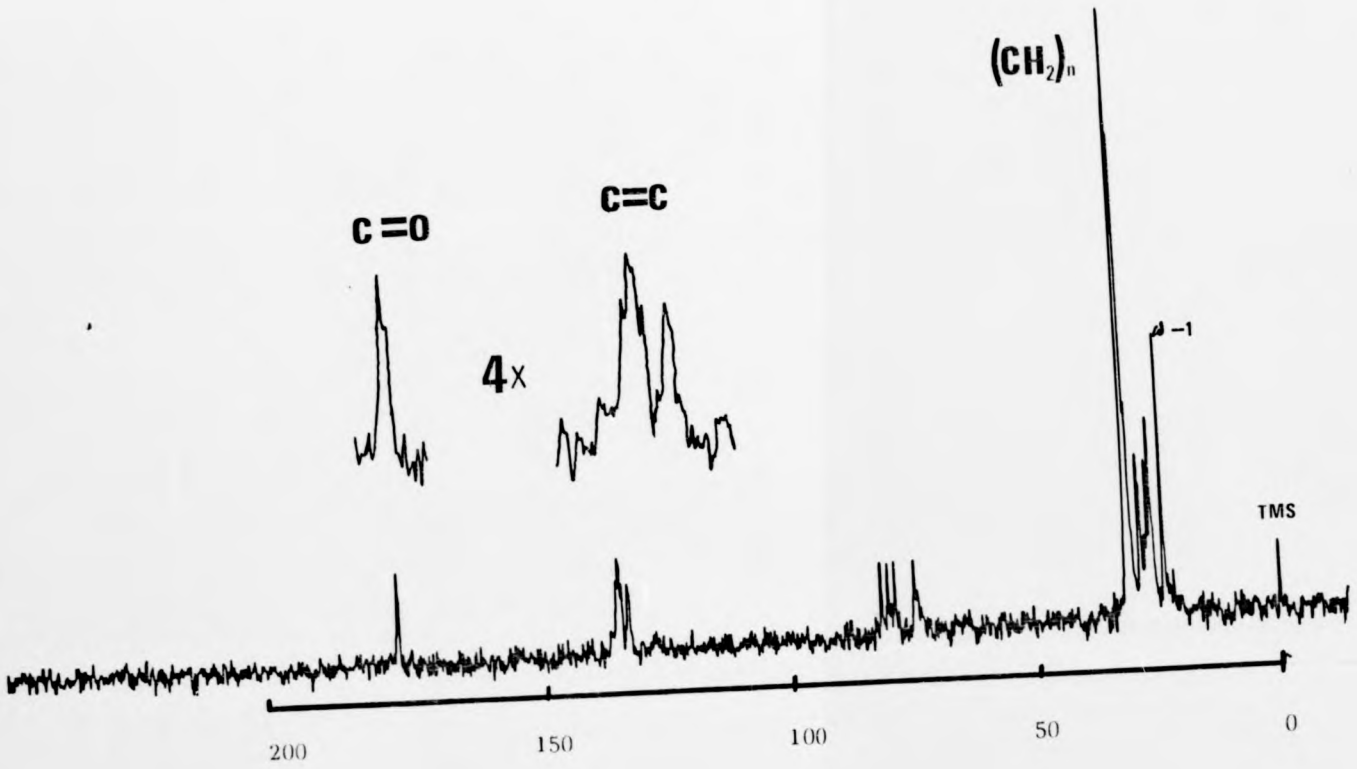
(CH2)n
C=O
C=C
4X
-1
TMS
200
150
100
50
0

Fig. 32a 22.63 MHz ^{13}C n.m.r. spectrum of PE from T.pyriformis grown on E.coli strain CY2. 200 FIDs were Fourier transformed on an 8K memory size.
conc. 20 mg/ml in $CDCl_3$ at 30^{o} .

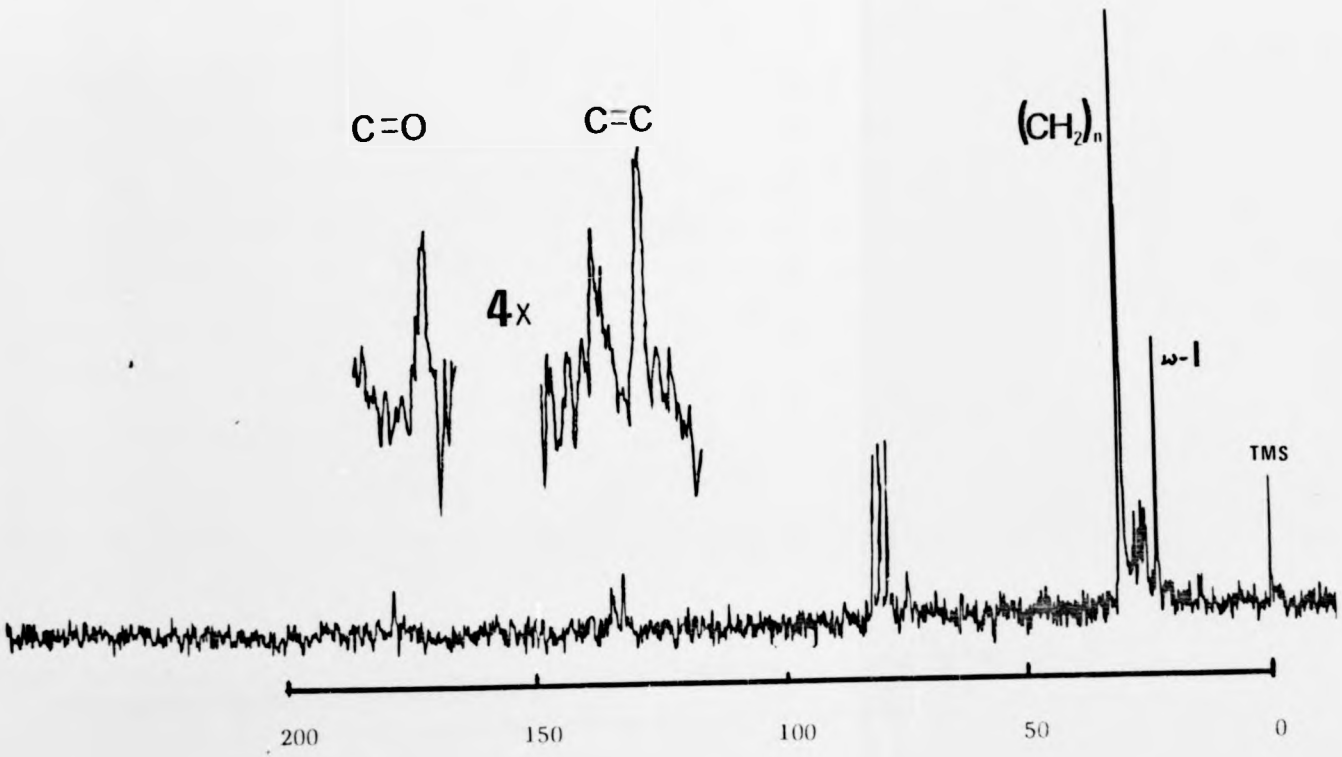
C=O
C=C
4X
(CH2)n
ω-1
TMS
200
150
100
50
0

Fig. 32b 22.63 MHz ^{13}C n.m.r. spectrum of PC from T.pyriformis grown on E.coli strain CY2. 200 FID's were Fourier transformed on an 8K memory size. conc. 10 mg ml in $CDCl_3$ at $30^{o}C$.

The olefin region shows evidence of more than mono-unsaturation as contrasted again with the case in E.coli. Polyunsaturation of fatty acid residues of phospholipids is more common in Eucaryotic membranes than in procaryotic ones. Specifically, Tetrahymena pyriformis has been shown to have more than half of its total fatty acid content in polyunsaturated forms (Erwin and Bloch, 1963). Also, in the separated fractions of PE and PC, there appear to be inconsistencies in the resonances between ω-1, and the main methylene envelope as was seen in the CY2, PE. These differences and their likely sources are dealt with in fuller detail in the discussion and in terms of the possible metabolic alterations that the E.coli lipid may have undergone.

The % ^{13}C enrichment of the phospholipids was determined as in Chapter 3, by comparing the intensities of the olefine protons and their ^{13}C satellite peaks of the ^{1}H n.m.r. of the fatty acid methyl esters from the phospholipids. This gave an enrichment of approximately 25%.

The ^{13}C enrichment was measured independently by mass spectrometry of the fatty acid methyl esters at 40°C on an A.E.I. MS 50 spectrometer, using the +ve ion mode; 100 sec/decode and high gain (courtesy of Dr.R.Mitchum, Warwick University). The unsaturated acid esters palmitoleic, oleic, linoleic and linolenic, which together constitute more than 70% of the total fatty acids in Tetrahymena at the growth temperature of these experiments (Nozawa et al.m, 1974) gave complex spectra of low order, characterized by a large peak at m/e of 74 from the species produced by β cleavage with hydrogen atom transfer (McLafferty, 1959). The spectra were not suitable for the calculation of the degree of ^{13}C enrichment. The saturated fatty acid esters, myristic acid and palmitic acid methyl esters, which constitute ~5 and 8% respectively of total fatty acid composition (Nozawa et al., 1974)

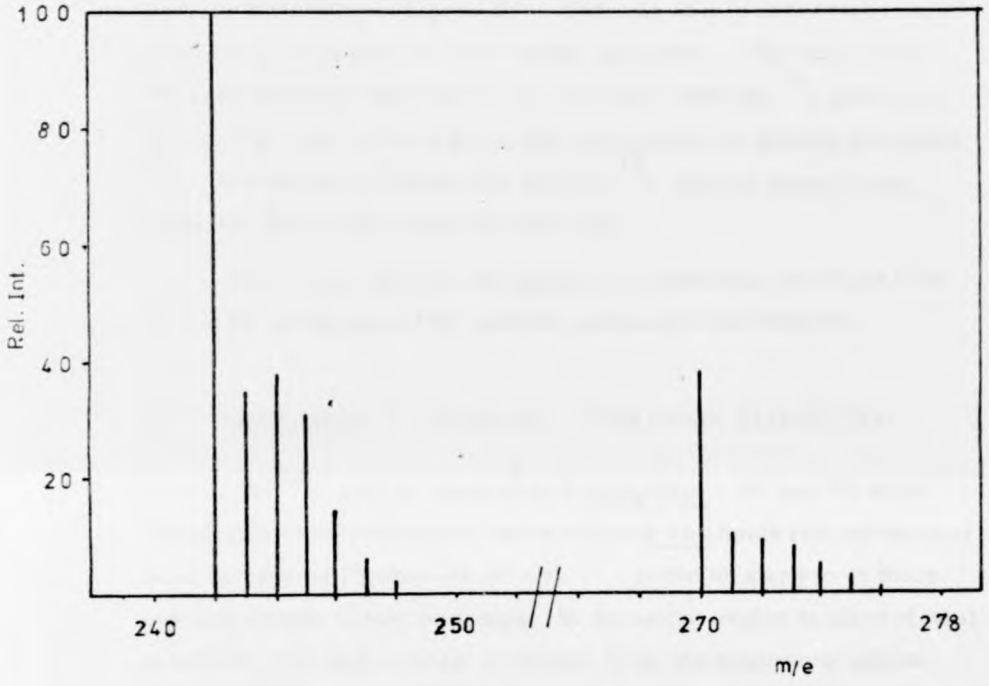

Fig. 33 Mass spec. of methyl myristate m/e 242
and methyl palmitate m/c 270.

gave simpler spectra (Figure 33). The peak at m/e 242 corresponds to the main molecular ion from methyl myristate. The peak at m/e 243 corresponds to that from metyl myristate with one ^{13}C atom etc. Comparison of the peak heights, after correction for natural abundance ^{13}C , enabled us to compute the ratio of ^{13}C labelled atoms to the maximum theoretically possible labelling.

This ratio, which is the degree of enrichment, was found to be $19.3 \pm 2\%$ in the case of the palmitic esters derived from PC.

C. DISCUSSION : EVIDENCE FOR CHAIN ELONGATION

The ^{13}C n.m.r. spectra of Tetrahymena PC and PE show considerable differences from those of the E.coli lipids from which they were derived (cf Figures 32 (a - b) . In the former two ,a more complex system is now resonating in the olefin region in place of what appeared to be only a single resonance from the mono-unsaturation from the E.coli lipids. Furthermore, between the ω-1 resonance and the main methylene envelope, there appears to be at least four resolved resonances as against only two [C(3) and C(11] in the phospholipids from E.coli (See Figure 16).

One interpretation probably is that scrambling of the label to previously unenriched carbons has occurred in the process of "tetrahymenization" of the E.coli lipids. But this surely would have led to direct ^{13}C - ^{13}C splittings of about 130 Hz which have not been observed. Another possible interpretation is that of the movement of the double bond without any other major alteration in the fatty acyl residue. There will have to be indeed a mixture of fatty acyl residues with double bonds that have wandered to various extents to produce the

three newly resolved peaks in the alkyl region and in fact, π-electrons that have wandered quite close to either end of the chain , would be required to give the different shifts in the olefin region; since monoenes with a fair number of saturated carbons attached on either side are known to have identical shifts in long-chain hydrocarbons (Levine et al., 1972a). Furthermore, monoene fatty acids are by far the minor unsaturates in Tetrahymena pyriformis (Holz and Conner, 1973). And yet another explanation, and one that is more likely, is that chain elongation with further unsaturation has occurred. Polyunsaturated fatty acids and in particular, γ-linolenic acid (6,9,12-octadecatrienoic acid) are the major fatty acids of Tetrahymena pyriformis (Erwin and Bloch, 1963). These authors have also shown that γ-linolenate occurs more on the choline than on the ethanolamine phosphatides (~ 30% of the fatty acid esterified to PC is γ-linolenate, as compared with only ~ 19% for PE).

Chain elongation is thought to be a normal process of fatty acid synthesis in higher organisms (Bishop and Stump, 1971). One suggested mechanism is an enzyme catalysed condensation of acetate, derived from acyl -CoA, with the acyl CoA derivative of the long chain fatty acid.

$$RCH_2CO\text{-}S.CoA + CH_3CO\text{-}S.CoA \xrightarrow[NADPH]{NADH} RCH_2CH_2CH_2CO\text{-}S.CoA + CoA\text{-}SH$$

There are also enzyme systems (desaturases) thought to be specific in introducing double bonds along the chain of the fatty acid via the expression :-

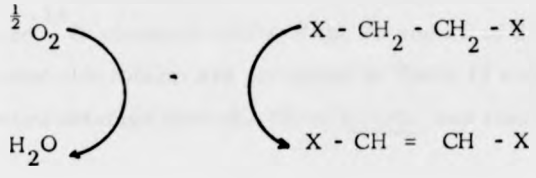

Erwin and Bloch (1963) have shown that when "hot" palmitic acid was fed to cultures of T.pyriformis , a large amount of label resulted in the γ-linolenate fraction of the phospholipids. The biological sequence of events appeared to favour palmitate against palmitoleate as a precursor for chain elongation and desaturation to γ-linolenate.

Our data shows evidence of these possible metabolic events. They indicate that (i) the level of ^{13}C enrichment in PC has decreased from its value in its E.coli precursor, (ii) changes in the relative intensities of different regions of the ^{13}C n.m.r. spectrum of the PC are commensurate with the process of chain elongation and desaturation, (iii) on the basis of non-equivalence of chemical environments, six of the enriched carbons in the γ-linolenate will experience shifts in their corresponding resonances in the palmitoleate residues and that by assuming the presence of these two fatty acids on each phospholipid we can explain the extra resolved resonances in the olefinic and acyl regions of the ^{13}C n.m.r. spectrum.

Chemical shifts were measured relative to tetramethyl silane, on an 8K (8192) data set. Under these conditions, and at an external magnetic field strength of 21 K gauss, the computer is in theory capable of measurement of chemical shifts to an accuracy of $\pm$ 0.01 ppm. However, given linewidths at half-peak height ($\Delta V_{\frac{1}{2}}$) of $\sim$ 3Hz for 10 mm samples of the chloroform solutions of lipids (see Chapter 4) an accuracy of $\pm$ 0.1 ppm is more likely in practice. Thus, barring large systematic errors, such as large discrepancies in temperature from sample to sample, the measured chemical shifts of the PE and PC should be comparable within these error limits unless the origins of such shifts are at considerable variance. Also, peaks as close as 0.2 ppm will be resolved. The measured ^{13}C chemical shifts of the PE and PC of the ciliate in deuteriated chloroform are presented in Table 12 and are compared with values obtained from the PE of E.coli and also the PE from egg yolk.

Table 12: ^{13}C chemical shifts of T. pyriformis phospholipids in $CDCl_3$ compared with those of lipids from other sources.

Resolved resonances along acyl residue.	Chemical shift p.p.m. from TMS at 45°C			
	Tetrahymena		E. coli	Egg yolk
	PC	PE	PE	PE
C1 α	173.1	173.0	173.8	173.8
C1 e			173.6	
C3	25.0	25.2	25.4	25.0
C5			29.9	
C7			30.6	
C9			130.1	
C11			27.2	
C13			29.5	
C15 (ω-1)	22.5	22.7	23.2	22.6
C16 (ω)			16.0	14.4
a	130.0	130.0		130.4
C=C b	129.5	129.5		129.5
c	127.6	127.6		128.1
d	29.8	30.5		30.0
e	29.3	30.1		29.6
f	-	29.3		
g	27.4	27.4		27.4
h	26.9	27.0		
i	26.1	26.3		
j	25.6	25.9		

To avoid ambiguity, only the carbons with confirmed chemical shifts are numbered with the nomenclature in Chapter 4 and the rest are lettered in order of decreasing chemical shift from tetramethyl silane (see Figures 34 (a -b). Clearly, from Table 12, it can be seen that the chemical shifts of the resolved resonances in both PE and PC from the ciliate are quite similar, suggesting a correspondingly similar equivalence of environment of these groups. γ-linolenate has been assumed the principal unsaturate in these two phospholipids. Compared with values from egg yolk PE, inconsistencies are apparent, reflecting perhaps possible differences in the degree of unsaturation and chain length of the fatty acyl residues in these systems. Also the values for the chemical shifts of corresponding resonances from E.coli PE differ from those of the former two by more than the experimental error involved in their measurements and again are indicative of alteration of these precursors in the ciliates as to be expected.

The % ^{13}C enrichment in each resolved resonance from the phospholipids of T. pyriformis are shown in Table 13, and are compared with corresponding values obtained for the PE from E.coli in Chapter 3. The same method of ratioing the intensity of each resolved peak, to that of the solvent peak ($CDCl_3$) and comparing these ratios with those similarly obtained for natural abundance spectrum has been employed. The % ^{13}C enrichment of T.pyriformis PE is still fairly comparable with those measured for the E.coli P.E. in Chapter 3. They are also reasonably close to the average value obtained by the radio-activity labelling method at the beginning of this experiment. For example, considering the enrichment in the carboxylate carbon alone, we have values of 50% and 65% in the ciliate and bacteria respectively, and a value of ~ 70% from the [1 - ^{14}C] acetate counts in the bacteria (Table 11). In contrast, the values as determined for the PC are much less than for the

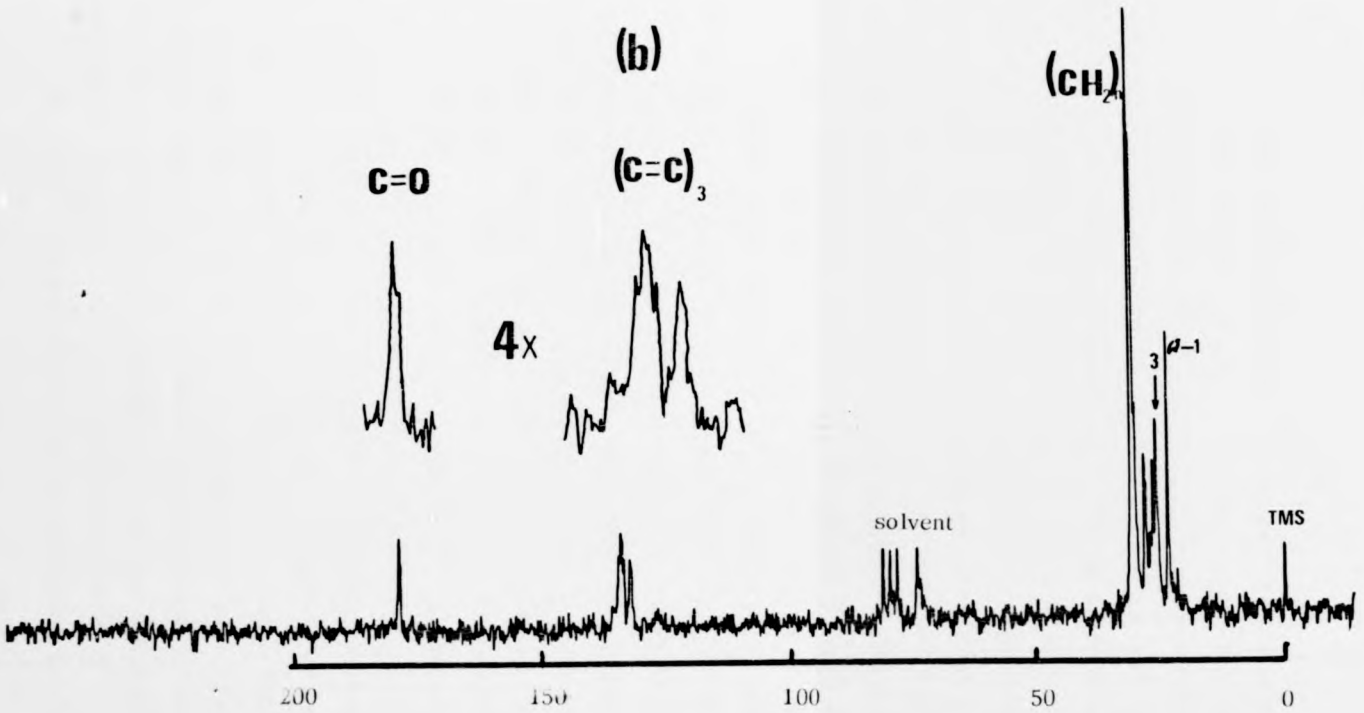
(b)
(CH2)n
C=O
(C=C)3
4X
3
α–1
solvent
TMS
200
150
100
50
0

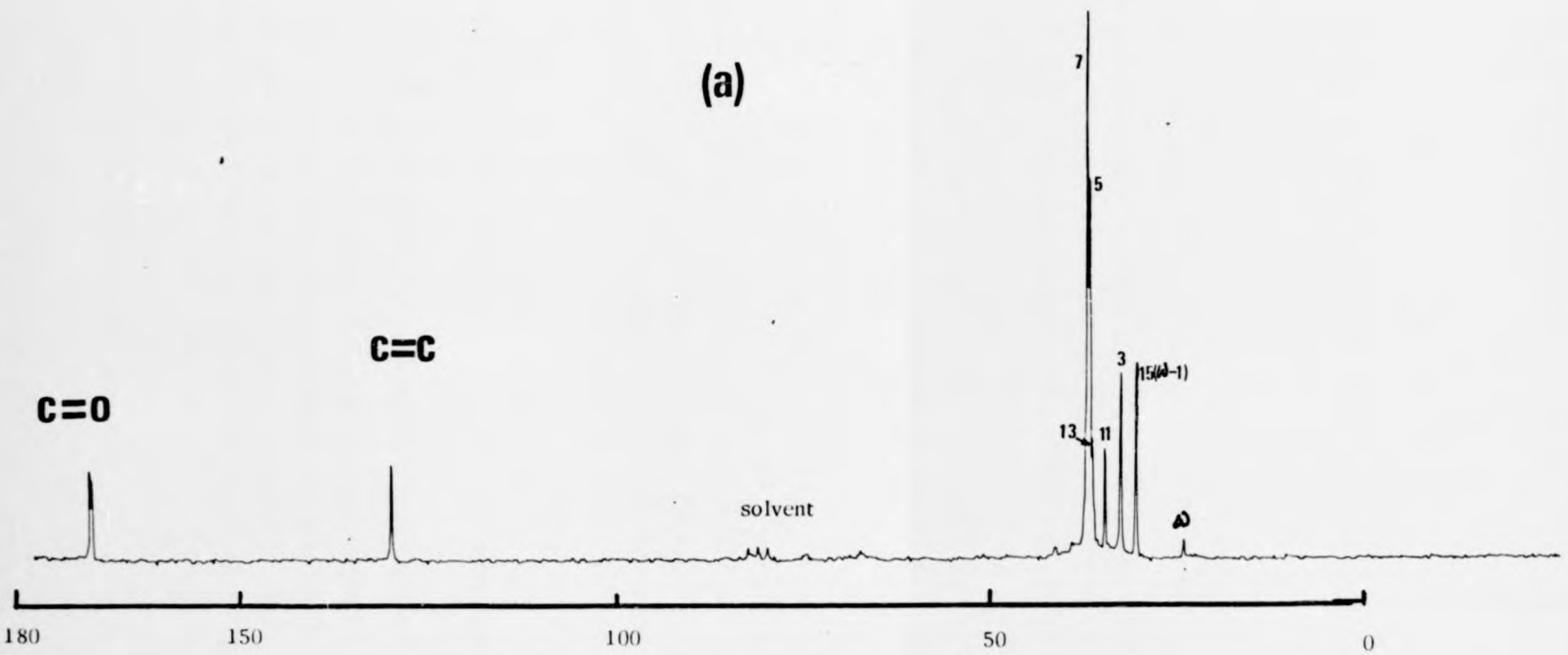

Fig. 34 Phosphatidyl ethanolamine from (a) E.coli and (b) T_1 pyriformis equivalent resonances are compared.

Table 13: % ^{13}C enrichment as estimated for each carbon of enriched T. Pyriformis lipids compared with PE in CY2

Resolved resonances along acyl residue	% ^{13}C enrichment		
	T. pyriformis		E. coli
	PE	PC	PE
C1 $^{\alpha}_{\beta}$	50	23	65 60
C3	44	16	47
C5, 7, 13			24
C9			70
C11			28
(x-1) C15	50	49	50
(ω) C16	n.a.*	n.a.*	5
a	53	23	
C=C b	52	25	
c	50	33	
d	20	19	
e	24	16	
f	22	16	

* natural abundance level of enrichment ~ 1.1%

a see text for numbering system.

of
in CY2

E. coli	
PE	
65	
60	
47	
24	
70	
28	
50	
5	

corresponding cases in their E.coli precursor , a value of only ~ 20% obtained for the carboxylate of PC. Clearly, any metabolic alteration that the fatty acyl residues of the E.coli lipids have undergone in the ciliate leading to the decrease in levels of enrichment must have affected the residues of the choline phospholipid more.

Further examination of Table 13 shows that this trend is not peculiar to only the carboxylate carbon but appears to affect all the newly unsaturated carbons and generally those carbons nearer the carboxylate end of the molecules. The well resolved peak at $\delta \sim 23$ppm, due to the penultimate carbon appears to retain its enrichment remarkably well as shown by values of 50% and 49% respectively for PE and PC from the ciliate and as compared with the corresponding value of 50% from PE of E.coli . A comparison of the relative intensities of certain regions of the spectrum helps to magnify this point. The region in question is the 22 - 30 ppm region of the ^{13}C n.m.r. spectrum (Figure 32) and the integrated areas under the main methylene envelope (J), and under the peaks between this envelope and the penultimate carbon (K), and also the area under the penultimate (ω-1) carbon itself (L) are considered. The ratio J : K : L is found to be of the order 3:2:1, for the PE or even cardiolipin derived from E.coli . For the Tetrahymena PE , a ratio of 3: 1.8 : 1 was obtained and for the PC, a value of 3: 1 : 1 . These relative intensities, in a situation where all the carbons in the skeleton are equally enriched, should give an indication of the number of nuclei resonating under any one peak or group of peaks. In a case where the level of enrichment varies from carbon to carbon, the intensities are also an index of % enrichment in each region and can be compared from spectrum to spectrum if the resonances have similar chemical shifts. Thus the decrease in K relative to J and L can have one or more of the following origins :-

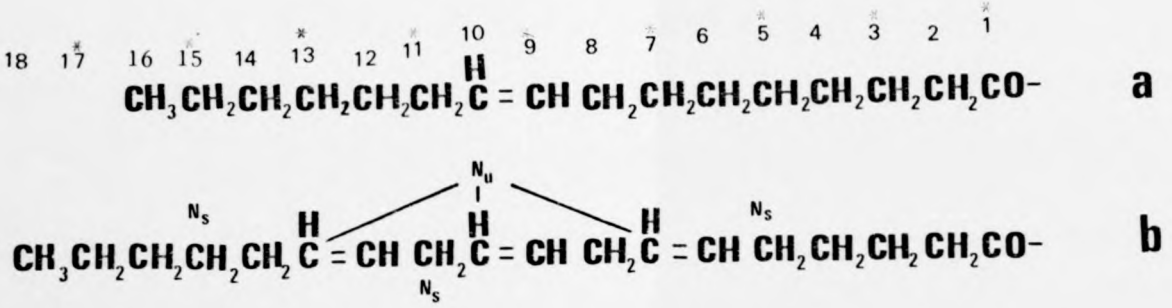

Fig. 35 Schematic of (a) palmitoleic (Δ^{9}) and (b) γ- linolenate $\Delta^{6,9,12}$
* showing ^{13}C enriched sites.

Nu those carbons that will shift as a result of unsaturation.
N_S those saturated carbons that may shift due to new environments

(a) the number of non-equivalent nuclei resonating under K has decreased. This is unlikely; in fact as we shall see later, more peaks are indeed resolved in this region and they are not due to ^{13}C - ^{13}C splittings.

(b) de novo fatty acid synthesis has led to a dilution of the labelled fatty acid with γ-linolenate synthesized ab initio. But such de novo effects are bound to lead to a uniform reduction along the entire chain length and not regional decreases.

(c) the chain elongation and chain desaturation have somehow led to regional decreases in enrichment of different parts of the acyl residue. Again, since no direct carbon spin coupling was observed, the mechanism by which this can arise is probably only through a partial breakdown of the acyl chain acyl CoA units during these metabolic alterations.

Figure 35 is a sketch of the two relevant unsaturated fatty acids superimposed on each other in an attempt to identify any resonances that may experience induced shifts from the effects of polymerisation and chain elongation in γ-linolenate. The chain at the top is that due to palmitoleate [cis -9, palmitoleic acid; (16 : 1 Δ^{9})] which has been shown to be the major unsaturate in E.coli and which is also not likely to be involved in chain elongation in T.pyriformis . And below is the skeleton of γ -linolenate [cis-6, cis-9, cis-12 Octadecatrienoic acid (18:3, $\Delta^{6,9,12}$)] which is the major unsaturate in T.pyriformis and will be derived from the

major saturated fatty acyl residue of E.coli which is palmitate (16)]

In chloroform solution, the phospholipids are likely to exist as inverted micelles of up to 60 - 70 molecules per micelle. The chemical shifts associated with the carboxylates, the ω-1 and the C3 in both residues would largely be unaffected by chain length and may be expected to be the same irrespective of relative abundance of each fatty acid in the lipid. Clearly polyunsaturation in the γ-linolenate will result in more olefinic nuclei being resolved at the intermediate field region of ~120-130Hz due to the increasing s character of these bonds. In γ-linolenate the three π-bonds are $\Delta^{6,9,12}$, and this means that resonances due to enriched carbons 5, 7 and 11, in palmitate now become carbons 7' 9' and 13' respectively in γ-linolenate and they now become unsaturated, which was not the case previously. These resonances marked N_u in Figure 35 will be lost from the acyl region to the olefinic region. How they will be resolved in this new region may depend on several factors, such as the degree of polarizability due to proximity to a dipole and/or stearic factors such as gauche-trans isomerism. Bearing in mind the "multiplicity" of species of fatty acids that may be present in these phospholipids, no attempt has been made to accurately assign the olefin region. One must point out, however, the resolution of at least 2 and at most 4 resonances in the olefinic region of the T.pyriformis lipids. Also it must be remembered that γ- linolenate is the principal unsaturate in this organism and that PC is likely to have more of this species in its acyl residues than PE. We are now left with three enriched sites to be accounted for viz-a-viz carbons 5', 11' and 15' in γ-linolenate, which are derived from carbons 3, 9 and 13 respectively in palmitate.

Now C5' in γ-linolenate has not moved very much farther from the molecular dipole at the carboxylate end than C3 in palmitoleate, so

that we expect not too dissimilar contributions to its shift from the polarisation of its bond induced by the electric field at this molecular dipole. However, C5' is now directly bound to an unsaturated carbon at C6'. Magnetic anisotropy in ^{13}C n.m.r. is not expected to be much more than about the ≤ 1 ppm equivalent in proton n.m.r. This shift if operating will lead to a new resonance in the ^{13}C n.m.r. spectrum of the phospholipid at about $25 + 1 = 26$ ppm, and this will still be in the K domain. Similarly, C15' which as C13 in palmitoleate resonated at δ 29.5 ppm, may be shifted upfield by a combination of several factors. For a beginning, it is allylic to the unsaturation at Δ^{12}, resulting in a downfield shift of less than 1 ppm again. But a reversal of this shift might result from stearic upfield shifts due to the greater tendency of γ-linolenate to form gauche bonds than is the case in palmitoleate. It has been suggested (Batchelor et al., 1972) that there exists a tendency towards a gauche bond β to a cis-unsaturate. Now if no other gauche bonds are assumed to exist other than by this process in these systems, we see that γ-linolenate is potentially capable of forming 6 gauche bonds as against 2 only in palmitoleate. Clearly, the possibility of an upfield shift due to these stearic factors is more favourable for C15' than for C13. The only enriched nucleus still unaccounted for is the C11 of the γ-linolenate. This centre is derived from the C 9 of the palmitate and in palmitoleic acid is the carboxylate-end centre of the only olefin along the chain, Δ^9. It is obvious, therefore, that the shift of this carbon will be considerably different in γ - linolenate from what it was in palmitoleate. These three resonances of saturated carbons that may experience shifts in the process of chain lengthening and desaturation are each marked Ns in Figure 35. It must be pointed out, however, that the assumption that palmitoleate and γ-linoleate are the principal fatty acids in this

organism, as reasonable as it appears, is a very simplistic one, considering that saturated fatty acid residues with equally high levels of ^{13}C abundance exist in these lipids albeit as minor components. For example, although γ - linolenate is derived from palmitate, not all the palmitate is exhausted in this process and PE in T.Pyriformis is known to have up to 13% of its fatty acids as palmitic acid. This will introduce further complications in the observed spectrum because the C11' of the γ -linolenate, for example, will presumably resonate at lower field than its C9 precursor in palmitate, due to the magnetic anisotropy from adjacent olefins on either side (Figure 35). In E.coli, the problem is not as acute because palmitate alone makes up almost half of the fatty acids and the only unsaturates found are monoenes. This is evident from the relatively simpler spectra obtained from the extracted phospholipids of this organism. Thus, it must be emphasized that the exercise described above was not one in accurately assigning chemical shifts. Rather, it represents an attempt to relate the observed additional complexity of the ^{13}C n.m.r. spectrum of the ciliate lipids, to possible metabolic alterations that the bacterial lipids had undergone.

D. BIOLOGICAL IMPLICATIONS

These findings may have a possible biological relevance in terms of elucidating the mechanisms of chain elongation and desaturation. Firstly, the enrichment at the methyl terminal end appears to be remarkably well preserved as contrasted with that at the carboxylate end. This is good evidence that the process of chain elongation is from the carboxylate end of the molecule . Clearly, the fatty acid will have to be cleaved from the glycerol ester linkage, before 2 carbon units can be added to its carboxylate end. Presumably, a hydrolytic enzyme cleaves the ester linkage which is then followed by the enzyme-catalyzed addition of one

acetate unit. This is then followed by re-esterification of the residue by an esterase and finally the desaturate introduces the double bonds. The last two steps may alternate freely. The interesting point, however, is that these enzymes are likely to be interacting with the rest of the chain during these processes. It is not unlikely, for instance, that the enzyme responsible for chain elongation binds its non-polar residue to the rest of the acyl chain while it exposes its active site to the carboxylate end of the molecule. In a similar way, the desaturase may bind non-specifically to the glycerol moiety while it exposes its active site to the centre to be desaturated. The interactions of these enzymes, and indeed other metabolic enzymes, with the acyl residue may lead to the reduction in enrichment of portions of the chain relative to others.

The observation that the PE still retains its enrichment level rather well compared to the PC, may at first suggest that the PE from E.coli undergoes much less pronounced alterations in being converted to Tetrahymena PE than in going to PC. It is not clear how this can happen unless one postulates that PC is synthesized at a much later stage in the metabolism of the lipids. In this manner, the fatty acids from PC are probably synthesized from the reassembly of almost or totally broken down E.coli fatty acids, whereas the PE is made from whole E.coli fatty acids with a simple single acetate condensation step. In short, it may be the greater participation of ab initio synthesis in the process of chain elongation that results in more reduced levels of enrichment in the PC.

CHAPTER 6

N.M.R. STUDIES OF PROTEIN DENATURATION

A. INTRODUCTION

The ability of various denaturants to alter the structure of proteins has been the subject of broad investigation for some time now (Tanford, 1968; Lumry and Bittonen, 1969). A common feature of many globular proteins is the fact that, in their native conformation, i.e. in the conformation in which they occur in their natural surroundings, most polar residues are located on the surface of the molecule in contact with solvent (usually aqueous) while the interior is made up to a large extent of non-polar amino acid side chains (Kendrew, 1961; Philips, 1966). Quite obviously, the folding of a long-chain polymer into a compact structure will result in a loss of freedom of motion of the chain and hence a decrease of configurational entropy. For a typical protein containing about 200 amino acids, folding into the native form at physiological temperatures could result in the loss of up to 800 KJ mol^{-1} of protein of structure stabilization free energy (Tanford, 1962). Clearly, this must be overcome by attractive forces of equal magnitude if the protein integrity is to be preserved. Current reasoning appears to be that the loss in entropy involved in protein folding is more than made up for, by the gain in entropy of water molecules in the surrounding environment.

The end product of denaturation may vary depending on the strength of the denaturing agent. Denaturants like urea or guanidine salts are known to unfold the protein "configuration" to an extent approaching the "random-flight" conformation of synthetic polymers. On the other hand, milder denaturing agents like acetone and various alcohols unfold the protein, but the α-helical structure is still recognisable (Callaghan and Martin, 1962; Timasheff et al., 1966).

The question of how these agents bring about their effect involves not only a consideration of their structures (they are usually simple organic molecules) but also an explanation of the nature of their interaction in aqueous solutions. In other words, the structure of water itself and any structural alteration brought about by the solubilisation of these molecules will have to be considered. But perhaps most importantly, an insight into the exact mechanism of denaturation will necessarily reflect upon the exact nature of the forces involved in protein stabilisation which is of such great biological importance and yet very poorly understood.

Aqueous urea solutions are known to inhibit micellar aggregation (Schick, 1964), solubilise hydrocarbons and affect the conformational properties of a wide range of polymers, including protein denaturation (McKenzie and Rolston , 1971). A lot of circumstantial evidence, from thermodynamic data mostly (Stokes, 1967) has implicated hydrophobic interactions in these systems. Yet another set of evidence demonstrates the requirement for the presence of free hydrogen atoms on the nitrogen atoms of denaturing agents (Gordon and Jencks, 1963, Robinson and Jencks, 1965), thus implicating the capacity to form hydrogen bonds as a requirement for denaturation. Furthermore, alkyl group substitution of urea in the methyl ureas is observed to decrease the solubility of simple peptides , providing conflicting evidence that the denaturation may not proceed via hydrophobic interactions after all. Studies of protein chemical shifts in water in the presence and absence of non-polar solutes (Clifford and Pethica, 1964; Finer et al., 1972) , have produced ambiguous results. On the other hand, proper application of n.m.r. relaxation data may prove to be the technique of choice in these systems. For example, measurement of relaxation times of water revealed increases of up to a factor of 2 in the presence of non-polar substances

The question of how these agents bring about their effect involves not only a consideration of their structures (they are usually simple organic molecules) but also an explanation of the nature of their interaction in aqueous solutions. In other words, the structure of water itself and any structural alteration brought about by the solubilisation of these molecules will have to be considered. But perhaps most importantly, an insight into the exact mechanism of denaturation will necessarily reflect upon the exact nature of the forces involved in protein stabilisation which is of such great biological importance and yet very poorly understood.

Aqueous urea solutions are known to inhibit micellar aggregation (Schick, 1964), solubilise hydrocarbons and affect the conformational properties of a wide range of polymers, including protein denaturation (McKenzie and Rolston , 1971). A lot of circumstantial evidence, from thermodynamic data mostly (Stokes, 1967) has implicated hydrophobic interactions in these systems. Yet another set of evidence demonstrates the requirement for the presence of free hydrogen atoms on the nitrogen atoms of denaturing agents (Gordon and Jencks, 1963; Robinson and Jencks, 1965), thus implicating the capacity to form hydrogen bonds as a requirement for denaturation. Furthermore, alkyl group substitution of urea in the methyl ureas is observed to decrease the solubility of simple peptides , providing conflicting evidence that the denaturation may not proceed via hydrophobic interactions after all. Studies of protein chemical shifts in water in the presence and absence of non-polar solutes (Clifford and Pethica, 1964; Finer et al., 1972) , have produced ambiguous results. On the other hand, proper application of n.m.r. relaxation data may prove to be the technique of choice in these systems. For example, measurement of relaxation times of water revealed increases of up to a factor of 2 in the presence of non-polar substances

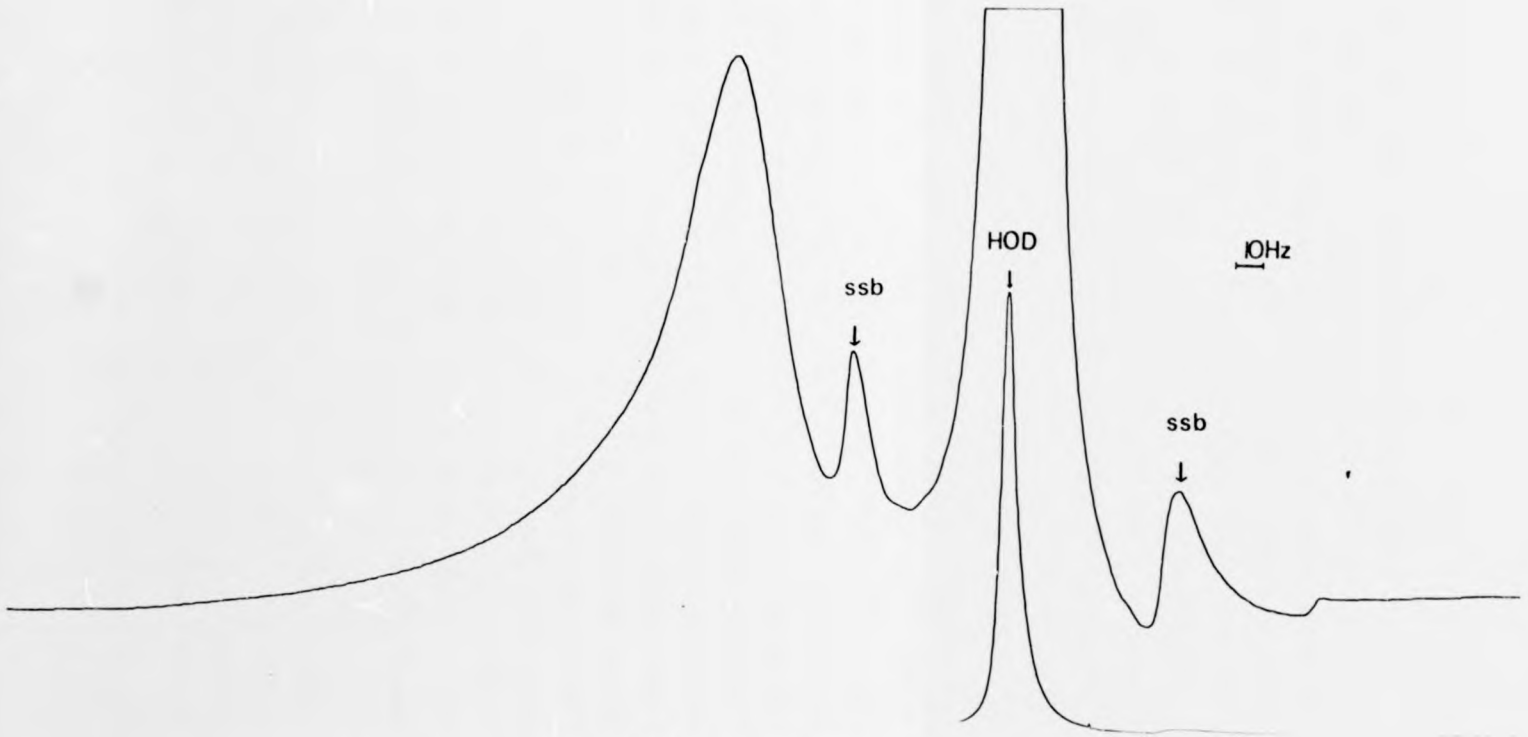

Fig. 36 **90.02 MHz proton nmr of 8M Urea**

as against the values in pure water, indicating an increase in the ordering of water in these solutions (Danyluk and Gore, 1964; Howarth, 1975).

We have applied the technique of ^{13}C spin-lattice relaxation times to the study of the urea-water-bovine serum albumin system. Specifically, we have measured relaxation times for urea solutions in the presence and absence of the protein over the concentration range of 2 - 10 M urea. We find (1) evidence corroborated by proton saturation experiments, i.e.double irradiation techniques leading to nuclear Overhauser enhancements (NOE), that urea disrupts the water structure with possible entropy increase (ii) no evidence for strong urea binding to sites on the protein (iii) weak urea-protein association may exist and probably facilitated by the removal of adsorbed oxygen on the protein .

B. NUCLEAR OVERHAUSER ENHANCEMENTS

A 90 MHz proton n.m.r. spectrum of an 8M urea solution in deuterium oxide, pH 7.0 and at 25°C is shown in Figure 36 . The exchange of protons between urea and water is sufficiently slow to permit the observation of two separate peaks. Acid or base catalysis of proton exchange in aqueous urea has been shown to be extremely effective $\sim 10^6$ mol^{-1} sec^{-1} , leading to the rapid collapse of the two peaks into a singlet (Vold et al., 1970). The exchange at neutral pH, only about 1.5 ± 0.5 sec^{-1} , leads to the two resolved peaks at about 3.673 KHz and 3.578KHz corresponding to the $-NH_2$ and HOD signals respectively. The separation of almost 100 Hz means that if the decoupler power is appropriately chosen, selective irradiation of each peak is possible, while the ^{13}C n.m.r. spectrum is being observed. The values of the signal-to-noise enhancements as obtained for the irradiation of (i) the urea protons only, (ii) the water protons only, and (iii) all the protons in the sample by broad band modulation are reported in Table 14 . Values have been measured for 2M and 8M urea; both representing the lower and higher urea concentration limits respectively in terms of effectiveness in protein

Fig. 36 90.02 MHz proton nmr of 8M Urea

TABLE 14

^{13}C SIGNAL -TO-NOISE RATIOS FOR THE SELECTIVE PROTON DECOUPLING [$^{13}C\{^{1}H\}$] OF AQUEOUS UREA SOLUTIONS. TEMPERATURE 30°C

Type of protons being irradiated	8 Molar Urea		2 Molar Urea	
	S/N	NOE	S/N	NOE
Not decoupled	6.7	-	2.8	-
Broad-band decoupled	15.5	1.2η	5.0	0.9η
H_2O (3,578 KHz)	15.4	1.2η	3.7	0.7η
Urea (3.673 KHz	10.7	0.8η	3.0	0.5η

[a] measurements are the means of at least three separate determinations.

η + 1 = maximum possible enhancement from a directly bound proton to ^{13}C nucleus.

fig 37a

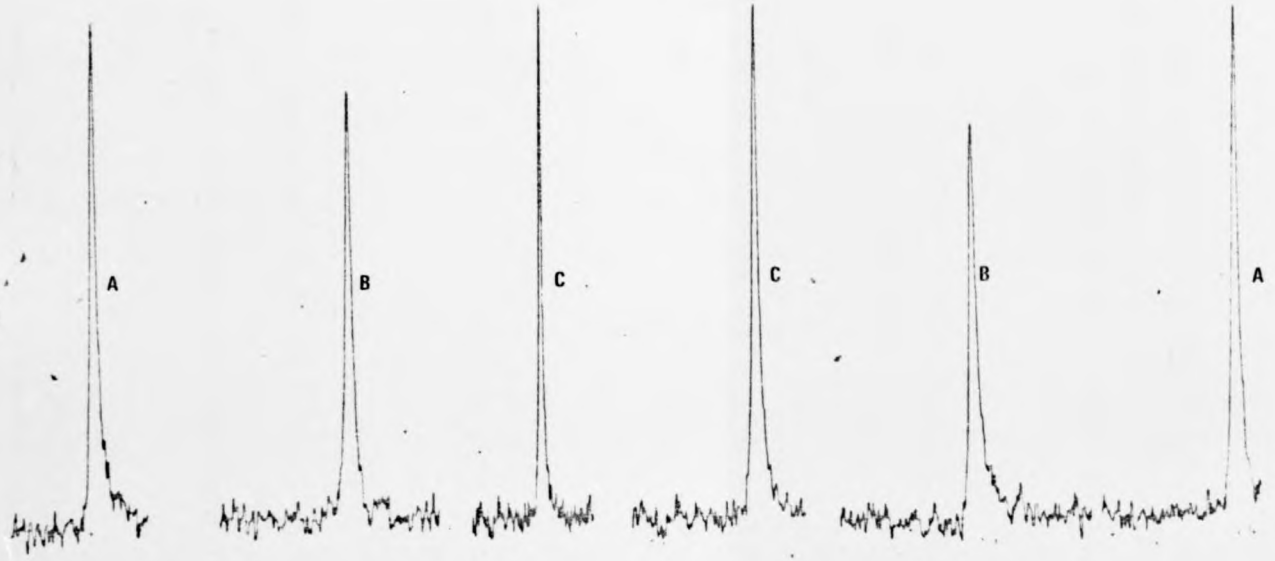

fig 37b

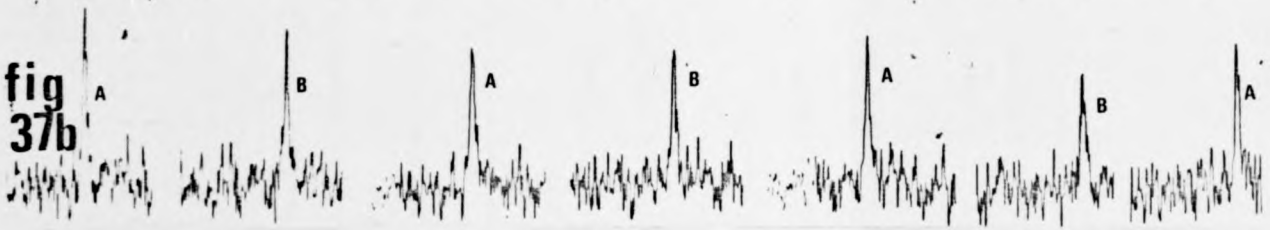

[^{13}C { ^{1}H }] experiments : variation of signal/noise with decoupling frequency.

Fig. 37a for 8M Urea Solution

Fig. 37b for 2M Urea Solution.

Decoupling frequency at (A) 3.578 KH_2 (B) 3.673 KH_2 and (C) fully modulated.

denaturation. Some of the spectra used for the calculation are shown in Figure 37.

C. ^{13}C SPIN-LATTICE RELAXATION STUDIES

T_1 values have been determined for (i) aqueous urea solutions and (ii) aqueous-urea-bovine serum albumin solutions, both at $30^{o}C$. Values for 1M concentration intervals over a urea concentration range of 2 -10M are presented in Table 15. All values presented are for the case of degassed solutions. Measurements of T_1s for corresponding undegassed solutions have not been reported but are mentioned in the discussion. A fixed protein concentration of 2% (w/v) was used throughout the experiment. The variation of T_1 with urea concentration is plotted in Figure 38a PRFT and corresponding log $(A\infty - At)$ vs t plots are included in Figure 39

D. DISCUSSION

The ^{13}C T_1 values observed for the carbonyl grouping in urea are in the range of 30 - 40 secs., Table 15.Estimation of the rotational correlation time based on the Debye equation

$$\tau_c = .74\ V\eta/3NoKT \qquad (11)$$

where V is the molar volume, η is the viscosity and No is Avogadro's number, give $\tau_c \sim 10^{-12}$s. Furthermore, the lack of directly bonded dipoles resulting on the whole in inefficent relaxation mechanisms, could account for these long T_1s.

The results of the double resonance experiments and those of the ^{13}C T_1 values of degassed aqueous solutions of urea are best interpreted in the light of the "structuring" affect of urea on water molecules. The recognition that water is an associated compound dates back a long time

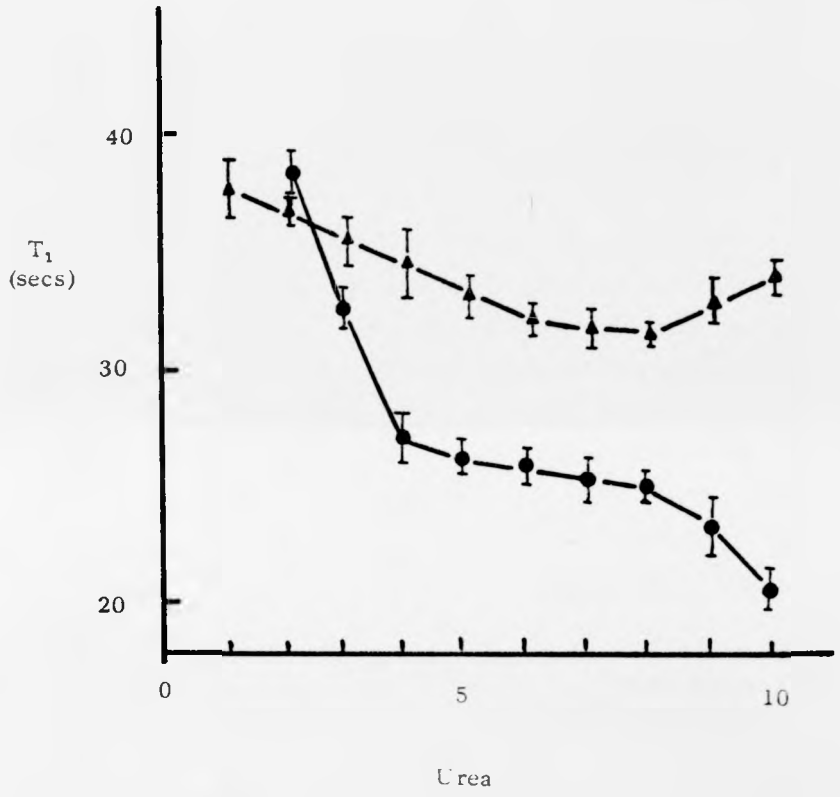

Fig. 38a ^{13}C T_1 as a function of Urea Concentration

▲ without protein ● plus a constant 2% (w/v) protein

Table 15: ^{13}C T_1 data for aqueous urea solutions in the presence and absence of bovine serum albumin at 20 mgs/ml.

Urea conc^n Molarity	No protein present		Protein present	
	T_1[a] sec	$T_1^{-1} \times 10^2$	T_1[a] sec	$T_1^{-1} \times 10^2$
1	36.4 ± 1.2	2.74	-	-
2	36.2 ± .5	2.76	38.4 ± .8	2.60
3	35.0 ± .8	2.85	31.6 ± .4	3.16
4	34.0 ± 1.4	2.94	26.2 ± 1.2	3.82
5	32.7 ± .6	3.06	26.0 ± .8	3.85
6	31.8 ± .5	3.14	25.4 ± .7	3.93
7	31.4 ± .7	3.18	25.2 ± .9	3.96
8	31.2 ± .3	3.20	25.0 ± .6	4.00
9	32.5 ± .8	3.07	22.8 ± 1.0	4.38
10	32.8 ± .6	3.05	20.2 ± .8	4.95

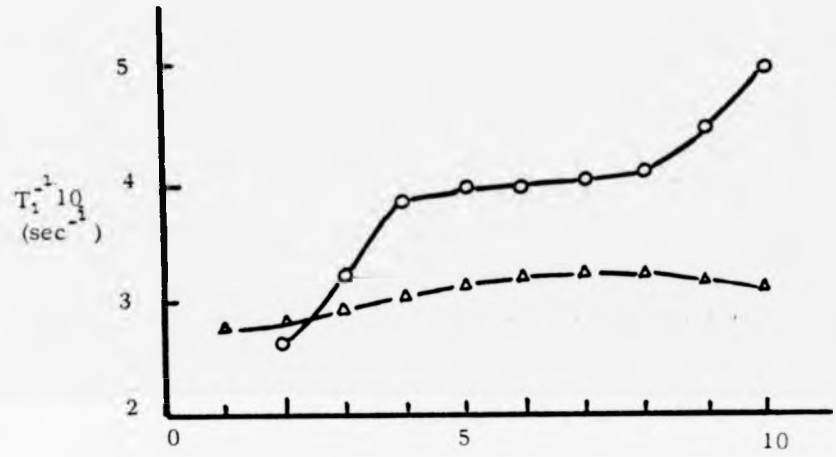

Fig. 38b

Plot of rate of ^{13} relaxation as a function of urea in the presence ○ absence △ of protein.


10
15
20
25
30
40
50
100

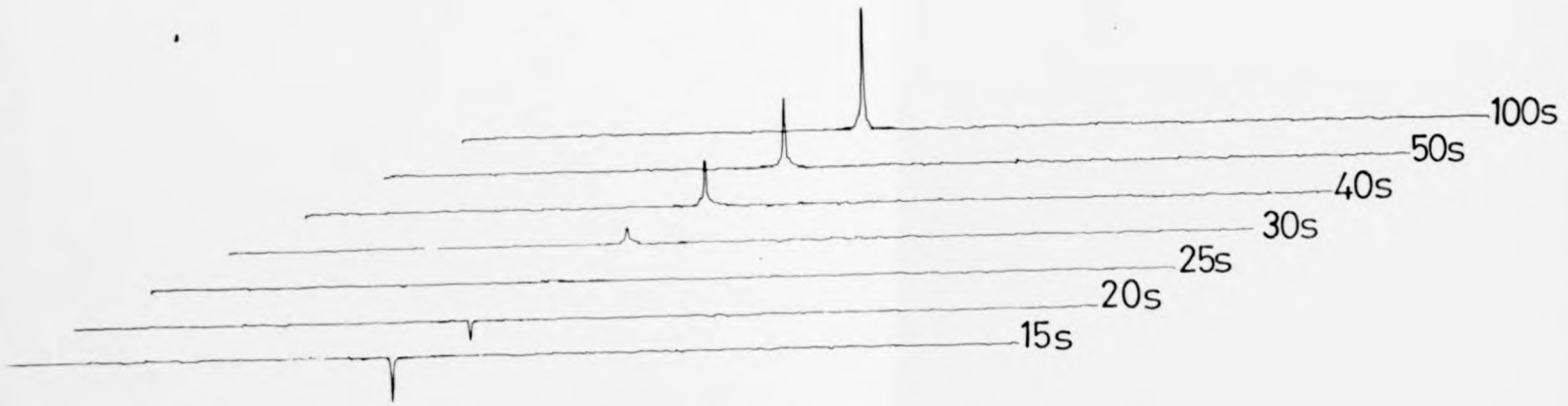

Fig. 39a PRFT of a 10M Urea Solution

Fig. 39a PRFT of a 10M Urea Solution

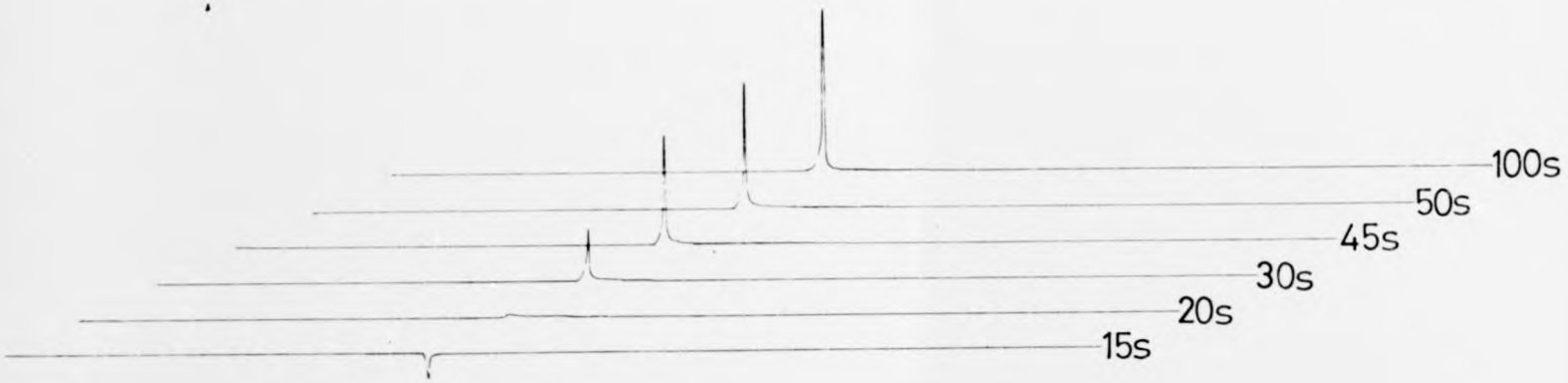

Fig. 39b PRFT for 10M Urea with 2% Protein
T is given on right of spectra from 15-100 secs.
(see text for details)

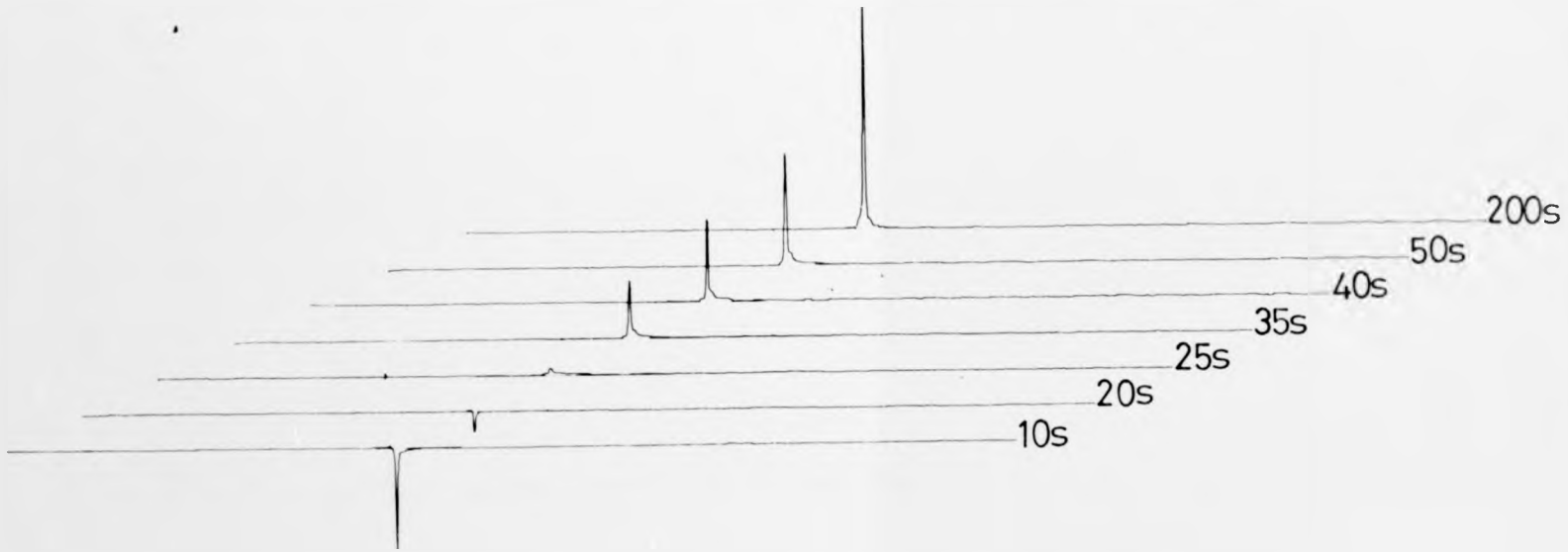

Fig.39c PRFT of 6M Urea Solution

Fig. 39c PRFT of 6M Urea Solution

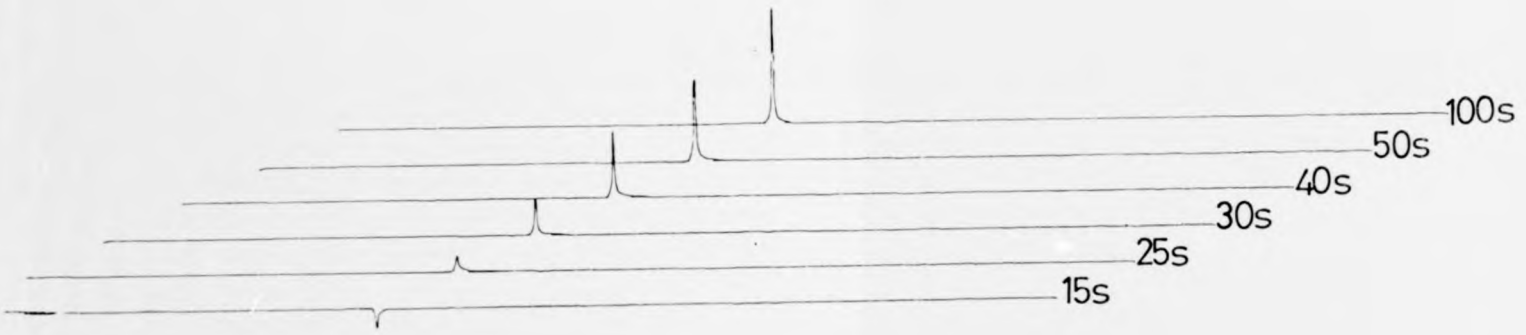

Fig. 39d PRFT for 6M Urea with 20 mgs/ml Protein

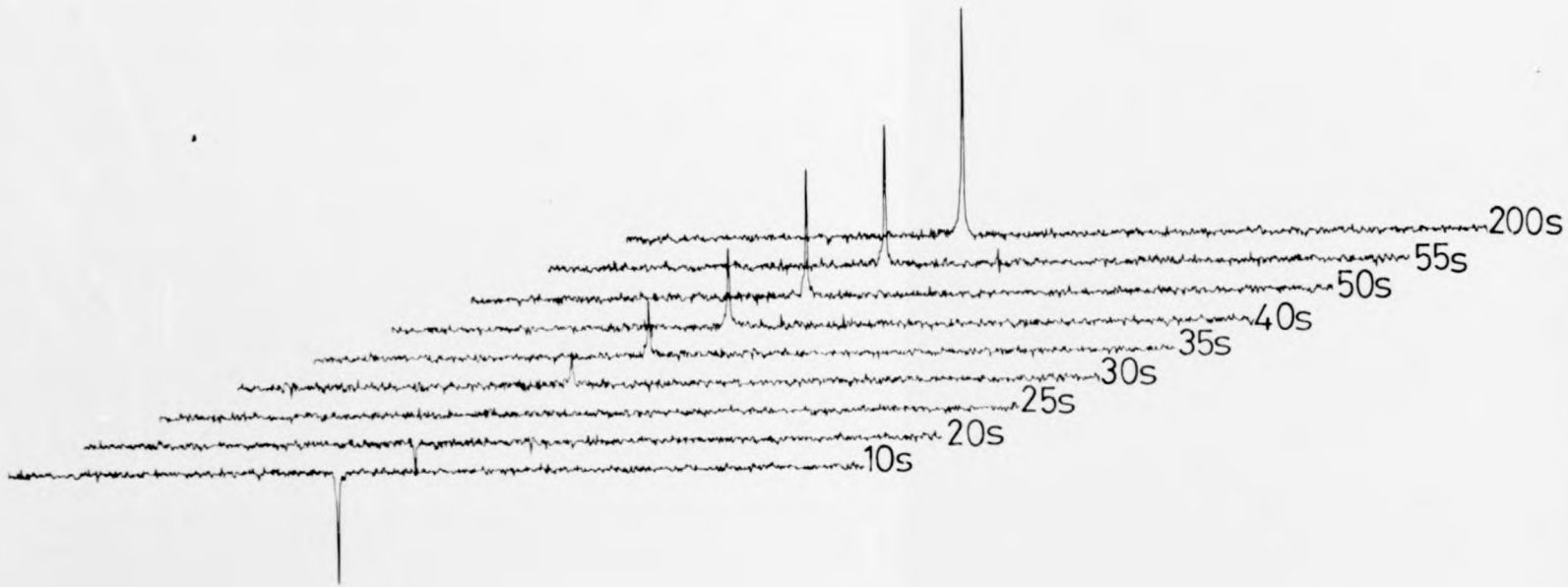

Fig. 39 PRFT of a 4M Urea Solution

Fig. 39e PRFT of a 4M Urea Solution

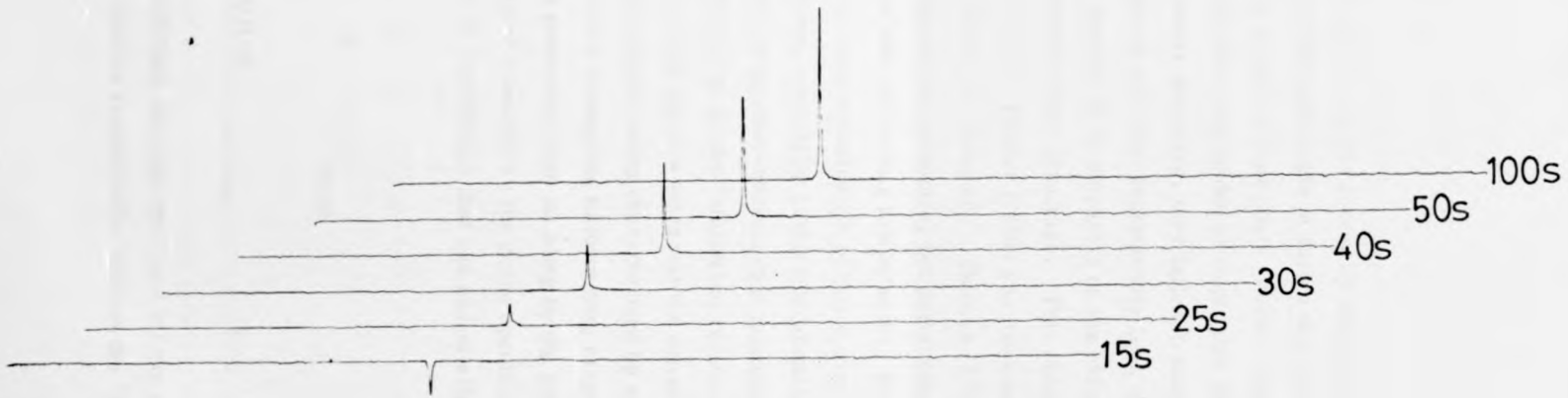

Fig. 39f PRFT for 4M Urea with 20 mgs/ml Protein

indeed. (Chadwell, 1927). It has generally been accepted that these interactions involve hydrogen bonds in such a way that each water molecule is directly bonded to four other "sister" water molecules. But whereas the older theories tended to emphasize the existence of "polymers" in the water structure, they failed to account for many of the observed properties and have consequently been superseded in most of the recent models by an emphasis on the existence of spatial networks in the extended water structure. This change in viewpoint was initiated by Bernal and Fowler (1933) who proposed a model based on a broken-down "ice structure" (Barnes 1929) with most of the hydrogen bonding still in existence, but permitting the hydrogen bonds to break down with increasing temperature. Perhaps more inclination towards a later modification of this theory by Franks and Franks (1968) is shown, especially in the interpretation of the solubility properties of aqueous-hydrocarbon mixtures. This new approach, often referred to as the "statistical treatment" represents water as a mixture of two species viz-a-viz the dense and the bulky species ; the bulky species being characterized by tetrahedrally bonded water molecules attempting to form long range associated structures and only prevented from so doing by the presence of freely tumbling, unassociated monomers : the dense species.
It is postulated that an equilibrium that can essentially be represented as

$$H_2O_{bulky} \rightleftharpoons H_2O_{dense}$$

and $$K = f/(1-f) \qquad (12)$$

where K is the equilibrium constant and f and 1-f are the mole fractions of bulky and dense species respectively, defines the "structural temperature "

of the liquid. Intermediate degrees of molecular energy and freedom meaning those molecules with $\leq 4 \geq O$, H-bonds (Figure 40) may exist but will not effectively alter the treatment, and the effect of a foreign molecule either as a "structure-maker" or "structure-breaker" will be measured by the extent to which it has shifted this equilibrium either to the left or right respectively. As the temperature increases, for example, more and more of the bulky species would have to be converted to the monomer species and vice versa ; temperature being regarded as a "structure breaker" of water therefore. Not only is the pictorial concept of this model suitable for this kind of qualitative interpretation, it fits quantitatively observations on the solution properties of non-ionic solutes in water. Walferen (1966) has defined a "structure breaker" as operationally a solute either ionic, or non-ionic, for which the ratio (Raman spectroscopic terms), $(I_2 / C_2) / (I_1 C_1)$ is less than unity The subscripts $_1$ and $_2$ refer to pure water and to solutions respectively. I refers to the integrated Raman intensity of the hydrogen-bond stretching band at 152 - 175 cm^{-1} and C refers to the stoichiometric water molarity. The ratio found for urea under these conditions is 0.8 and that for sucrose which is considered a "structure maker" is 1.6.

We think that the results from the signal enhancement studies back up the involvement of urea-water association in these solutions. Consistently, the signal-to-noise of the ^{13}C n.m.r. peak of the urea carbonyl is larger when the water peak alone is irradiated than in the undecoupled case. Not only that, the actual enhancement is 2.3, the same as when the decoupling is broad band modulated and as contrasted with a value of only 1.6 when the urea protons are irradiated. It is unlikely that any association of the urea molecules with neighbouring water molecules short of direct hydrogen bonding to the carbonyl of the urea will produce such an efficient dipolar spin coupling: the estimated

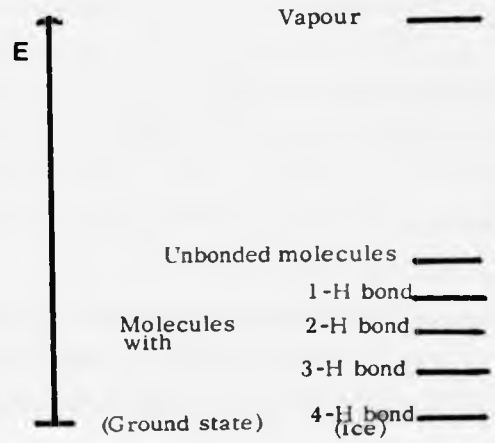

Fig. 40 Schematic representation of energy levels for H_2O molecules with degrees of H-bonded structures.

(Nemethy & Scheraga, (1962) J. Chem. Phys. 36, 3382)

maximum enhancement from a directly bound hydrogen on carbon is only about 3. The surprisingly high solubility of urea (Ellerton and Dunlop, 1966) of up to 10 molar at 25°C is suggestive of some solute-solvent interaction. Also the upfield shift of the chemical shift of the urea protons with increasing temperature (Finer et al, 1972) is evidence of the severing of hydrogen bonds to the urea molecule as temperature increases.

The variation of viscosity with urea concentration in aqueous urea solutions is more pronounced than the variation of T_1. A factor of 1.4 change in viscosity in going from 1- 8M urea (Jager et al., 1965) contrasted with an observed T_1 change of a factor of only 1.1 over the same concentration range indicates perhaps increased motional freedom as the concentration is raised. In fact, the relaxation time is observed to increase suddenly in going from 8 molar to 10 molar solutions (Figure 38a) One possible explanation for this is that the observed relaxation time is actually contributed to by different urea species in aqueous solution and that it is the shift in the statistical distribution of these species (which are presumably in some sort of equilibrium with each other), that determines the T_1 observed. It has been suggested that the resolution of two dielectric relaxations in 8M urea (Pottel and Adoph, 1972) implies independently tumbling urea and water molecules. Our results here do not fit this model but instead indicate a coexistence of species with different correlation times for the urea molecule at least. If, as the double irradiation experiments suggest, hydrogen bonding between urea and water molecules is significant, then it is conceivable that the "bound" urea entity may tumble as a whole; in other words, the tumbling rate of the bound species will be considerably influenced by the rotational correlation time of the water "monomer" bound to it, resulting perhaps in two different correlation times for urea. The exchange of the urea

molecule between "sites", i.e. bound and free species, may be within the relevant range of determining T_1. Presumably, as the urea concentration is raised, the ratio of free/bound urea molecules increases and consequently, the contribution of the bound species to the observed T_1 diminishes. A comparison of the ratios of the number of water molecules per molecule of urea shows a rapid decrease in going from 1 - 10M urea solutions at 20° (c.f. > 52 molecules of water to 1 molecule of urea at 1 molar, as contrasted with < 3 molecules of water to every molecule of urea at 10 Molar urea solutions) indicating, perhaps, that if there is going to remain any "bulky" species of the water structure as previously referred to, then the equilibrium between hydrogen bonded urea-water unions and free urea molecules will be established long before the 10M urea concentration is reached. This is so because for reasons of geometry, urea cannot be accommodated in the tetrahedral spatial net-work of the bulky water species.

Having postulated a strong participation of urea molecules in the water structure, the question remains as to how the new environment would affect protein solubility and eventual denaturation. The denaturation of bovine serum albumin by urea is pH dependent, proceeds fastest above the 6M urea concentration range and of course is temperature dependent as well. At neutrality and an urea concentration of about 7M, the scheme for the denaturation can be represented as :

$$A_1 \longleftrightarrow A^* \longleftrightarrow \Sigma A_{ac} \begin{cases} \xrightarrow{k_2} \Sigma S_1 \\ \xrightarrow{k_3} \Sigma A_2 \xrightarrow{k_4} \Sigma I \end{cases} \qquad (13)$$

where A_1 is the native monomer conformation of the protein and A^* is an activated complex of A_1, thought to be converted rapidly to conformationally altered albumin A_{ac} (McKenzie et al., 1963). The A_{ac} species are

indistinguishable electrophoretically from the native form but are identifiable by means of other physical techniques such as optical rotation (Kauzmann and Simpson, 1953) and viscosity (Mackenzie et al., 1963). The S_1 and A_2 series are electrophoretically distinguishable from the native form. S_1 has ~ 5 - 30% mobility of A_1 and A_2 has mobilities between S_1 and A_1. (Katz and Denis, 1969). After long exposure, ≥ 4 days, water and salt insoluble components begin to appear. The sign Σ indicates the formation at each stage of multiple species depending on urea concentration; the so-called "micro-heterogeneity" element.

The multiplicity of the protein species present in urea solutions make it almost unreasonable to dismiss outright any form of urea protein association. In fact the relaxation time of the urea molecule in the presence of protein is considerably decreased over all the concentration range studied except for the very low urea concentration at ≤ 2M. This decrease may just be purely due to the corresponding increase in viscosity with the presence of protein; at neutral pH, the relative viscosity of urea solution in the presence (η) and absence (η_0) of protein is found to be 1.8 and 1.4 for 2M and 7M urea respectively, at a fixed protein concentration of 20 mgs/ml. The relative change in T_1 for these solutions is of the order of ≤ 1.3 up to an urea concentration of 9M and only rises to 1.6 at 10M urea (Figure 38a). Clearly, these changes are within the range of the increase in solution viscosity and hence may not represent any strong binding of the urea to the protein. On the other hand, the very long relaxation time at low urea concentration (< 4M) in the presence of protein (see Figure 38a) is evidence that, at least at these concentrations where the denaturant is considered least effective, the urea molecules are still tumbling relatively freely as if there was no protein present. These long T_1 values are also probably evidence that it is the viscosity increase associated with the unfolded conformers of the protein : a factor of ~ 5 increase in intrinsic viscosity for the protein solution in going from

native to denatured conformers at neutral pH (Mackenzie et al, 1963), which is responsible for the drop in T_1 s at higher urea concentrations. An interesting observation, however, is that the relaxation rates (see Figure 38b), depict the urea molecule as being in a medium of identical "fluidity" over the concentration range of 4 - 8 M urea in the presence of protein. This is clearly not the case in the absence of protein where a steady increase in the rate of relaxation is observed in raising the concentration. This identifies the protein as being solely responsible for this observation. If we are going to interpret the changes as being purely an increase of viscosity brought about by the unfolding of denatured protein, then it is quite likely that the plateau in this concentration range indicates the presence of conformers at the same stage of denaturation in the least (see equation 13) or at worst conformers with identical viscosities. It seems that raising the urea concentration above 8M produces a new species with radically different viscosities .

In summary then, it seems that the results point towards a fairly strong participation of urea in the water structure. This participation is almost certainly via hydrogen bonding between the water molecules and incoming urea molecules. If the equilibrium water structure involving tetrahedrally hydrogen bonded water molecules and free, tumbling monomers is accepted as near enough to the true picture, then conceptually an urea molecule can form a hydrogen bond with at least one molecule. If this new association considerably alters the properties of the newly associating water molecule, more monomers will have to be released from the bulky species of the water, resulting in a shift to the right of the equilibrium. The result, an increase in the "structural temperature" of the water , could conceivably be sufficient to offset the almost 800 $Kjmole^{-1}$ structural stabilization energy associated with protein folding. Our

results provide no evidence of strong "ligand-type" associations between the urea and incoming protein. Weaker associations cannot be similarly ruled out. Indeed, even if strong association between only a few easily saturable sites on the protein and very few urea molecules exist, it is possible we may have missed it given the extremely high urea concentration range we are operating at. However, there appears to be evidence that different urea strengths lead to different conformers of the denatured species.

Finally, mention is due of the corresponding T_1 data obtained from undegassed solutions. They have not been included here because we think that they are ambiguous. Although the urea solutions behave fairly according to prediction, the presence of protein in these solutions seems to result in relaxation times higher than to be expected. We think that differential solubilities of molecular oxygen in these solutions might account for some of these discrepancies.

CONCLUDING REMARKS

It was found most convenient to present this thesis in its present form, i.e. on the basis of one chapter containing the results of a similar series of experiments. It must not be assumed, however, that a connection does not exist from experiment to experiment.

The results of ^{13}C enrichment of lipids described in Chapter 3, for example, made it feasible to study these systems by relaxation techniques as described in Chapter 4. Also the enrichment of PC as described in Chapter 5 shows that the application of ^{13}C T_1 to a very important phospholipid of "higher" organisms is now a relatively simple matter. Besides, by appropriate choice of labelling agents, e.g. the use of [2-^{13}C] acetate, other carbons which have been impossible to study in these systems may be resolved. The protein denaturation studies described in Chapter 6 are (inasmuch as proteins are an integral part of *in vivo* membranes) related to the rest of the work as well.

Finally, mention is due of another aspect of the n.m.r. of membranes which we have attempted, without success, to investigate. This is the design of an n.m.r. lipophilic probe that can be introduced into the bilayer without appreciable perturbation of the native state of the membranes. An ideal membrane system to use is the erythrocyte "ghost" preparation which is easy to come by and can be prepared fairly easily. Ideal also as the probe are small organic molecules with a fair amount of equivalent protons that will give a readily detectable n.m.r. signal in the concentration range of interest. We have tried simple hydrocarbons such as Hexamethyl ethane (C_8H_{18}), diphenyl ($C_{12}H_{10}$), hexa methyl benzene, ($C_{12}H_{18}$) etc., which, because of their smallness and reasonably simple structures , would hopefully not perturb the bilayer significantly. It appears that rather harsh methods that lead to membrane disorganisation are required to transfer these probes across the "membrane-water" interface.

GLOSSARY OF TERMS AND ABBREVIATIONS

∂	Chemical shift in parts per million.
FID	Free induction decay.
FT	Fourier transform.
NMR	Nuclear magnetic resonance.
NOE	Nuclear Overhauser effect.
T_1	Spin-lattice relaxation time.
T_2	Spin-spin relaxation time.
PRFT	Partially relaxed Fourier transform.
S/N	Signal-to-noise ratio.
BSA	Bovine serum albumin.
CL	Cardiolipin.
DML	Synthetic dimyristoyl lecithin.
DPL	Synthetic dipalmitoyl lecithin.
PC	Phosphatidyl choline.
PE	Phosphatidyl ethanolamine.
PE* or PE[1-^{13}C] acetate	PE derived from biosynthetic ^{13}C enrichment with [1-^{13}C] acetate.
PE/DPL	PE-DPL mixtures.
PE/PS	PE-PS mixtures.
PL	Phospholipid.
PEPF	Phospholipid exchange protein factor.
PS	Phosphatidyl serine.

All other symbols and abbreviations used are explained in the text.

BIBLIOGRAPHY

Abragam, A. (1961) "The Principles of Nuclear Magnetism", Oxford Univ. Press.

Ackers, G.K. (1967) Biochemistry 242, 3237.

Ames, G.F. (1968) J. Bacteriol. 95, 833.

Ashworth, J.M., Kornberg, H.L. and Nothmann, D.L. (1965) J. Mol. Biol. 11, 654.

Atkinson, D., Hauser, H., Shipley, G.G. and Stubs, J.M. (1974) Biochim. Biophys. Acta 339, 10.

Bangham, A.D. (1972) Ann. Rev. Biochem. 41, 753.

Bangham, A.D. and Horne, R.W. (1964) J. Mol. Biol. 8, 660.

Barnes, W.H. (1929) Proc. Roy. Soc. (London) A125, 670.

Barrat, M.D., footnote in Salsbury, N.J., Chapman, D. and Jones, G.P. (1970) Trans. Faraday Soc. 66, 1554.

Barsukov, L.I., Shapiro, Yu.e., Viktorov, A.V. and Volkova, V.I. (1975) Chem. Phys. Lipids 14, 211.

Batchelor J.C. (1974) Ph. D. Thesis, Yale University, U.S.A.

Batchelor, J.C., Cushley, R.J. and Prestegard, J.H. (1974) J. Org. Chem. 39, 1698.

Batchelor, J.C., Prestegard, J.H., Cushley, R.J. and Lipsky, S.R. (1972) Biochem. Biophys. Res. Comm. 48, 70.

Bernal, J.D. and Fowler R.H. (1933) J. Chem. Phys. 1, 515.

Birdsall, N.J.M., Ellar, D.J., Lee, A.J., Metcalfe, J.C. and Warren, G.B. (1974) Biochim. Biophys. Acta 380, 344.

Birdsall, N.J.M., Feeney, J, Lee, A.G., Levine, Y.K. and Metcalfe, J.C. (1972) J. Chem. Soc. 1441.

Bishop, D.G. and Stumpf, P.K. (1971) in "Biochemistry and Methodology of Lipids", Johnson, A.R. and Davenport, J.B. ed; Wiley-Interscience, New York, ch. 19, p.361.

Blazyk, J.F. and Steim, J.M. (1972) Biochim. Biophys. Acta 226, 737.

Bligh, E.G. and Dyer, W.J. (1959) Can. J. Biochem. Physiol. 37, 911.

Bloembergen, N., Purcell, E.M. and Pound, R.V. (1948) Phys Rev. 73, 679.

Bretscher, M.S. (1973) Science 181, 622.

Burger, S.P., Fujii, T., Hanahan, D.T. (1968) Biochemistry 7, 3682.

Burnett, L.J. and Harmon, J.F. (1972) J. Chem. Phys. 57, 1293.

Bystrov, V.F., Shapiro, Yu. E., Viktorov, A.V., Barsukov, L.I. and Bergleson, L.D. (1972) Febs Letts. 25, 337.

Callaghan, P. and Martin N.H. (1962) Biochem. J. 83, 144.

Caroll, K.K., Cuts, J.H. and Murray, G.D. (1968) Can. J. Biochem. 46, 899.

Chadwell, C. (1927) Chem. Revs. 4, 375.

Chan, S.I., Feigenson, G.W. and Seiter, C.H.A. (1971) Nature 231, 110.

Chapman, D. (1968) in "Biological Membranes: Physical Fact and Function", Chapman, D. ed; vol. 1, Academic Press, London, New York.

Chapman, D. (1973) in "Biological Membranes", vol. 2, Chapman, D and Wallach, D.F.H. ed. Academic Press, London, New York.

Chapman, D., Byrne, P. and Shipley, G.G. (1966) Proc. Roy. Soc. A.290, 115.

Chapman, D. and Morrison, A. (1966) J. Biol. Chem. 241, 5044.

Chapman, D. and Penkett, S.A. (1966) Nature 211, 1304.

Chapman, D., Williams, R.M. and Ladbrooke, B.D. (1967) Chem. Phys. Lipids 1, 445

Clifford, J. and Pethica, B.A. (1965) Trans. Faraday Soc. 60, 1483.

Coleman, R. (1973) Biochim. Biophys. Acta 300, 1.

Colley, C.M. and Metcalfe, J.C. (1972) Febs Letts. 24, 241.

Cronan, J.E.Jr. and Batchelor J.G. (1973) Chem. Phys. Lipids 11, 196.

Cronan, J.E. Jr. and Vagelos, P.R. (1972) Biochim. Biophys. Acta 265, 25.

Curds, C.R. and Cockburn, A. (1968) J. Gen. Microbiol. 54, 343.

Danielli, J.F. and Davson, H. (1935) J. Cell. Comp. Physiol. 5, 495.

Danyluk, S.S. and Gore (1964) Nature (London) 203, 748.

De Siervo, A.J. (1969) J. Bacteriol. 100, 1342.

Dietrich, J. and Henning, U. (1970) Eur. J. Biochem. 14, 258.

De Vries, J.J., Berendsen, H.J.C. (1969) Nature (London) 221, 1139.

Ellerton, H.D. and Dunlop, P.J. (1966) J. Phys. Chem. 70, 1831.

Elworthy, P.H. (1959) J. Chem. Soc. 1951.

Elworthy, P.H. and McIntosh (1961) J. Pharm. Pharmacol. 13, 633.

Elworthy, P.H. and McIntosh (1964) J. Phys. Chem. 68, 3448.

Engelman, D.M. (1972) Chem. Phys. Lipids 8, 298.

Erwin, J. and Bloch, K. (1963) J. Biol. Chem. 238, 1618.

Farrar, T.C., Becker, E.D. (1971) Pulse Fourier Transform Nuclear Magnetic Resonance, Academic Press, New York.

Farrar, T.C., Druck, S.J., Shoup, R.R. and Becker, E.D. (1972) J. Amer. Chem. Soc. 94, 699.

Finer, E.G. (1974) J. Mag. Res. 13, 76.

Finer, E.G., Flook, A.G. and Hauser, H. (1972) Biochim. Biophys. Acta 260, 59.

Finer, E.G., Franks, F. and Tait, M.J. (1972) J. Amer. Chem. Soc. 94, 4424.

Franks, H.S. and Franks, F. (1968) J. Chem. Phys. 48, 4746.

Freeman, R. and Hill, H.D.W. (1971) J. Phys. Chem. 54, 3367.

Gent, M.P.N. and Prestegard, J.H. (1974) Biochemistry 13, 4027.

Gilvarg, C. and Davies, B.D. (1956) J. Biol. Chem. 222, 307.

Godici, P.E. and Landsberger, F.R. (1974) Biochemistry, 13, 362.

Goldman, S.S. and Albers, R.W. (1973) J. Biol. Chem. 248, 867.

Gordon, J.A. and Jencks, W.P. (1963) Biochemistry 2, 47.

Grant, D.M. and Cheney, B.V. (1967) J. Amer. Chem. Soc. 89, 5315.

Hansen, J.R. and Lawson, K.D. (1970) Nature 225, 542.

Harder, M.E., Beacham, I.R., Cronan, J.E. Jr., Beacham, K., Honegger, J.L. and Silbert, D.F. (1972) Proc. Nat. Acad. Sci. U.S.A. 69, 3105.

Hauser, H. (1971) Biochim. Biophys. Res. Commun. 45, 1049.

Hauser, H., Finer, E.G. and Chapman, D. (1970) J. Mol. Biol. 53, 419.

Heatley, F. (1976) Private communication.

Hinz, H.J. and Sturtevant, J.M. (1972) J. Biol. Chem. 247, 6071.

Holz, G.G. Jr. and Conner, R.L. (1973) in "Biology of Tetrahymena" Elliot, A.M. ed. Dowden, Hutchinson and Ross Inc., Strondsburg, Penn. ch. 4.

Howarth, O.W. (1975) J. Chem. Faraday Trans I, 71, 2303.

Hsu, C.C. and Fox, C.F. (1970) J. Bacteriol. 103, 410.

Huang, C., Charlton, J.P., Shyr, C.I. and Thompson, T.E. (1970) Biochemistry 9, 3422.

Hubbel, W.H. and McConnell, H.M. (1968) Proc. Nat. Acad. Sci. U.S.A. 61, 12.

Inoue, Y., Nishioka, A. and Chujo, R. (1973) Die Makromol. Chem. 168, 163.

Israelachvili, J.N. and Mitchell, D.J. (1975) Biochim. Biophys. Acta 389, 13.

Jacobson, K. and Papahadjopoulos, D. (1975) Biochemistry 14, 152.

Jager, L., Nyvlt, J., Horacek, S. and Gottfried (1965) Collection Czech. Chem. Comm. 30, 2117.

Johnson, S.M., Bangham, A.D., Hill, M.W. and Korn, E.D. (1971) Biochim. Biophys. Acta 233, 820.

Kaemasa, Y., Akamatsu, A. and Nojima, S. (1967) Biochim. Biophys. Acta 144, 382.

Kaneshiro, T. and Marr, A.G. (1962) J. Lipid Res. 3, 184.

Karabatsos, G.J. (1960) J. Amer. Chem. Soc. 83, 1230.

Kates, M. (1972) in "Techniques of Lipidology - Laboratory Techniques in Biochemistry and Molecular Biology". Work, T.S. and Work, E. ed. Vol III, p.355, North Holl. Publ. Co., Amsterdam.

Katz, S. and Denis, J. (1969) Biochim. Biophys. Acta 188, 247.

Kauzmann, W. and Simpson, R.B. (1053) J. Amer. Chem. Soc. 75, 5154.

Kendrew, J.C. (1961) Sci. Am. 205, 96.

Kornberg, R.D. and McConnell, H.M. (1971) Biochemistry 10, 1111.

Kulmann, K.F., Grant, D.M. and Harris, R.K. (1970) J. Chem. Phys. 52, 3439.

Law, J.H. (1961) Bacteriol. Proc. 129.

Lee, A.G., Birdsall, N.J.M., Levine, Y.K. and Metcalfe, J.C. (1972) Biochim. Biophys. Acta 255, 43.

Lees, A.M. and Korn, E.D. (1966) Biochemistry 5, 1475.

Levine, Y.K., Birdsall, N.J.M., Lee, A.G. and Metcalfe, J.C. (1972a) Biochemistry 11, 1416.

Levine, Y.K., Partington, P., Roberts, G.C.K., Birdsall, N.J.M., Lee, A.G. and Metcalfe, J.C. (1972b) Febs Letts. 23, 203.

Levine, Y.K. and Wilkins, M.H.F. (1971) Nature New Biol. 230, 69.

Levy, G.C. and Nelson, G.L. (1972) Carbon-13 Nulcear Magnetic Resonance for Organic Chemists, Wiley-Interscience, New York.

Litman, B.J. (1973) Biochemistry 12, 2545.

Lumry, R. and Biltonen, R. (1969) in "Structure and Stability of Biological Macromolecules", Timasheff, S.N. and Fasman, G.D., ed., Marcell Dekker, New York, p. 65.

Luzzati, V.(1968) in "Biological Membranes - Physical Fact and Function", vol. 1, Chapman, D. ed.

McKenzie, H.A. and Ralston, T. (1971) Experientia 27, 617.

McKenzie, H.A., Smith, M.B. and Wake, R.G. (1963) Biochim. Biophys. Acta 69, 222.

McLafferty, F.W. (1959) Anal Chem. 31, 82.

McLaughlin, S. and Harary, H. (1974) Biophys. J. 14, 200.

Metcalfe, J.C., Birdsall, N.J.M., Feeney, J., Lee, A.G., Levine, Y.K. and Partington, P. (1971a) Nature 233, 199.

Metcalfe, J.C., Birdsall, N.J.M. and Lee, A.G. (1972) Febs Letts. 21, 335.

Metcalfe, J.C., Metcalfe, S. and Engelman, D.M. (1971b) Biochim. Biophys. Acta 241, 412.

Michaelson, D.M., Horwitz, A.F. and Klein, M.P. (1973) Biochemistry 12, 2637.

Michaelson, D.M., Horwitz, A.F. and Klein, M.P. (1974) Biochemistry 13, 2605.

Nagle, J.F. (1973) J. Chem. Phys. 58, 252.

Nozawa, Y., Fukushima, H. and Iida, H. (1975) Biochim. Biophys. Acta 406, 248.

Nozawa, Y., Iida, H., Fukushima, H. and Ohnishi, A. (1974) Biophys. Biochem. Acta 367, 134.

Nozawa, Y. and Thompson, G.A. (1971) J. Cell. Biol. 49, 712.

Oldfield, E. and Chapman, D. (1972) Febs Letts. 21, 303.

Overath, P., Schairer, H.U. and Stoffel, W. (1970) Proc. Nat. Acad. Sci., U.S.A. 64, 606.

Overath, P. and Träuble, H. (1973) Biochemistry 12, 2625.

Papahadjopoulos, D., Jacobson, K., Nir, S. and Isac, T. (1973) Biochem. Biophys. Acta 311, 330.

Papahadjopoulos, D. and Miller, N. (1967) Biochim. Biophys. Acta 135, 624.

Penkett, S.A., Flook, A.G. and Chapman, D. (1968) Chem. Phys. Lipids 2, 273.

Philips, M.C. (1966) Sci. Am. 215, 78.

Philips, M.C., Finer, E.G. and Hauser, H. (1972) Biochim. Biophys. Acta 290, 397.

Philips, M.C., Ladbrooke, B.D. and Chapman, D. (1970) Biochim. Biophys. Acta 196, 35.

Pottel, R. and Adoph, D. in personal communication to Finer, E.G., Franks, F. and Tait, M.J. (1972b) J. Amer. Chem. Soc. 94, 4424.

Price, H.I. and Lewis, W.C.M. (1929) Biochem. J. 23, 1030.

Ramsey, N.F. (1950) Phys. Rev. 78, 699.

Roberts, R.B., Abelson, P.H., Cowie, P.B., Bolton, E.T. and Britten, R.J. (1963) in "Studies of Biosynthesis in Escherichia coli", Carnegie Institute of Washington, 113.

Robinson, D.R. and Jencks, W.P. (1965) J. Amer. Chem. Soc. 87, 2462.

Sackmann, E. and Moehwald, H. (1973) J. Chem. Phys. 58, 5407.

Saffman, P.G. and Delbrück, M. (1975) Proc. Nat. Acad. Sci. U.S.A. 72, 3111.

Schick, M.J. (1964) J. Phys. Chem. 68, 3585.

Sheetz, M.P. and Chan, S.I. (1972) Biochemistry 11, 4573.

Seiter, C.H.A. and Chan, S.I. (1973) J. Amer. Chem. Soc. 95, 7541.

Sessa, G. and Weissman, G. (1968) J. Lipid Res. 9, 310.

Shapiro, Yu. E., Victoriv, A.V., Volkova, V.I., Barsukov, L.I., Bystrov, V.F. and Bergelson, L.D. (1975) Chem. Phys. Lipids 14, 227.

Shimschick, E. and McConnell, H.M. (1973) Biochemistry 12, 2351.

Shoolery, J.N. (1959) J. Chem. Phys. 31, 1427.

Silbert, D.F. and Vagelos, P.R. (1967) Proc. Nat. Acad. Sci. U.S.A. 56, 1579.

Sims, P.J., Waggoner, A.S., Wang, C. and Hoffman, J.F. (1974) Biochemistry 13, 3315.

Singer, S.J. (1974) Ann. Rev. Biochem. 43, 805.

Singer, S.J. and Nicholson, G.L. (1972) Science 175, 720.

Steim, J.M. (1968) Advan. Chem. Ser. 84, 259.

Steim, J.M., Tourtelotte, M.E., Reinert, J.C., McElhaney, R.N. and Radar, R.L. (1969) Proc. Nat. Acad. Sci. U.S.A. 63, 104.

Stokes, R.H. (1967) Aust. J. Chem. 80, 2087.

Strecker, H.J. (1951) J. Biol. Chem. 189, 815.

Tanford, C. (1962) J. Amer. Chem. Soc. 84, 4240.

Tanford, C. (1968) Advan. Protein Chem. 23, 121.

Thompson, T.E. and Henn, F. (1970) in "Membranes of Mitochondria and Chloroplasts", ACS Monograph No. 165, Racker, E., ed. New York. ch. 1.

Timasheff, S.N., Townend, R. and Mescanti, L. (1966) J. Biol. Chem. 241, 1863.

Träuble, H. and Eibl, H. (1974) Proc. Nat. Acad. Sci. U.S.A. 71, 214.

Träuble, H. and Haynes, D.H. (1971) Chem. Phys. Lipids 7, 324.

Träuble, H. and Overath, P. (1973) Biochim. Biophys. Acta 307, 491.

Veksli, Z., Salsburg, N.J. and Chapmen, D. (1969) Biochim. Biophys. Acta 183, 434.

Vogel, H.J. and Bonner, D.M. (1956) J. Biol. Chem. 218, 97.

Vold, R.L., Daniel, E.S. and Chan, S.O. (1970) J. Amer. Chem. Soc. 92, 6771.

Walfaren, G.E. (1966) J. Chem. Phys. 44, 1546.

Wallach, D. (1967) J. Chem. Phys. 47, 5258.

Wallach, D. (1969) J. Chem. Phys. 73, 307.

Walter, W.V. and Hayes, R.G. (1971) Biophys. Biochem. Acta 249, 528.

Wilkins, M.H.F. (1971) Nature (London) New Biol. 230, 72.

Wilson, G. and Fox, C.F. (1971) J. Mol. Biol. 55, 49.

Wirtz, K.W.A. and Zilversmit, D.B. (1970) Febs Letts. 7, 44.

Woessner, D.E. (1962) J. Chem. Phys. 36, 1.

Yost, P. (1971) in "Structure and Function of Biological Membranes" Rotfield, L., ed. New York, Academic Press, ch. 3.

Zimmer, G. and Schirmer, H. (1974) Biochim. Biophys. Acta 345, 314.

ADDENDUM

1. Chapman, D. and Dodd, G.H., (1971) in "Structure and Function of Biological Membranes", Rothfield ed. Acad. Press. Ch. 2.
2. Clowes, A.W., Cherry, R.J. and Chapman, D., (1971), Biochim. Biophys. Acta. 249, 301.
3. De Kruijff, B., Cullis, P.R. and Radda, G.K., (1975), Biochim. Biophys. Acta. 406. 6.
4. Huang, C, (1969), Biochemistry. 8, 344.
5. Ladbrooke, B.D. and Chapman, D., (1969), Chem. Phys. Lipids. 3, 304.
6. Philips, M.C., Williams, R.M. and Chapman, D., (1969). Chem. Phys. Lipids. 3, 234.
7. Seelig, A. and Seelig, J., (1974), Biochemistry. 13, 4839.
8. Seelig, A. and Seelig, J., (1975), Biochim. Biophys. Acta. 406. 1.
9. Tinker, D.O. and Pinteric, L., (1971), Biochemistry. 10, 860.